

**University of Alberta**

Reusable Ru and Rh Catalyst-Organic Frameworks for Ester  
Hydrogenations and Enyne Cycloisomerizations

by

Michael Jason Hass

A thesis submitted to the Faculty of Graduate Studies and Research  
in partial fulfillment of the requirements for the degree of

Master of Science

Department of Chemistry

©Michael Jason Hass

Spring 2011

Edmonton, Alberta

Permission is hereby granted to the University of Alberta Libraries to reproduce single copies of this thesis and to lend or sell such copies for private, scholarly or scientific research purposes only.

Where the thesis is converted to, or otherwise made available in digital form, the University of Alberta will advise potential users of the thesis of these terms.

The author reserves all other publication and other rights in association with the copyright in the thesis and, except as herein before provided, neither the thesis nor any substantial portion thereof may be printed or otherwise reproduced in any material form whatsoever without the author's prior written permission.

## **Examining Committee**

Steven H. Bergens, Chemistry

Jillian M. Buriak, Chemistry

Natalia Semagina, Chemical and Materials Engineering

## Abstract

A method was developed to immobilize and reuse a catalyst for the asymmetric cycloisomerization of enynes. Immobilization is achieved through use of metal containing monomers, which are reacted with a cycloolefin via an alternating ring-opening metathesis polymerization, assembling a three-dimensional catalyst-organic framework. For example,  $[\text{RhCl}((R)\text{-5,5'-dinorimido BINAP})_2]$  was copolymerized with *cis*-cyclooctene using *trans*- $\text{RuCl}_2(\text{CHPh})(\text{PCy}_3)_2$  as a catalyst. After supporting the resulting framework on barium sulphate, silver(I) hexafluoroantimonate was added in the presence of enyne substrates to generate cationic rhodium(I) sites. These catalytic rhodium(I) sites catalyzed the asymmetric cycloisomerization of enynes, and afforded a maximum of 620 turnovers and >99% *ee* over the course of six runs. This catalyst was also used for batch reactions with turnovers as high as 800. The maximum number of turnovers reported in literature for a homogeneous non-tandem cycloisomerization reaction is ten.

## Acknowledgements

I would like to thank Steve Bergens for being intolerable when it was required!

## Table of Contents

### Chapter 1

#### Introduction

General definitions	1
Asymmetric catalysis, and immobilization	1
Polymer-supported catalysts for asymmetric C-C bond forming reactions	4
Introduction to olefin metathesis	7
Immobilized ring-closing metathesis catalysts	11
Immobilization of Rh-BINAP catalysts	14
Introduction to cycloisomerization of enynes	20
Rh-catalyzed asymmetric cycloisomerization	21
Pioneering work by Xumu Zhang	21
Mechanism of Rh-catalysed cycloisomerization	24
Synthesis of natural products	26
Research objectives	33

### Chapter 2

#### Supported Catalyst-Organic Framework for the Asymmetric Cycloisomerization of 1,6-Enynes

Introduction	35
Results and Discussion	36

Section A: Synthesis of ( <i>R</i> )-5,5'-dinorimido-BINAP	
<b>(13)</b>	36
Hydrogenation of ( <i>R</i> )-5,5'-dinitro-BINAP dioxide ( <b>19</b> )	39
Synthesis of ( <i>R</i> )-5,5'-dinorimido-BINAP ( <b>13</b> )	40
Characterization of NMR-distinct atropisomers of <b>13</b>	42
Section B: Preparation of ROMP-Active Catalyst Monomers	
	48
Synthesis and characterization of [Ru(N-BINAP)((1-3;5-6-η)-C <sub>8</sub> H <sub>11</sub> )]BF <sub>4</sub> ( <b>23</b> )	48
Synthesis and characterization of [RhCl(N-BINAP)] <sub>2</sub> ( <b>22</b> )	54
Section C: Preparation of Catalyst-Organic Frameworks through Alternating-ROMP Assembly.	
	62
Alternating ROMP assembly of <b>23</b> and COE	66
Alternating ROMP assembly of <b>22</b> and COE	72
Section D: Investigations into the Hydrogenation of Esters using a Supported Noyori-Type Ketone Hydrogenation Catalyst.	
	81
Reusability of Ru-based catalyst organic framework <b>27</b> for the hydrogenation of esters	81

Section E: Investigations into the Efficacy and Reusability of the Immobilized Catalyst for the Cycloisomerization of 1,6-Enynes	85
Preparation of Substrates	86
Reusability of Rh-based catalyst organic framework <b>28</b> for the cycloisomerization of 1,6-enynes	89
Enantiomeric excess determination of ( <i>Z</i> )-3-(cyclohexylmethylene)-4-(( <i>E</i> )-prop-1-enyl)tetrahydrofuran ( <b>32</b> )	93
<b>Chapter 3</b>	
<b>Concluding remarks</b>	104
<b>Chapter 4</b>	
<b>Experimental Section</b>	109
General procedures and materials	109
Synthesis of ( <i>R</i> )-5,5'-diamino-BINAP dioxide ( <b>20</b> ).	110
Synthesis of [Ru( $\eta^6$ -anthracene)((1-3;5-6- $\eta$ )-C <sub>8</sub> H <sub>11</sub> )]BF <sub>4</sub> ( <b>24</b> )	111
Synthesis of [Ru( $\eta^5$ -C <sub>8</sub> H <sub>11</sub> )(N-BINAP)]BF <sub>4</sub> ( <b>23</b> )	112
Synthesis of [RhCl(N-BINAP)] <sub>2</sub> ( <b>25</b> )	112
Procedure for the ROMP-Assembly of Catalyst Organic Framework ( <b>28</b> )	113
Preparation of <i>cis</i> -2-Penten-1-Bromide ( <b>35</b> )	116
Preparation of 3-cyclohexyl-2-propyn-1-ol ( <b>33</b> )	117

((2Z)-3-Pent-2-enyloxy-prop-1-yl)cyclohexene ( <b>31</b> )	117
Preparation of 3-phenyl-2-propyn-1-ol ( <b>34</b> )	119
((2Z)-3-Pent-2-enyloxy-prop-1-yl)benzene ( <b>29</b> )	119
General Procedure for Low-Loading Cyclizations	121
General Procedure for High-Loading Cyclizations	122
Enantiomeric Excess Determination of <b>32</b>	123
Enantiomeric Excess Determination of <b>30</b>	124
<b>References</b>	125



## List of Tables

### Chapter 1

<b>Table 1-1:</b> RCM reactions in H <sub>2</sub> O at room temperature using supported catalyst <b>7</b> .	14
<b>Table 1-2:</b> Hydrogenation of β-ketoesters using <b>10</b> .	17

### Chapter 2

<b>Table 2-1:</b> Rh(I)-catalyzed asymmetric hydrogenation of dehydroamino acids using BINAP phosphinite ligands.	38
<b>Table 2-2:</b> Rh(I)-catalyzed isomerization of N,N-diethyl geranylamine using <b>5</b> at 100°C in THF.	39
<b>Table 2-3</b> Atropisomer ratios obtained from the Diels-Alder and radical reactions of N-aryl maleimides.	47
<b>Table 2-4:</b> Hydrogenations of Methyl Benzoate in THF, through reuse of Catalyst-Organic Framework.	84
<b>Table 2-5:</b> Cycloisomerization of <b>31</b> through reuse of Catalyst Framework <b>9</b> .	92
<b>Table 2-6:</b> Cycloisomerization of <b>29</b> through reuse of Catalyst Framework <b>9</b> .	97
<b>Table 2-7:</b> Cycloisomerization of <b>31</b> In Different Solvents	99

**Table 2-8.** Cycloisomerization of **29** Using Further Additions of Substrate before Attempted Reuse. 101

**Table 2-9.** Cycloisomerization of **31** with High Loadings of Substrate. 103

## List of Figures

### Chapter 1

- Figure 1-1:** Enantiomers of Thalidomide and Ketamine. 2
- Figure 1-2:** Common, commercially available olefin metathesis catalysts. 11

### Chapter 2

- Figure 2-1:** (*R*)-5,5'-dinorimido BINAP, **13**, a ROMP-active ligand used in the preparation of Catalyst-Organic Frameworks. 36
- Figure 2-2:** Chiral environment of an (*S*)-BINAP Ru complex as described by Kitamura *et al.* 37
- Figure 2-3:** Diastereomeric rotamers of **13**. 43
- Figure 2-4:**  $^{31}\text{P}$  NMR of one isomer of **13** after 5 minutes at room temperature (162.1 MHz,  $\text{CD}_2\text{Cl}_2$ .) 44
- Figure 2-5:**  $^{31}\text{P}$  NMR spectra of **13** in  $\text{CD}_2\text{Cl}_2$  recorded at a) 30 minutes, b) 60 minutes and c) 18 hours. (202.3 MHz,  $\text{CD}_2\text{Cl}_2$ , 27°C) 45
- Figure 2-6:**  $^1\text{H}$  NMR Spectrum of  $[\text{Ru}(\text{C}_8\text{H}_{11})(\text{N-BINAP})]\text{BF}_4$  (**230**) before and after reflux at 40°C for 48h. (399.8 MHz, 27°C,  $\text{CD}_2\text{Cl}_2$ .)  
\* = residual solvent signal, + = displaced anthracene. 52
- Figure 2-7:**  $^{31}\text{P}$  NMR Spectrum of  $[\text{Ru}(\text{C}_8\text{H}_{11})(\text{N-BINAP})]\text{BF}_4$  (**23**) before and after reflux at 40°C for 48h. (161.2 MHz, 27°C,  $\text{CD}_2\text{Cl}_2$ .)

**Figure 2-8:** Conformation of the thermodynamically stable isomer of  $[\text{Ru}(\text{C}_8\text{H}_{11})(\text{N-BINAP})]\text{BF}_4$ , (**23a**). 54

**Figure 2-9:**  $^1\text{H}$  NMR of **22** taken at  $27^\circ\text{C}$ . \* = residual  $\text{CH}_2\text{Cl}_2$  signals; + = residual  $\text{C}_2\text{H}_4$  signals. (399.8 MHz,  $\text{CD}_2\text{Cl}_2$ ,  $27^\circ\text{C}$ ). 56

**Figure 2-10:**  $^{31}\text{P}$  NMR of  $[\text{RhCl}(\text{N-BINAP})]_2$  (**22**) recorded 15 minutes after mixing. (162.1 MHz,  $27^\circ\text{C}$ ,  $\text{CD}_2\text{Cl}_2$ .) 57

**Figure 2-11:**  $^{31}\text{P}$  NMR of  $[\text{RhCl}(\text{N-BINAP})]_2$  (**22**) recorded a) 15 minutes, b) 30 minutes, c) 60 minutes and d) 90 minutes after mixing. (162.1 MHz,  $27^\circ\text{C}$ ,  $\text{CD}_2\text{Cl}_2$ .) 58

**Figure 2-12:**  $^{31}\text{P}$  NMR of **21** at room temperature. (162.1MHz,  $\text{CD}_2\text{Cl}_2$ ,  $27^\circ\text{C}$ ). 61

**Figure 2-13:** NMR spectra recorded of the prepared catalyst-organic framework **26** from the alternating-ROMP assembly of **23a** with COE. a)  $^1\text{H}$  NMR spectrum (400 MHz,  $\text{CD}_2\text{Cl}_2$ ,  $27^\circ\text{C}$ ), b)  $^{31}\text{P}$  NMR spectrum (162.1 MHz,  $\text{CD}_2\text{Cl}_2$ ,  $27^\circ\text{C}$ ). 65

**Figure 2-14:** NMR spectra recorded for the catalyst-organic framework (**27**) prepared through alternating-ROMP assembly of **23a** with COE after the addition of dpen. a)  $^1\text{H}$  NMR spectrum (400 MHz,  $\text{CD}_2\text{Cl}_2$ ,  $27^\circ\text{C}$ ), b)  $^{31}\text{P}$  NMR spectrum (162.1 MHz,  $\text{CD}_2\text{Cl}_2$ ,  $27^\circ\text{C}$ ). 66

**Figure 2-15:** Dicationic, inactive Rh-dimer formed upon hydrogenation of  $[\text{Rh}(\text{BINAP})(\text{NBD})]^+$ . 68

**Figure 2-16:**  $^{31}\text{P}$  NMR of alternating-ROMP assembled catalyst-organic framework **28**. (161.2 MHz, 27°C,  $\text{CD}_2\text{Cl}_2$ .) 72

**Figure 2-17:**  $^1\text{H}$  NMR Spectra during alternating-ROMP assembly of **22** and COE with **1** at RT a) 0 hr (before addition of Grubbs' I, b) 24hr. \* = Residual  $\text{CH}_2\text{Cl}_2$ . (399.8 MHz,  $\text{CD}_2\text{Cl}_2$ , 27.0°C). 77

**Figure 2-18:**  $^1\text{H}$  NMR spectra of COE polymerization before and after addition of excess  $\text{C}_2\text{H}_4(\text{g})$ . 78

**Figure 2-19:**  $^1\text{H}$  NMR spectrum of **32** as prepared through reuse of catalyst-organic framework **28**. 91

**Figure 2-20:** Effects of addition of **35** in the  $^1\text{H}$  NMR spectra of a sample of ( $\pm$ )-**32**. (500 MHz,  $\text{C}_6\text{D}_6$ , 27°C). a) 0 mol %; b) 4 mol %; c) 6 mol %; d) 8 mol %. 94

**Figure 2-21:** Determination of the *ee* of **32** using ~8 mol % of **35** through  $^1\text{H}$  NMR spectroscopy. (500 MHz,  $\text{C}_6\text{D}_6$ , 27°C) a) racemic **32** prepared using  $[\text{Rh}(\text{NBD})_2]\text{BF}_4$ ; b) **32** prepared using framework **28** as the catalyst; **32** as prepared in b with racemic **32** added. 95

## List of Schemes

### Chapter 1

- Scheme 1-1:** Wilkenson's catalyst supported on polystyrene beads. 6
- Scheme 1-2:** Common operation modes of olefin metathesis. (a) Ring-Opening Metathesis (ROM), (b) Ring-Opening Metathesis Polymerization (ROMP), (c) Cross Metathesis (CM), (d) Ring-Closing Metathesis (RCM). 9
- Scheme 1-3:** Formation and collapse of the metallacyclobutane intermediate during metathesis catalysis. 9
- Scheme 1-4:** Preparation of PEG-supported second generation Hoveyda-Grubbs metathesis catalyst (**5**). 12
- Scheme 1-5:** Preparation of PEG-linked NHC ligand, and reaction with Hoveyda-Grubbs 1st generation catalyst to form supported metathesis catalyst **7**. 13
- Scheme 1-6:** Synthesis of immobilized BINAP-based ligand on silica support. 15
- Scheme 1-7:** Synthesis of immobilized catalyst **11**. 18
- Scheme 1-8:** Proposed mechanism, and competing pathways for the intramolecular cycloisomerization of enynes by cationic rhodium-diphosphine species. 25

**Scheme 1-9:** Catalyst containing copolymer prepared by Ralph and Akotsi for the asymmetric hydrogenation of ketones<sup>87</sup>. 29

**Scheme 1-10:** Three-dimensional representation of catalyst-organic framework after alternating copolymerization, **15**, as synthesized by Ralph<sup>89</sup>. 32

## Chapter 2

**Scheme 2-1.** Synthesis of (*R*)-5,5'-diamino-BINAP (**16**). 41

**Scheme 2-2:** Synthesis of ROMP active ligand, *N*-BINAP (**13**).

41

**Scheme 2-3:** Preparation of a ROMP active **23** for the asymmetric hydrogenation of ketones. 49

**Scheme 2-4:** Preparation of ROMP active Catalyst Monomer, **22**.

55

**Scheme 2-5:** Preparation of catalyst-organic framework using **23a**.

64

**Scheme 2-6:** Expected three-dimensional structure of catalyst organic framework **26**. 65

**Scheme 2-7.** Preparation of catalyst-organic framework (**28**) through alternating-ROMP assembly. 70

**Scheme 2-8:** Three-Dimensional structure of **28** after alternating ROMP assembly. 71

**Scheme 2-9:** 1,6-Enyne substrates used in the evaluation of the catalyst organic framework. 86

**Scheme 2-10:** Literature Procedure for the Synthesis of (2*Z*)-3-Pent-2-enyloxy-prop-1-yl)benzene, **29**. 87

**Scheme 2-11:** Modified Preparation of (2*Z*)-3-Pent-2-enyloxy-prop-1-yl)benzene, **29**. 88



## List of Equations

### Chapter 1

**Equation 1-1:** Rhodium-catalyzed 1,4-addition of phenylboronic acid to 2-cyclopentenone. 19

**Equation 1-2.** The intramolecular cycloisomerization reaction of 1,6-Enynes. a) Thermal cyclization of 6-Octen-1-yne at 400°C 21

**Equation 1-3:** Reaction Scope for the rhodium-BINAP catalyzed intramolecular cycloisomerization of enynes to produce a) chiral tetrahydrofurans<sup>75</sup>, b) lactams<sup>77</sup>, c) lactones<sup>78</sup>, d) cyclopentanes<sup>80</sup>, and e) cyclopentanones<sup>80</sup>. 23

**Equation 1-4:** Synthesis of (+)-Blastmycinolactol through precursor production by cationic rhodium-BINAP catalyzed cycloisomerization, and kinetic resolution of racemic enynes. 26

**Equation 1-5:** Synthesis of (4*R*)-(Z)-dehydrohomopilopic aldehyde, a precursor in the synthesis of (+)-pilocarpene. 27

**Equation 1-6:** Asymmetric synthesis of (-)-Platensimycin, through formation of a spirocycle intermediate. 28

**Equation 1-7:** Synthesis of a ROMP-active Ru-BINAP metal-containing monomer from (*R*)-5,5'-dinorimido-BINAP(**13**). 32

## List of Abbreviations

2MeTHF	2-methyltetrahydrofuran
acac	acetylacetone
BINAP	2,2'-bis(diphenylphosino)-1,1'-binaphthyl
CM	Cross Metathesis
COE	<i>cis</i> -cyclooctene
CPME	cyclopentylmethylether
DCE	1,2-dichloroethane
DLS	dynamic light scattering
EDCI	1-(3-dimethylaminopropyl)-3-ethylcarbodiimide hydrochloride
<i>ee</i>	Enantiomeric Excess
ESI	electrospray ionization
equiv	equivalents
GC	gas chromatography
GPC	gel permeation chromatography
h	hour(s)
HOBt	1-hydroxybenzotriazole hydrate
HPLC	high performance liquid chromatography
Hz	Hertz
KH	Potassium hydride

M	Metal
MALDI	matrix-assisted laser desorption/ionization
MeOH	methanol
MHz	Megahertz
min	minute(s)
mL	milliliter(s)
mm	millimeter(s)
mmol	millimole(s)
mol	mole(s)
MS	mass spectrometry
N-BINAP	( <i>R</i> )-5,5'-dinorimido-BINAP
NHC	N-Heterocyclic Carbene
NMR	Nuclear Magnetic Resonance
Norphos	(2 <i>R</i> ,3 <i>R</i> )-(-)-2,3-Bis(diphenylphosphino)-bicyclo[2.2.1]hept-5-ene
PCy <sub>3</sub>	tricyclohexylphosphine
Pd/C	palladium on carbon
PEG	polyethylene glycol
Ph	phenyl
Py	pyridine, or benzene with a nitrogen.
PS	polystyrene
psi	pounds per square inch

psig	pounds per square inch gauge pressure
RCM	ring closing metathesis
Rh	rhodium
ROMP	ring opening metathesis polymerization
ROP	ring opening polymerization
Ru	ruthenium
rt	room temperature
sol	solvent
<sup>t</sup> BuOK	potassium <i>tert</i> -butoxide
THF	tetrahydrofuran
TO	turn overs
TOF	time of flight
TON	turn over number

## List of Compounds

- 1  $\text{trans-RuCl}_2(\text{=CHPh})(\text{PCy}_3)_2$ , 1<sup>st</sup> Generation Grubbs catalyst
- 2  $\text{trans-RuCl}_2(\text{=CHPh})(\text{PCy}_3)(\text{NHC})$ , 2<sup>nd</sup> Generation Grubbs catalyst
- 3 (1,3-Bis-(2,4,6-trimethylphenyl)-2-imidazolidinylidene)dichloro(*o*-isopropoxyphenylmethylene)ruthenium
- 4 2,6-Diisopropylphenylimidoneophylidene molybdenum(VI)bis(hexafluoro-*t*-butoxide), Schrock's catalyst
- 5 Polyethyleneglycol supported Hoveyda-Grubbs 2<sup>nd</sup> Generation Catalyst
- 6 N-tosyldiallylamine
- 7 PEG-supported Hoveyda-Grubbs 2<sup>nd</sup> Generation catalyst
- 8 Silica-supported 5,5'-diamino BINAP
- 9 *trans*- $\text{RuCl}_2(\text{silica-supported } 5,5'\text{-diamino BINAP})(\text{benzene})$
- 10  $[\text{Rh}(\text{COD})(\text{silica-supported } 5,5\text{-diamino BINAP})]\text{BF}_4$
- 11  $[(\text{PS-PEG supported BINAP})\text{Rh}(\text{acac})]$
- 12 *trans*- $[\text{RuCl}_2(\text{Norphos})(\text{Py})_2]$
- 13 (*R*)-5,5'-dinorimido-BINAP
- 14 *trans*- $[\text{RuCl}_2(\text{N-BINAP})\text{Py}_2]$
- 15 *trans*-- $[\text{RuCl}_2(\text{N-BINAP})\text{Py}_2]$  based Catalyst-Organic Framework
- 16 (*R*)-5,5'-diamino BINAP
- 17 (*R*)-BINAP
- 18 (*R*)-BINAP dioxide

- 19 (*R*)-5,5'-dinitro BINAP dioxide
- 20 (*R*)-5,5'-diamino BINAP dioxide
- 21 [Rh(NBD)(N-BINAP)]BF<sub>4</sub>
- 22 [RhCl(N-BINAP)]<sub>2</sub>
- 23 [Ru(N-BINAP)((1-3;5-6-η)-C<sub>8</sub>H<sub>11</sub>)]BF<sub>4</sub>
- 24 [Ru(η<sup>6</sup>-anthracene)((1-3;5-6-η)-C<sub>8</sub>H<sub>11</sub>)]BF<sub>4</sub>
- 25 [RhCl(N-BINAP)]<sub>2</sub>
- 26 [Ru(N-BINAP)((1-3;5-6-η)-C<sub>8</sub>H<sub>11</sub>)]BF<sub>4</sub> based Catalyst-Organic Framework
- 27 [Ru(N-BINAP)((1-3η)-C<sub>8</sub>H<sub>11</sub>(dpn))]BF<sub>4</sub> based Catalyst-Organic Framework
- 28 [RhCl(N-BINAP)]<sub>2</sub> based Catalyst-Organic Framework
- 29 ((2*Z*)-3-Pent-2-enyloxy-prop-1-yl)benzene
- 30 (*Z*)-3-benzylidene-4-((*E*)-prop-1-enyl)tetrahydrofuran
- 31 ((2*Z*)-3-Pent-2-enyloxy-prop-1-yl)cyclohexene
- 32 (*Z*)-3-(cyclohexylmethylene)-4-((*E*)-prop-1-enyl)tetrahydrofuran
- 33 3-phenyl-2-propyn-1-ol
- 34 3-cyclohexyl-2-propyn-1-ol
- 35 *cis*-2-penten-1-bromide
- 36 europium tris[3-(heptafluoropropylhydroxymethylene)-(+)-camphorate]

## Chapter 1

### Introduction

Asymmetric catalysis is an ever-growing field of chemistry that is inherently multidisciplinary with applications in the fragrance<sup>1</sup>, flavouring<sup>1</sup>, agrochemical<sup>2</sup>, and pharmaceutical industries<sup>3</sup>. In 1992, the United States Food and Drug Administration placed stringent regulations on the pharmaceutical industry regarding the use of racemates as drugs<sup>4</sup>. Often, one enantiomer of a chiral pharmaceutical has the desired bioactivity, whereas the other enantiomer is inactive or toxic. Although the use of racemic drugs is still allowed, both enantiomers of any prospective agent must undergo full toxicological testing, leading to increased time and cost of development. One widely known example of why these restrictions were put in place is thalidomide, (*R,S*)-2-(2,6-dioxopiperidin-3-yl)-1*H*-isoindole-1,3-(2*H*)-dione (Figure 1-1), where one enantiomer, (*R*)-thalidomide, is an active sedative, and the other, (*S*)-thalidomide is a teratogen<sup>5</sup>. Racemic thalidomide had been prescribed as a sedative for pregnant women during the mid- to late-1950s, before the teratogenic effects were known. Note, however that the use of enantiopure (*R*)-thalidomide is not viable, as racemization occurs *in vivo*. Ketamine ((*R,S*)-2-(2-chlorophenyl)-2-methylamino-cyclohexan-1-one) is an example where both enantiomers of the compound are bioactive, but to different degrees.

The *S*-enantiomer (Figure 1-1) is on the order of four times more active than the *R*-enantiomer when binding to NDMA receptor sites in the brain<sup>6</sup>. In this case, *S*-ketamine is preferred over the racemate in the treatment of pain in cancer patients. Such differences in biological activity between enantiomers are the major driving force behind development of asymmetric synthesis in both industrial and academic laboratories<sup>7</sup>.

Available methods to prepare enantiomerically enriched compounds include chirality transfer reactions, resolution of racemic compounds, transformation of naturally occurring chiral compounds, and enantioselective catalysis<sup>7</sup>. Asymmetric catalysis is one of the most efficient methods to amplify chirality. More specifically, a small amount of homochiral catalyst produces many equivalents of near homochiral product. Catalysis also forms less waste and byproducts than stoichiometric large-scale industrial chemistry, and its increased use will improve the atom-economy of current and future industrial transformations<sup>8</sup>.

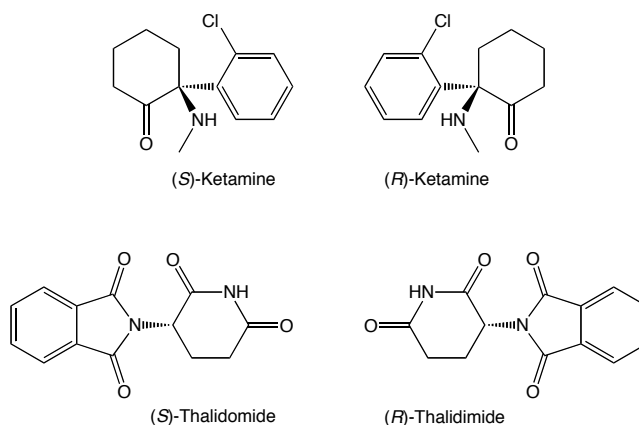


**Figure 1-1:** Enantiomers of Thalidomide and Ketamine.



Asymmetric catalysis is widely utilized to prepare natural products. One example among many is the palladium catalyzed diyne cyclization step in the total synthesis of (+)-streptazolin<sup>9</sup>. (+)-Streptazolin is a lipophilic antibiotic, first isolated from *Streptomyces viridochromogenes*<sup>10</sup>, and is noted for containing a naturally occurring internal urethane moiety in the tricyclic skeleton. The (+)-streptazolin derivative 3,9-dihydrostreptazolin<sup>10</sup> and certain Diels-Alder adducts<sup>11</sup>, such as with naphthoquinones show excellent antimicrobial and cytotoxic activity. Several studies have been carried out on the total synthesis of (+)-streptazolin, and Trost's use of Pd catalysis remains a very elegant synthesis of (+)-streptazolin with enantioselective control.

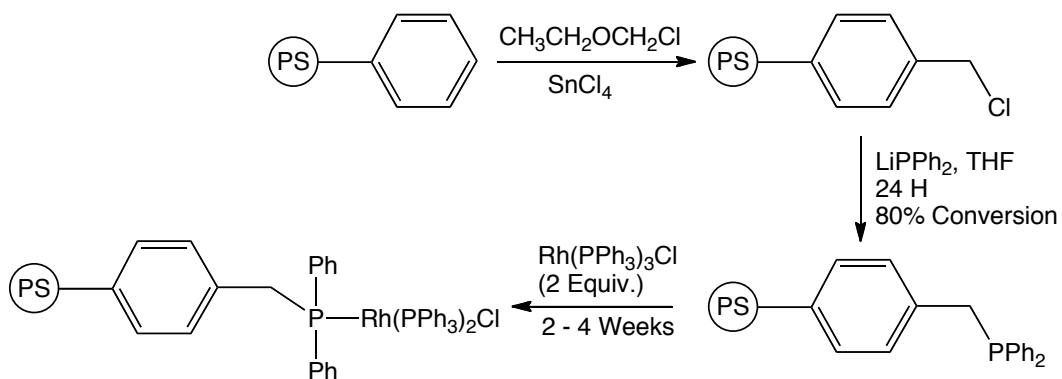
There are, however, disadvantages to the utilization of asymmetric catalysis via transition metal chemistry. For example, catalysts used are typically air sensitive, expensive, and toxic. Also, and often overlooked, the cost of the chiral ligand(s) can be more substantial than the metal centre itself<sup>12</sup>. Further, any toxic metals and ligands contained in the catalyst must be completely removed from the products in order to adhere to health and safety standards. Regulations for the pharmaceutical industry limit the amount of allowable residual metal impurities to less than 10 ppm<sup>13</sup>, thus catalyst residue removal will add cost and development time to drug production and discovery.

The immobilization of homogeneous catalysts, with the aims of easy isolation and reusability, is a logical step towards reducing the cost of enantioselective catalysis. Heterogeneous catalysis offers ease of catalyst separation, less product contamination, and adds the potential for catalyst reuse. Homogeneous catalysis, however, offers the ability to study the reaction on a molecular level, and it typically allows for ready variation of ligand structure, leading to rapid catalyst screening and development. Various methods of catalyst immobilization are documented in recent review articles<sup>14, 15</sup>, and a detailed survey is beyond the scope of this chapter. The interested reader is directed towards reviews on the following common methods of immobilization: non-covalent tethering<sup>15</sup>, electrostatic interactions<sup>16</sup>, biphasic or ionic-liquid systems<sup>17</sup>, encapsulation<sup>18</sup>, metal-organic frameworks<sup>19</sup> and covalent tethering<sup>12</sup>. Rh[diphosphine]<sup>+</sup> compounds, specifically, have been immobilized through interactions with ion exchange resins<sup>20</sup>, direct attachment of diphosphine ligands to PS-PEG copolymers<sup>21</sup>, copolymerization of isopropenylphenyl diphosphine-Rh compounds with ethyleneglycol dimethacrylate<sup>22</sup>, and grafting ligands onto silica supports<sup>23</sup>. Methods that have been developed to covalently link catalysts and supports include radical copolymerization of modified ligands and vinyl arenes<sup>24</sup>, copolymerization between amines and isocyanates<sup>25</sup>, grafting of modified chiral ligands onto polymeric resins<sup>26</sup>, and metal-organic frameworks<sup>19</sup>.

Polymerizable functional groups are often incorporated into ligands, such as vinyl arenes are in  $R_2P$ -(vinyl arene) that are radically co-polymerized with styrene and various linkers such as divinyl benzenes, or ROMP (ring opening metathesis polymerization) active functionalities such as norbornene groups<sup>27</sup>. Such functionalized ligands must often be polymerized before coordination to the metal, as the presence of the metal impedes the polymerization. Although Buchmeiser and others have carried out ROMP with certain metal containing monomers (MCMs)<sup>27, 28</sup>, the common practice is to metallate after polymerization of the ligand<sup>29</sup>. Metallation is attempted by reacting a common metal precursor with the polymerized ligand. The extent of metallation, or the number of occupied ligand sites after reaction with the metal precursor, is often low (17-65%), and is likely limited by mass transport of the precursor to the free ligand sites<sup>30</sup>, resulting in low catalyst loadings and wasted ligand. Consequently, an excess of metal precursors as well as reaction time are used, increasing both the time required to prepare a catalyst and the amount of waste generated.

In a seminal example, Grubbs reported in 1971 the first successful immobilized polyphosphine-rhodium hydrogenation catalyst<sup>31</sup> (Scheme 1-1). After functionalizing the polymer by electrophilic chloromethylation<sup>32</sup>, 80% of the benzyl chlorides were then replaced by reaction with lithiodiphenylphosphine. The immobilized ligand was then exposed to a

two-fold excess of tris(triphenylphosphine)chlororhodium(I) over four weeks. Elemental analysis indicated that only 17% of the available phosphines had been metallated. Although the immobilized catalyst was successfully reused 10 times at after maximum activity (400 turnovers) was observed for the hydrogenation of cyclohexene in benzene. However, the excess reagents required during preparation and poor overall yield of supported catalyst make this methodology impractical.



**Scheme 1-1:** Wilkinson's catalyst supported on polystyrene beads.

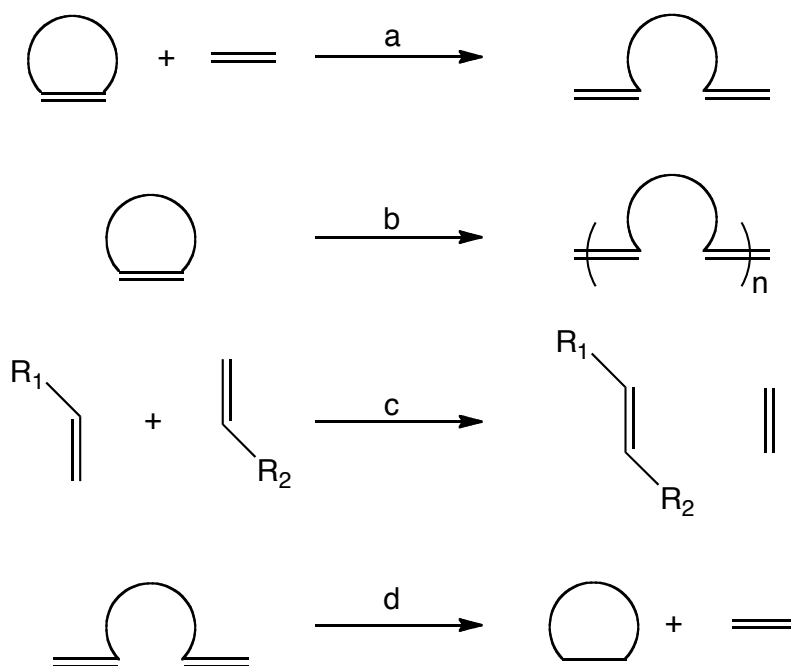
A more direct methodology to prepare polymerized homogeneous catalysts is to include the metal during polymerization, through the utilization of a MCM with ligands that contain a polymerizable unit. MCM's have been utilized to incorporate catalysts in polymers by both ROMP<sup>27, 28</sup> and by radical polymerization<sup>33</sup>. This approach also provides the ability to more directly compare the activities between homogeneous and heterogeneous systems. For example, Kroll<sup>28</sup> and Abd-El-Aziz<sup>27</sup> reported the grafting of a norbornene unit onto terpyridine and benzene, or toluene

ligands respectively. Norbornene was chosen as it contains a highly strained double bond that is reactive to ROMP.<sup>34</sup> Through grafting norbornene functional groups onto ligands, researchers hoped to, and succeeded in, utilizing the characteristic ROMP behaviour of norbornene for preparation of supported catalysts.

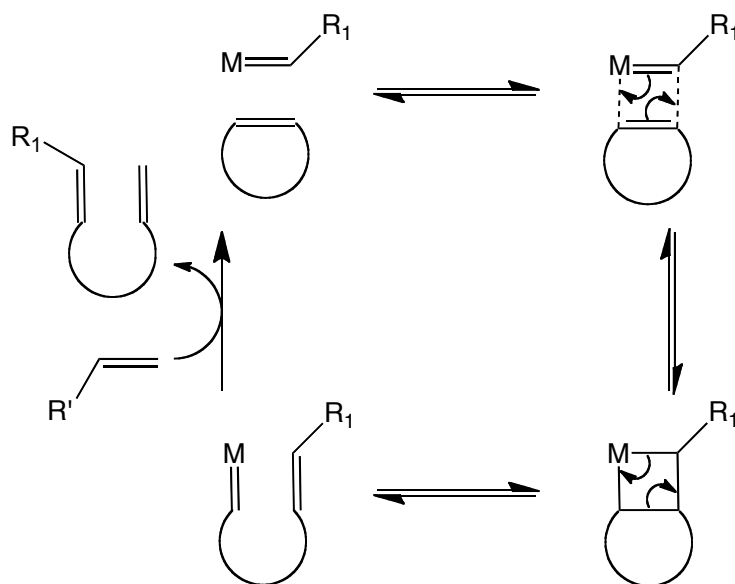
The majority of the published research on immobilization of homogeneous catalysts has been directed towards the development of hydrogenation catalysts. The number of published papers on the immobilization of catalysts capable of different coupling reactions is relatively small. The following section consists of an introduction to metathesis, and the methods used to immobilize metathesis catalysts.

Olefin metathesis is the skeletal rearrangement of a pair of alkenes through redistribution of the groups at the ends of carbon-carbon double bonds.<sup>35, 36</sup> Olefin metathesis can be carried out in an enantioselective manner<sup>37</sup>, and it can be carried out with multiple modes of operation. The common modes are ROMP<sup>38</sup>, ring-closing metathesis<sup>39</sup> (RCM), and cross metathesis<sup>40</sup> (CM). Ring opening metathesis (Scheme 1-2a) is a reaction primarily driven by ring strain, wherein cyclic olefins react with a metal alkylidene to form a metallacyclobutane intermediate, as shown in Scheme 1-3. This metallacyclobutane opens to generate a new metal alkylidene with a pendant olefin; the metal alkylidene then reacts with a free olefin (in this example ethylene,  $R_1 = H$ ) in the same manner to generate a diene.

ROMP (Scheme 1-2b) is very similar to ROM. During ROMP, the propagating metal alkylidene reacts with another cyclic olefin to generate a polymer. Cross metathesis (Scheme 1-2c) involves the transalkyldination of two terminal alkenes, through the initial reaction of one terminal alkene with the metathesis catalyst to generate a new metal-alkylidene, and further reactions with another terminal alkene, along with the loss of ethylene. Ring-closing metathesis (RCM) is the reverse of ROM, and involves the formation, and subsequent collapse of a metallacyclobutane as described above between a terminal olefin and catalyst. The newly generated metal-alkylidene has a pendant alkene group that can insert as previously described, leading to a newly formed cyclic olefin. Figure 1-2 shows some of the most common commercially available metathesis catalysts.



**Scheme 1-2:** Common operation modes of olefin metathesis. (a) Ring-Opening Metathesis (ROM), (b) Ring-Opening Metathesis Polymerization (ROMP), (c) Cross Metathesis (CM), (d) Ring-Closing Metathesis (RCM).



**Scheme 1-3:** Formation and collapse of the metallacyclobutane intermediate during metathesis catalysis.

The ruthenium catalysts **1** and **2** are commonly known as Grubbs' first<sup>41</sup> and second<sup>42</sup> generation catalysts, for their order of discovery. **3** is known as the Hoveyda-Grubbs second generation catalyst, and was prepared by reaction between Grubbs 2<sup>nd</sup> generation catalyst and a styrenyl ether in the presence of cuprous chloride<sup>43</sup>. The Grubbs', and Hoveyda-Grubbs' catalyst operates in the presence of alcohols, carboxylic acids and aldehydes<sup>44</sup>, but do not function in the presence of amines<sup>45</sup> and free phosphines<sup>46</sup>. The opposite is true for the molybdenum containing catalyst **4**<sup>47</sup>, developed independently by Schrock in 1990<sup>48</sup>. Grubbs' catalysts are air stable, and tolerant of a wider variety of functional groups, whereas Schrock metathesis catalysts are air-sensitive and less tolerant to different functional groups. Both systems are active and selective towards the different modes of metathesis, allowing for a wide scope of reactions.



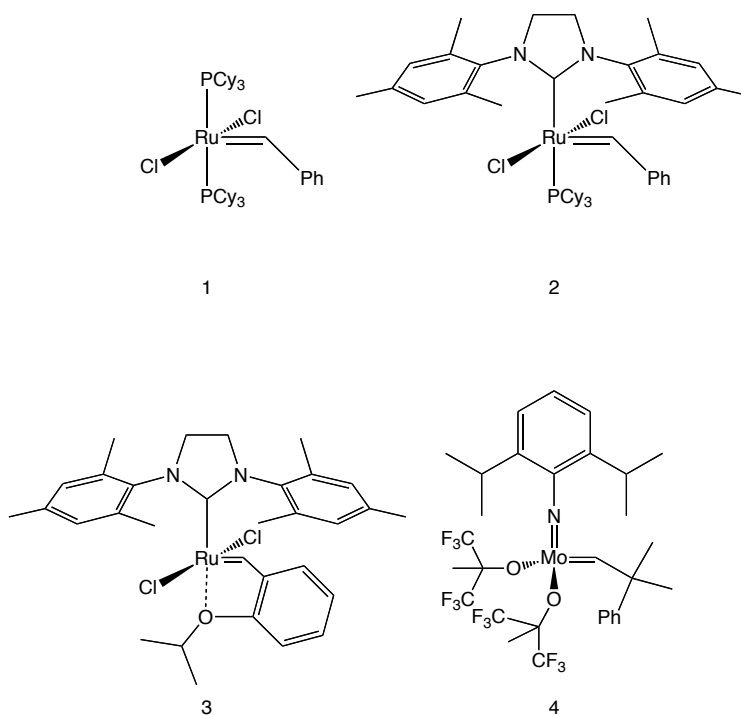
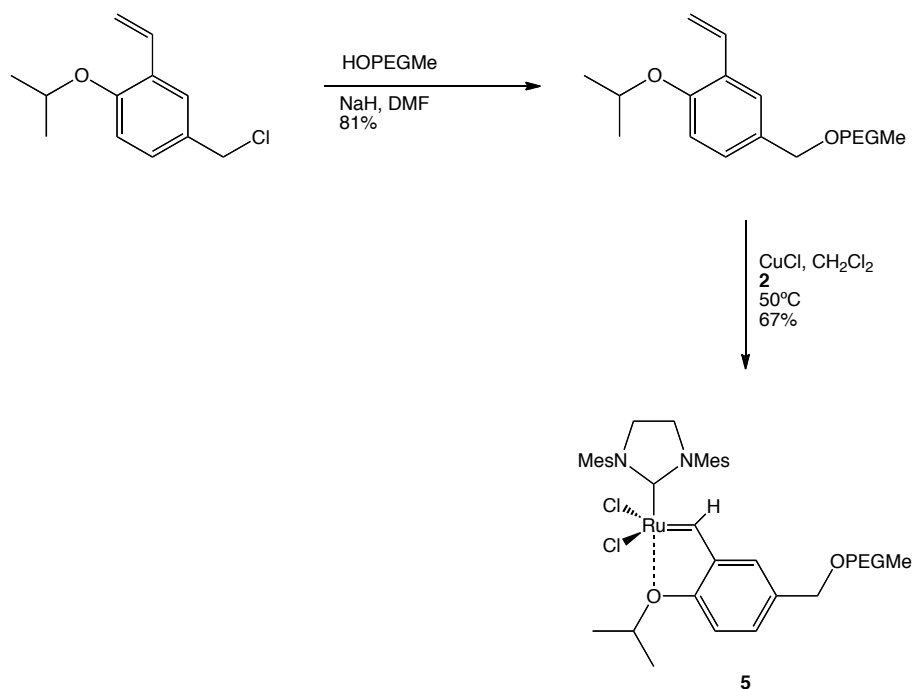


**Figure 1-2:** Common, commercially available olefin metathesis catalysts.

Zaman et al. supported the Hoveyda-Grubbs 2<sup>nd</sup> generation catalyst, **3**, by alkylidene exchange, through reaction between **3** and an isopropoxystyrene-modified polyethyleneglycol-resin, to give a PEG-supported catalyst **5** shown in Scheme 1-4. A study with <sup>1</sup>H NMR spectroscopy showed that the chemical environment of the ruthenium centre in the supported catalyst was similar to that of **3**, specifically, the chemical shift of the benzylidene proton in the supported catalyst was  $\delta = 16.5$  ppm, whereas in **3** it is  $\delta = \sim 16.3$  ppm.<sup>49</sup> The initial activity of the supported catalyst towards RCM of the benchmark substrate N-tosyldiallylamine (**6**) was equivalent to that of the homogeneous catalyst **3**. The supported catalyst was reused 5 times, but the activity had dropped

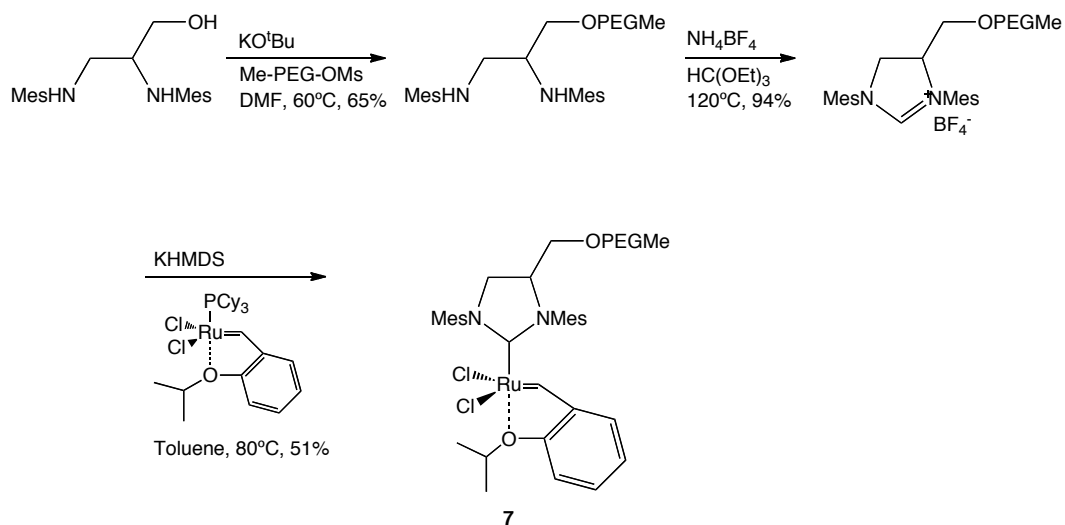
by ~10% in the fifth run. The supported metathesis catalyst was air stable, and was removed from the reaction mixture for reuse by precipitation or water-extraction. The water-solubility of this PEG-bound catalyst and general air-stability are very promising.



**Scheme 1-4:** Preparation of PEG-supported second generation Hoveyda-Grubbs metathesis catalyst (**5**).

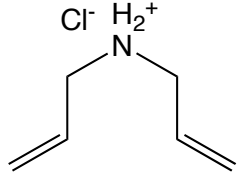
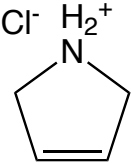
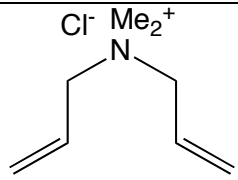
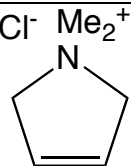
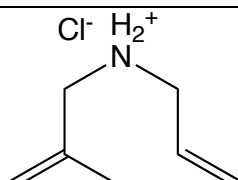
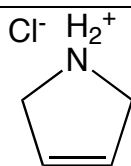
Grubbs-type metathesis catalysts have also been tethered by bonding the N-heterocyclic carbene (NHC) ligand<sup>50</sup> to the support. Specifically, the phosphine-free catalyst, **7**, was anchored through linkage of the NHC ligand to PEG, as shown in Scheme 1-5, and was capable of RCM reactions with water-soluble  $\alpha,\omega$ -dienes in aqueous media. Table 1-1 shows a general scope of the reaction; it is seen that RCM is most

successful on the least sterically hindered  $\alpha,\omega$ -dienes. Metathesis reactions in water are generally difficult to accomplish because ruthenium-methylidenes are unstable under aqueous conditions.<sup>51</sup> While **7** was capable of metathesis reactions on water-soluble substrates, there were no attempts to recover or reuse the supported catalyst.



**Scheme 1-5:** Preparation of PEG-linked NHC ligand, and reaction with Hoveyda-Grubbs 1st generation catalyst to form supported metathesis catalyst **7**.

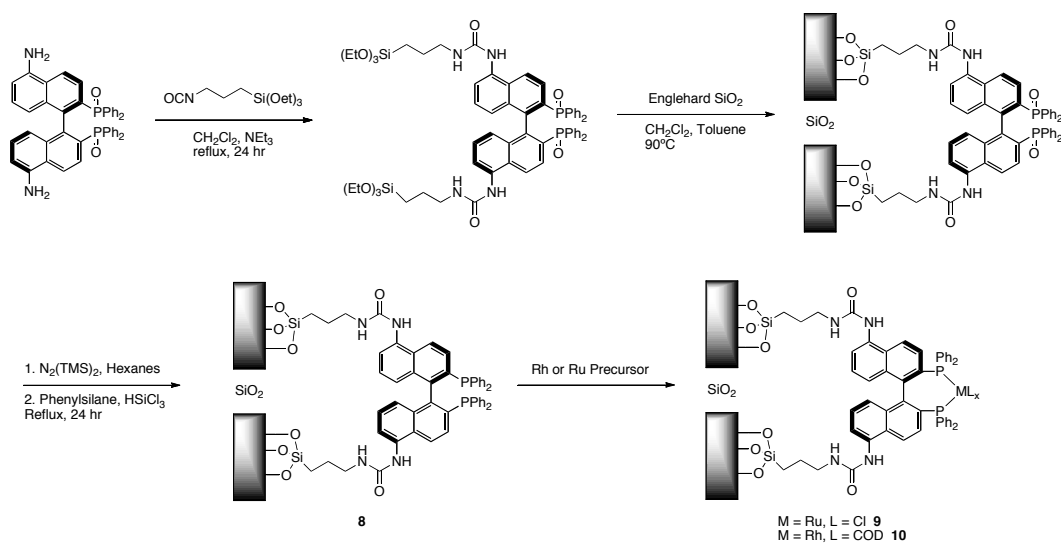
**Table 1-1:** RCM reactions in H<sub>2</sub>O at room temperature using supported catalyst 7.

Substrate	Product	Sub : Cat	Yield (%)	Time (h)
		20 : 1	67	36
		20 : 1	5	24
		20 : 1	42	24

The following section will focus on the immobilization of rhodium-BINAP catalysts, ([Rh(BINAP)]<sup>+</sup>). [Rh(BINAP)]<sup>+</sup>, the active catalyst species, is capable of many different reactions, including hydrogenation<sup>52</sup>, hydroboration<sup>53</sup>, hydroformylation<sup>54</sup>, cycloisomerization reactions<sup>55</sup>, and the isomerization of allylic alcohols<sup>56</sup>.

Recently, the van Koten group synthesized immobilized Rh- and Ru-BINAP complexes on silica as catalysts for asymmetric hydrogenation<sup>57</sup>. The immobilized catalysts were prepared by covalent attachment of a 3,3'-triethoxysilylpropyl-1-ureyl-modified BINAP-dioxide.

As shown in Scheme 1-6 this ligand was prepared in four steps from commercially available BINAP. The ligand was reacted with Engerhard SiO<sub>2</sub> via displacement of ethoxy groups on the ureyl linking groups. The remaining free silanol groups were capped with hexamethyldisilazane, and phosphine oxides were reduced by reaction with trichlorosilane in phenylsilane yielding the supported ligand **8**. The Ru- and Rh-precursors, [RuCl<sub>2</sub>(benzene)]<sub>2</sub> and [Rh(COD)]<sub>2</sub>BF<sub>4</sub>, were reacted with **8** to generate the supported catalysts **9** and **10**, respectively.

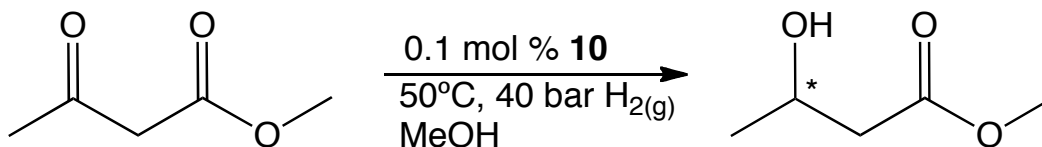


**Scheme 1-6:** Synthesis of an immobilized BINAP-based ligand on silica support.

Supported catalyst **9** was prepared for the hydrogenation of  $\beta$ -ketoesters and enamides, catalyst **10** was prepared solely for the hydrogenation of enamides. The Ru-BINAP catalyst **9** was used for five reuse cycles without loss in yield or *ee* for the hydrogenation of

methylacetoacetate, as shown in Table 1-2. Comparably, **9** was also capable of the hydrogenation of enamide substrates (*Z*)- $\alpha$ -(acetamido)-cinnamic acid and (*Z*)- $\alpha$ -(acetamido) acrylic acid with complete conversion and *ee* of 85 and 72 % respectively, although with higher loadings of Ru (2 mol %). The Rh-BINAP catalyst **10** was also capable of the asymmetric hydrogenation of the enamide substrates, with complete conversion, and *ee*'s of 85 and 60 %, respectively. Although the *ee* is lower for the acrylic acid in the rhodium case, the reaction is carried out with a higher loading of substrate, at 150 equiv (0.6 mol% Rh) compared to the 50 equiv in the ruthenium case. Reuse was attempted for the hydrogenation of the cinnamic acid substrate, the first attempted run had poor yield (56 %), with no *ee*. The failure to reuse the catalyst was attributed to catalyst decomposition due to oxidation. No data was given regarding metal contaminants in the products.

**Table 1-2:** Hydrogenation of methylacetoacetate using **10**.

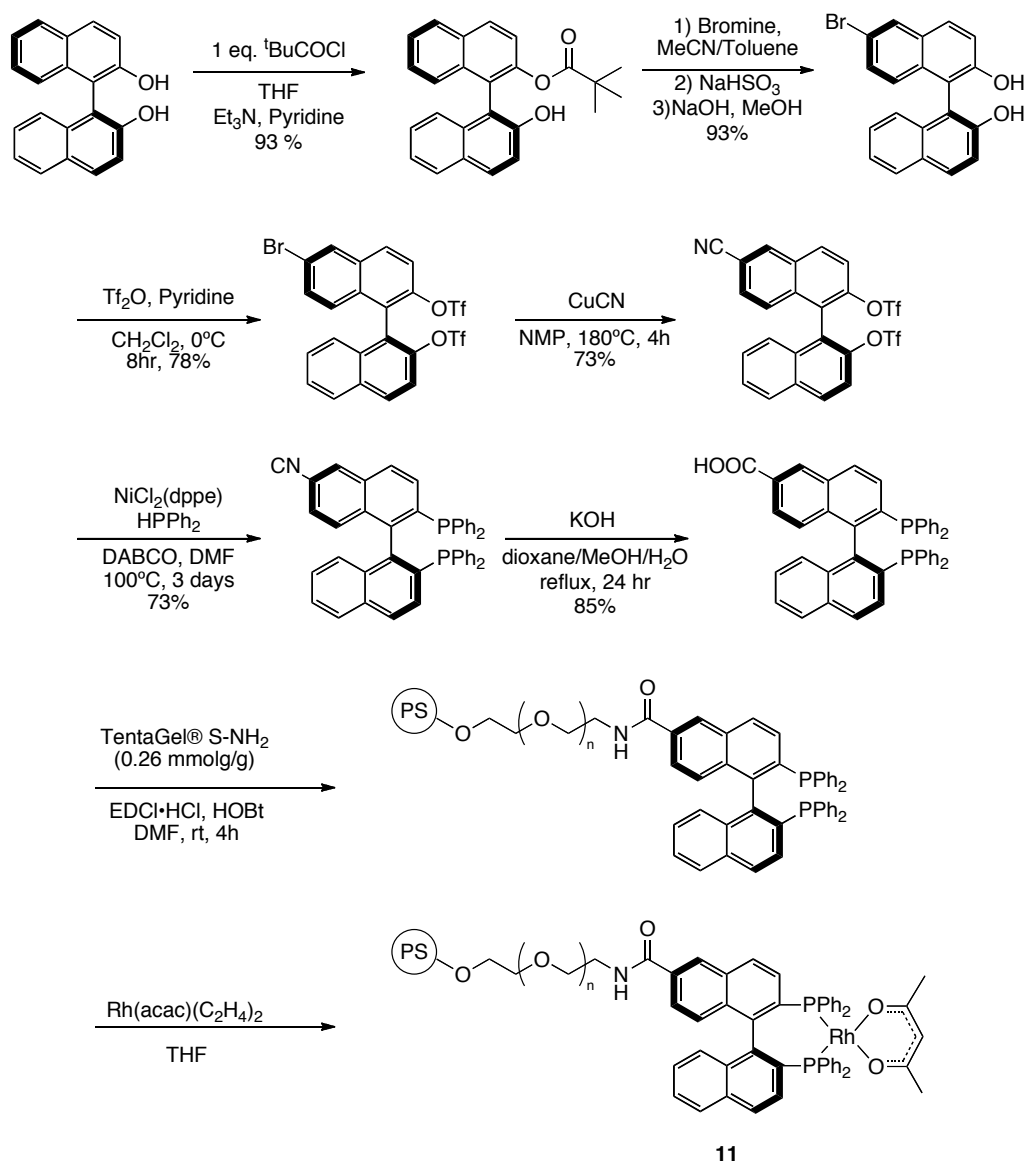


Run	Yield (%) <sup>a</sup>	<i>ee</i> <sup>b</sup>
1	100	>99
2	100	>99
3	100	>99
4	100	>99
5	100	>99
6	100	>99

<sup>a</sup>Yield determined by <sup>1</sup>H NMR spectroscopy and GC. <sup>b</sup>*ee* determined by chiral GC.

Otomaru *et al.* reported the development of an amphiphilic resin-supported Rh-(*S*)-BINAP catalyst for the asymmetric 1,4-addition of phenylboronic acid under aqueous conditions. The supported ligand was prepared from a mono-substituted BINAP carboxylic acid which was synthesized from optically pure BINOL in six steps (Scheme 1-7), utilizing a method for mono-brominated BINOL as devised by Cai *et al.*<sup>58</sup> The amide condensation between the mono-substituted BINAP carboxylic acid and the PS-PEG resin (TentaGel® S-NH<sub>2</sub>, 0.26 mmol/g NH<sub>2</sub>) was carried out in the presence of 1-(3-dimethylaminopropyl)-3-ethylcarbodiimide hydrochloride (EDCI) and 1-hydroxybenzotriazole hydrate (HOBt) in

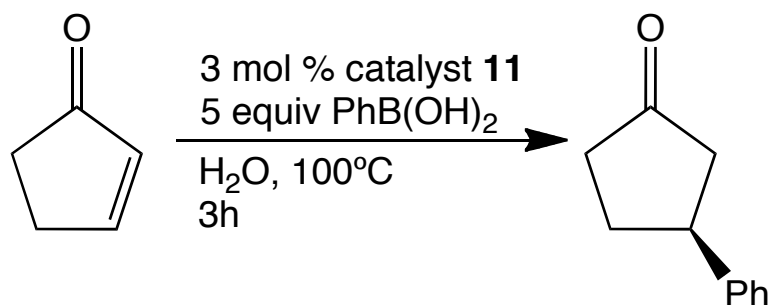
dimethylformamide (DMF). Elemental analysis showed that the content of the BINAP unit in the resin after condensation was 0.17 mmol/g, showing that 65% of the BINAP motif was incorporated into the resin. The resin-supported ligand was then reacted with  $[\text{Rh}(\text{acac})(\text{C}_2\text{H}_4)_2]$  (acac = acetylacetonate) to yield the supported catalyst **11** with quantitative metallation of the BINAP sites.



**Scheme 1-7:** Synthesis of immobilized catalyst **11**.



Catalyst **11** was used for 5 consecutive runs of the reaction shown in Equation 1-1 with little change to the enantioselectivity. Yields obtained were as high as 99 %, with *ee* of 93 – 94 %. To recycle the catalyst, the reaction mixture was extracted with diethyl ether, leaving the active catalyst in the aqueous layer, while removing the products.



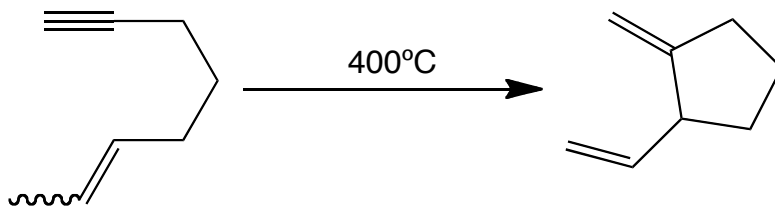
**Equation 1-1:** Rhodium-catalyzed 1,4-addition of phenylboronic acid to 2-cyclopentenone.

High reaction temperatures (100°C) are required as the ancillary ligand acetylacetonate (acac) is strongly coordinating. Removal of acac via either protonation, or by reaction with PhB(OH)<sub>2</sub> is not favoured at lower temperatures. As a result, greater amounts of phenylboronic acid are used compared to the homogeneous case, to compensate for the increased rate of phenylboronic acid hydrolysis, which increases the formation of the side product benzene.<sup>59</sup> Although this is a promising method for recyclable catalysis in water, severe detractors such as the

high-reaction temperatures and excess reagents required make this methodology impractical in comparison with the homogeneous reaction<sup>60</sup>.

A carbon-carbon bond forming reaction that recently has garnered significant attention is the cycloisomerization of 1,n-enynes. The ene reaction (also known as the Alder-ene reaction) was discovered in the 1940s by Alder<sup>61</sup>, and is the addition of an olefin with an allylic proton to an unsaturated carbon-carbon bond. The thermal cycloisomerization of 1,6-enynes was discovered in 1962 by Huntsman *et al.*<sup>62</sup> where neat 6-octen-1-yne was heated at 400°C yielding a cyclic 1,4-diene (Equation 1-2). Thermal cycloisomerizations of enyne substrates were prevalent in literature until the 1980s,<sup>63, 64</sup> but the elevated temperatures required to overcome the high activation energy barriers, combined with the limited scope of substrates that are compatible with this reaction<sup>65</sup> resulted in the stagnation of the field. The discovery by the Trost group in 1984 of a Pd-catalyzed intramolecular Alder-ene reaction<sup>66</sup> rejuvenated the field. Extensive studies into catalytic systems have expanded the range of metals that catalyze the cycloisomerization of 1,n-enynes to include platinum<sup>67</sup>, nickel<sup>68</sup>, gold<sup>69</sup>, silver<sup>70</sup>, ruthenium<sup>71</sup>, and iridium<sup>72</sup>. Asymmetric cycloisomerizations that utilize chiral catalysts have been reported relatively recently. Of particular interest among these reactions is the rhodium-catalyzed cycloisomerization of 1,6-enynes<sup>55</sup>, because of the

excellent enantiomeric excess (*ee*) afforded by the process and because of the wide scope of substrates that are compatible with rhodium catalysts.

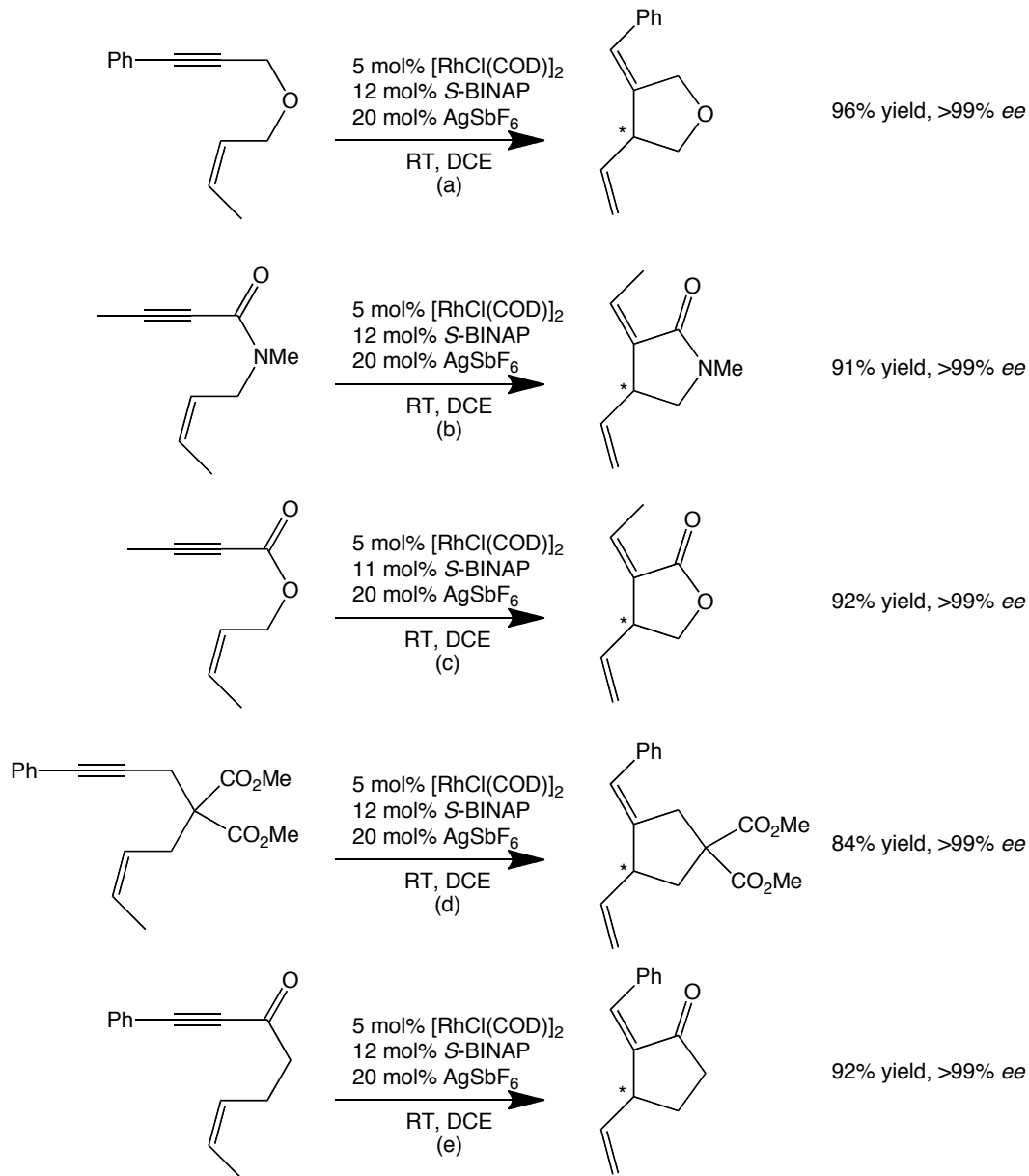


**Equation 1-2.** The thermal cycloisomerization of 6-octen-1-yne at 400°C

The rhodium-catalyzed asymmetric isomerization of 1,6-enyne substrates was initially reported in 2000 by Xumu Zhang *et al*<sup>73</sup>. In this initial report, the catalytically active cationic species  $[\text{Rh}(\text{diphosphine})(\text{s})_2]^+$ , where s = substrate or solvent, was generated *in situ* from reaction between  $[\text{RhCl}(\text{diphosphine})]_2$  and 2 equivalents (equiv)  $\text{AgSbF}_6$  in 1,2-dichloroethane.  $[\text{RhCl}(\text{BINAP})]_2$  was initially reported to be an ineffective catalyst precursor for the cycloisomerization. The Zhang group later reported that  $[\text{Rh}(\text{BINAP})]^+$  was a more active system in the cycloisomerization of 1,6-enynes when the catalyst was prepared *in situ* from the moderately air stable Rh precursor  $[(\text{COD})\text{RhCl}]_2$  (COD = 1,5-cyclooctadiene)<sup>74</sup>. This catalyst system, always prepared *in situ*, operates effectively in the presence of a wide variety of functionalities and is utilized in the synthesis of natural products and pharmaceuticals. It is an elegant method to produce chiral carbo- and heterocycles with very high *ee*, often greater than 99%. This system has been utilized to produce different

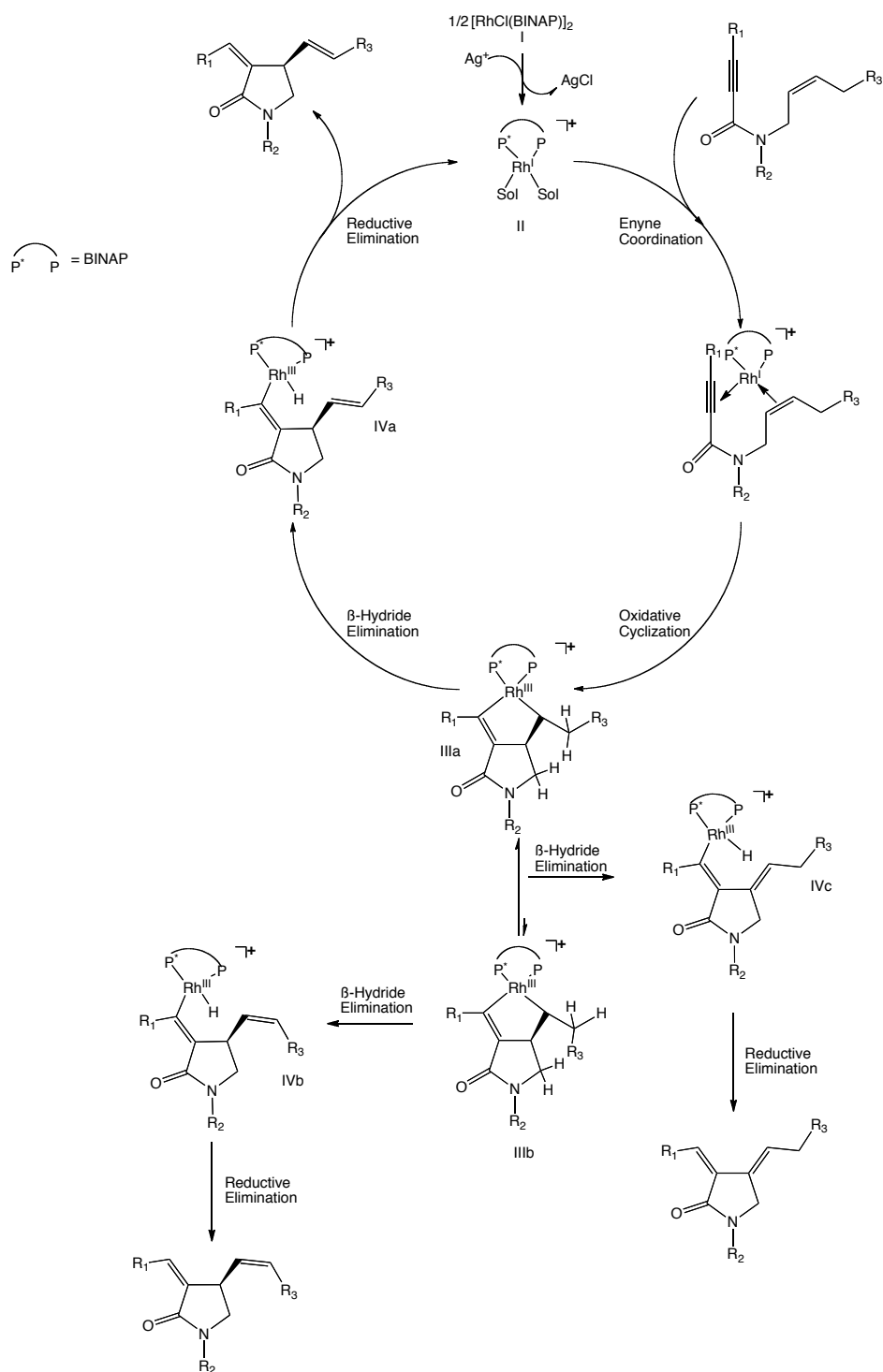
chiral products including tetrahydrofurans<sup>74, 75</sup> (Equation 1-3a), lactams<sup>76, 77</sup> (Equation 1-3b), lactones<sup>78, 79</sup> (Equation 1-3c), cyclopentanes<sup>76</sup> (Equation 1-3d) and cyclopentanones<sup>76</sup> (Equation 1-3e). Natural products that have been synthesized with this methodology include (-)-blastmycinolactol<sup>77</sup>, (+)-pilocarpene<sup>78</sup>, and platensimycin<sup>79</sup>.

Although the homogeneous system generates most products in very high *ee*, the turnover numbers (TON) are prohibitively low. The reasons why high loadings of Rh, BINAP, and AgSbF<sub>6</sub> are required are not discussed in the literature. We believe that high catalyst loadings and short durations are utilized in an effort to avoid product inhibition and isomerization. Consistent with this assertion is the report by Hashmi *et al.* that increasing the temperature to 80°C results in the formation of a cyclic 1,3-diene, rather than the desired 1,4-diene.<sup>80</sup>



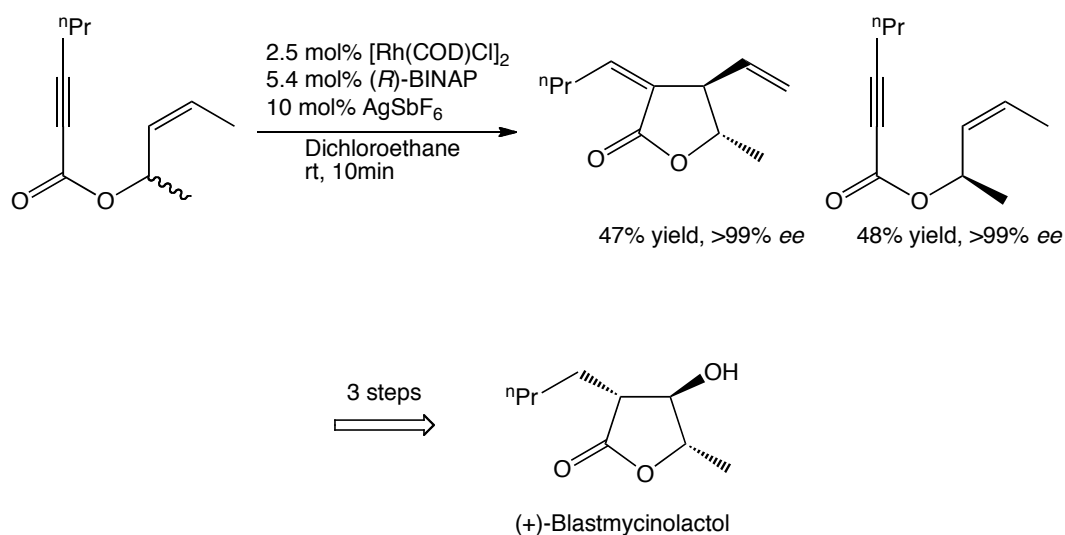
**Equation 1-3:** Examples of the rhodium-BINAP catalyzed intramolecular cycloisomerization of enynes to produce chiral a) chiral tetrahydrofurans<sup>75</sup>, b) lactams<sup>81</sup>, c) lactones<sup>77</sup>, d) cyclopentanes<sup>76</sup>, and e) cyclopentanones<sup>76</sup>.

The mechanism of the cycloisomerization proposed by Zhang *et al.* is shown in Scheme 1-8<sup>81</sup>. Conversion of the inactive chloro-bridged dimer (**I**) *in situ* to the active cationic disolvento species  $[\text{Rh}(\text{BINAP})(\text{sol})_2]^+$  (**II**) is achieved through abstraction of the bridging chlorides with a silver(I) source that contains a weakly-coordinating anion, such as  $\text{SbF}_6^-$  or  $\text{BF}_4^-$ . Zhang then proposes that the enyne substrate coordinates to the active catalyst **II** yielding the intermediate as shown. This intermediate is then believed to undergo an oxidative cycloisomerization to form a metallacyclopentane (**IIIa**) in one concerted step. This metallacyclopentane can exist as two conformers, labeled **IIIa** and **IIIb** for clarity. Steric interactions and crowding favours the formation of conformer **IIIa**. Subsequent  $\beta$ -hydride elimination leads to the formation of the *E*-alkene and a rhodium-hydride species (**IVa**). C-H reductive elimination from **IVa** generates the product and the active catalyst **II**.  $\beta$ -Hydride elimination within **IIIb** would lead to the formation of the *Z*-alkene (**IVb**). Subsequent C-H reductive elimination yields the desired 1,4-diene product. It is likely that the desired product is formed due to greater concentrations of **IIIa** than **IIIb**, as this is the favoured conformer due to steric interactions.



**Scheme 1-8:** Proposed mechanism for the intramolecular cycloisomerization of enynes by cationic rhodium-diphosphine species.

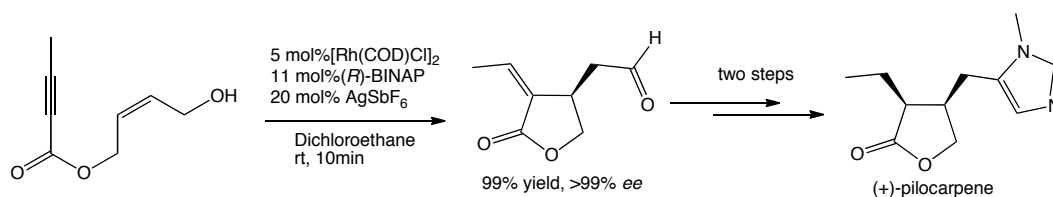
(-)-Blastmycinolactol is a known degradation product of (+)-antimycin, a known antifungal-antibiotic compound isolated from a family of *Streptomyces*. Zhang and coworkers reported a kinetic resolution of enyne esters using the cationic rhodium catalyst  $[\text{Rh}(\text{diphosphine})]^+$  for the asymmetric synthesis of (-)-blastmycinolactol. The process involves the reaction of racemic 1,6-enyne esters via the cycloisomerization coupled with a tandem 1,3-hydrogen shift. The product lactone (Equation 1-4) was produced in 99 % *ee* and 47 % yield, a total of 9.4 turnovers. This yield is particularly remarkable, considering 50% is the highest theoretical yield; in fact, the (*R*)-enriched starting material was obtained in 99 % *ee* and 48 % yield. The product (-)-blastmycinolactol was obtained in three steps after the cycloisomerization reaction.



**Equation 1-4:** Synthesis of (+)-blastmycinolactol through kinetic resolution of racemic enynes.



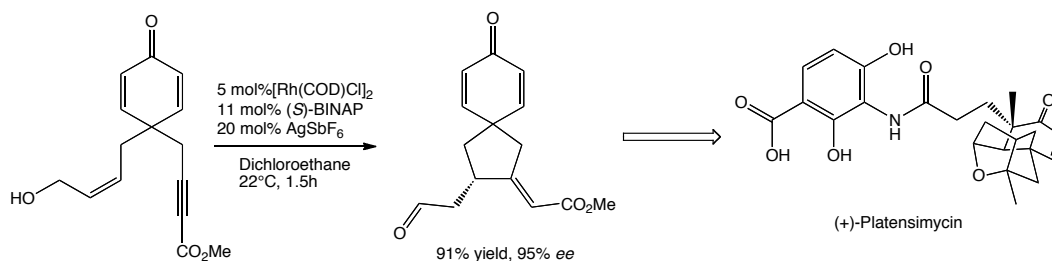
(+)-Pilocarpine is a natural product that contains the  $\alpha$ -methylene- $\gamma$ -butyrolactone moiety, which is a recurring motif in many natural products, including (+)-isopilocarpene, and (+)-isopilosine. Buchi *et al.* had previously synthesized a key intermediate in the synthesis of (+)-pilocarpine, (4*R*)-(Z)-dehydrohomopilopic aldehyde, in 5 steps with 20 % overall yield and 92 % *ee*<sup>82</sup>. Zhang and coworkers used the [Rh(diphosphine)]<sup>+</sup> catalyst system to form the aldehyde in > 99 % *ee* and 99 % yield (Equation 1-5)<sup>78</sup>. This example contains an allylic alcohol which, upon cycloisomerization undergoes a 1,3-hydrogen shift to form the aldehyde. Such isomerizations are common among [Rh(diphosphine)]<sup>+</sup> catalysts<sup>56</sup>.



**Equation 1-5:** Synthesis of (4*R*)-(Z)-dehydrohomopilopic aldehyde, a precursor in the synthesis of (+)-pilocarpene.

(-)-Platensimycin is a compound with promising antibacterial properties as there is the possibility for treatment of drug-resistant bacteria due to a unique mechanism of action *in vivo*<sup>84</sup>. Nicolaou and coworkers reported the total racemic synthesis of (±)-platensimycin in 2006<sup>83</sup> and, in

2007, reported the asymmetric synthesis of (-)-platensimycin<sup>79</sup>. The asymmetric synthesis reported utilized Zhang-type conditions for the cycloisomerization of an enyne ester forming the targeted spirocycle in 91 % yield and 95 % *ee* (Equation 1-6). (-)-Platensimycin can be obtained from 11 further steps from this spirocycle.

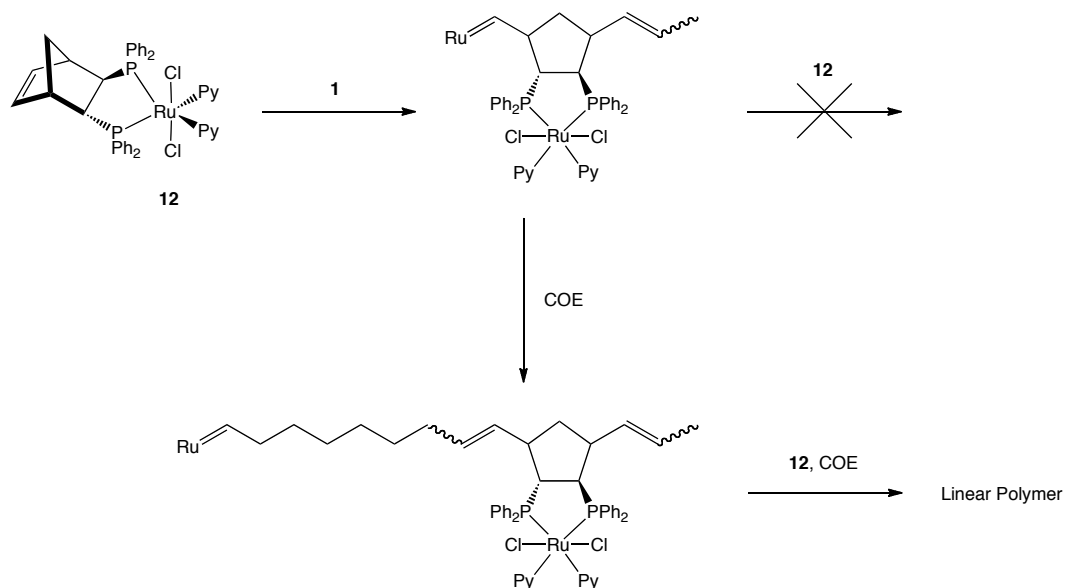


**Equation 1-6:** Asymmetric synthesis of (-)-platensimycin, through formation of a spirocycle intermediate.

The previous examples illustrate the adaptability and versatility of this cycloisomerization.  $[\text{Rh}(\text{BINAP})]^+$  as a catalytic system provides a method to produce carbo- and heterocyclic compounds of varying size with high enantioselectivity and can be used for kinetic resolution of racemic substrates.

As seen in the previous examples, the synthesis of supported catalysts all follow a common route that involves the coordination of a metal precursor to a ligand after it has been covalently attached to support<sup>84</sup>. The Bergens' group is one of the few in the literature to utilize a metal-containing monomer directly in the assembly of a catalyst-organic framework. The Bergens' group utilizes ROMP assembly with the metal-

containing monomer and a spacer monomer *cis*-cyclooctene (COE) to affect an alternating copolymer. The initial work was done with the Ruthenium-Norphos (Norphos = 2,3-bis(diphenylphosphino)-bicyclo[2.2.1]hept-5-ene) compound, **12**, where it was co-polymerized in the presence of COE yielding a linear polymeric catalyst<sup>85</sup>. (Scheme 1-9)



**Scheme 1-9:** Catalyst containing copolymer prepared by Ralph and Akotsi for the asymmetric hydrogenation of ketones<sup>85</sup>.

Co-polymerization was required as polymerization of **12** alone did not occur as the steric hindrance upon one event of metathesis between **1** (Figure 1-1) and **12** was great, and prevented further reaction. Stoichiometric experiments confirmed that the polymerization would not proceed with only **1** and **12** present. Investigations with molecular models support the belief that steric crowding at the propagating ruthenium-alkylidene is too high to react with another molecule of **12**. Thus, the

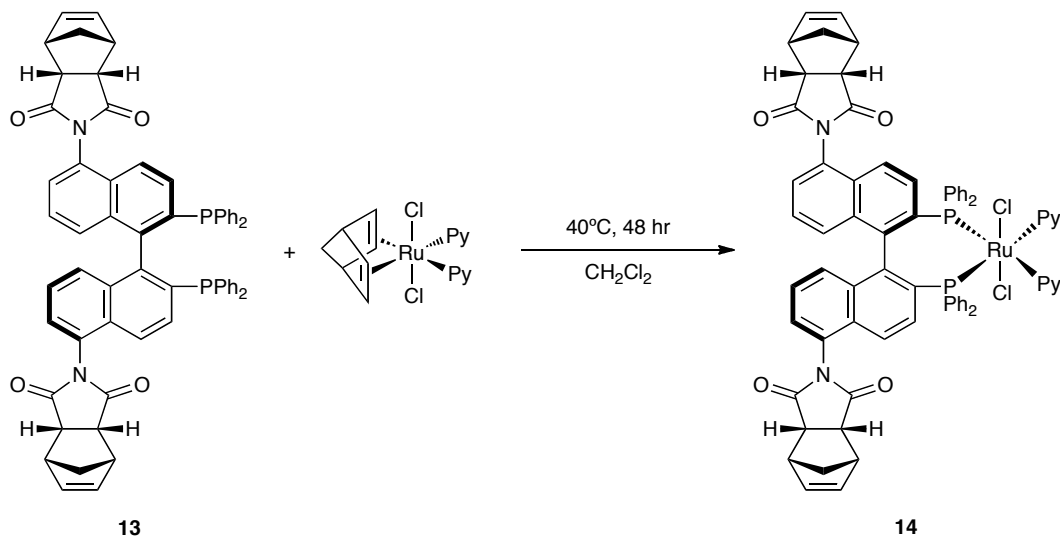
alternating ROMP polymerization with COE as a co-monomer was developed as a means to insert space and overcome the steric hindrance found at the propagating ruthenium-alkylidene. Intrinsically, COE is less reactive to ROMP than Norphos as there is less ring strain in a COE molecule; the energy of ring strain in *cis*-COE is 7.4 kcal/mol<sup>86</sup>, while in norbornene it is 18.8 kcal/mol<sup>87</sup> causing COE to be less reactive towards metathesis. COE would react with the propagating ruthenium-alkylidene after reaction between **1** and **12**; while COE is less reactive it is more sterically favoured to react with the propagating alkylidene, inserting an eight-carbon spacer between the metal-containing monomer and the propagating species. The less hindered alkylidene will then be able to react with one equivalent of the more-reactive **12**, and so on to form a linear alternating polymer.

The Py (Py = pyridine) groups coordinated to the ruthenium were then replaced with (*R,R*)-dpen (dpen = 1,2-diphenylethylenediamine), to generate a Noyori-type hydrogenation catalyst, which was then supported on BaSO<sub>4</sub>. This supported catalyst was then used for the hydrogenation of 1-acetonaphthone for 10 reuses with TON of 450 to 500 per run and 85 % *ee*. When published, this was the highest number of reuse obtained for a polymer-bound asymmetric catalyst with no significant drop in *ee*. This methodology for the preparation of a supported polymer-bound asymmetric catalyst was then adapted to BINAP-based systems (BINAP

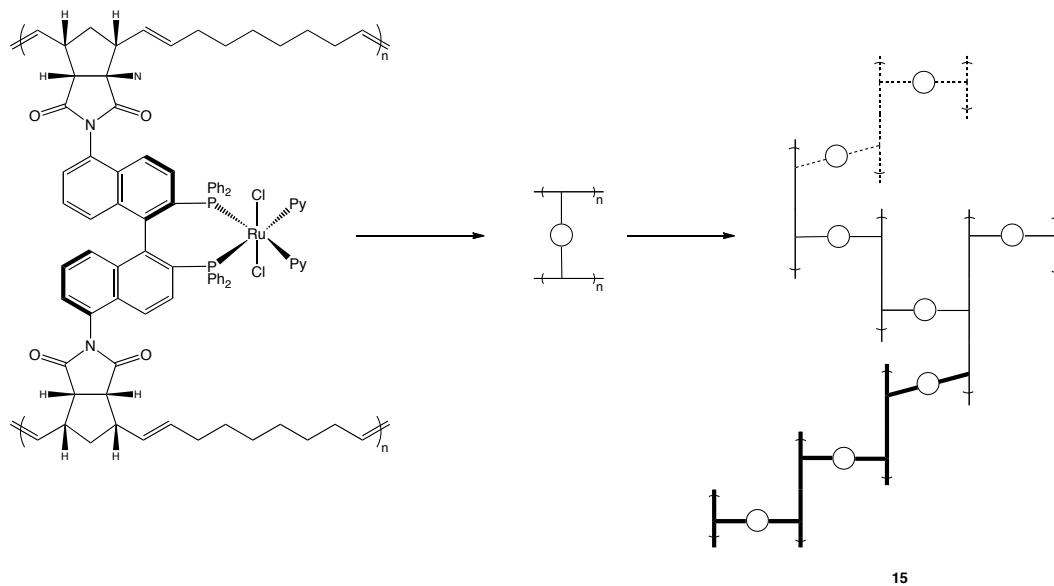
= 2,2'-bis(diphenylphosphino)-1,1'-binaphthyl) through the preparation of (*R*)-5,5'-dinorimido BINAP (**13**). BINAP was chosen for this treatment because it is one of the most widely used ligands in asymmetric catalysis. This ligand also affords higher selectivity and *ee* in the hydrogenation of ketones than does Norphos.

**13** is synthesized from commercially available (*R*)-BINAP in five steps. Through electrophilic substitutions done on BINAP dioxide, the norimido moieties are placed on the 5,5'-positions of the ligand. The Ru-BINAP catalyst precursor, **14**, was synthesized (Equation 1-7) and polymerized in the presence of COE using **1** (Figure 1-1). Each molecule of **13** has two norimido olefin groups, which lead to a cross-linked, three-dimensional catalyst-organic framework upon alternating ROMP-assembly (**15**). This three-dimensional structure of **15** is shown in Scheme 1-10. The three-dimensional structure directly contrasts with the previous linear catalyst-organic framework prepared from the alternating-ROMP of **12**. Again, displacement of the Py ligands with dpen affords a catalyst-organic framework with Noyori-type ruthenium sites. Ralph then used the prepared framework for the hydrogenation of 1'-acetonaphthone for 25 consecutive reuses without loss in activity at 1000 : 1 substrate: catalyst loading without loss of activity or selectivity, affording 100 % conversion with 96 % *ee*. No ruthenium leaching was detected (ICP-MS) in any products from the use of the supported catalyst. This is on record as the

highest number of reuses obtained for a polymeric asymmetric hydrogenation catalyst.



**Equation 1-7:** Synthesis of a ROMP-active Ru-BINAP metal-containing monomer from (*R*)-5,5'-dinorimido-BINAP(**13**).



**Scheme 1-10:** Three-dimensional representation of catalyst-organic framework after alternating copolymerization, **15**, as synthesized by Ralph<sup>88</sup>.

LaRocque and Sullivan both attempted to adapt this ROMP-assembly to prepare immobilized cationic rhodium catalysts for the cycloisomerization of 1,6-enynes. The precursors utilized were  $[\text{Rh}(\text{NBD})_2]\text{BF}_4$  (NBD = norbornadiene) and  $[\text{RhCl}(\text{C}_2\text{H}_4)_2]_2$ , respectively. The catalyst-organic framework prepared by LaRocque is similar in nature to that prepared by Ralph *et al.*, while the framework prepared by Sullivan contains another level of crosslinking due to the  $\mu$ -chloride ligands in the metal-containing monomer. The cycloisomerization of 1,6-enynes attempted by LaRocque were preceded by hydrogenation of the catalyst to liberate norbornene as norbornane. The attempted cycloisomerization reactions occurred in low yields, and catalyst reuse was not accomplished. At best, a yield of 80 % was obtained for the cycloisomerization of enyne substrates, at a catalyst loading of 10 mol % rhodium, an effective TON of 8. It was apparent during catalysis that the catalyst dissolved into the reaction solvent during the first attempted run. It is probable that the leached rhodium species was what performed the reaction. Sullivan prepared a less soluble catalyst than LaRocque. With the inclusion of  $\mu$ -chloride ligands in the monomer,  $\text{AgSbF}_6$  was required as additive. Reactions were run with loadings of 20 : 4 : 1 = substrate : additive : rhodium; twice the TON of the best in the literature. Sullivan successfully reused the catalyst for a total of 148 turnovers; the highest number of

turnovers for this reaction known at the time. The catalyst was, however, plagued by drastic losses of activity over time, most likely due to oxidation of the catalyst.

The goal of my project was to extend the process toward the asymmetric rhodium-catalyzed intramolecular cycloisomerization of 1,6-enynes at higher substrate loadings, and with better reuse. With a high TON immobilized catalyst, reusability, along with the requirement of only using the additive for the first batch reaction would make this more suited for commercial applications. This system would also, in principle, be suitable for a flow-reactor.



## Chapter 2

### Supported Catalyst-Organic Framework for the Asymmetric Cycloisomerization of 1,6-Enynes

As discussed in Chapter 1, a key development in our laboratory is the preparation of the ROMP-active ligand, **13**, shown in Figure 2-1. The polymerized form of this ligand was evaluated with a ruthenium catalyzed asymmetric hydrogenation of 1'-acetonaphthone at 40°C, and it provided over 25 reuses (ketone : Ru = 1000 : 1 per run), with no changes in enantiomeric excess or detectable ruthenium leeching. To date it is the highest number of reuses for an immobilized, polymer-based chiral catalyst. Further, previous students in this laboratory demonstrated that rhodium complexes of **13** show activity towards the cycloisomerization of 1,6-enynes; however, these previous systems suffered from rapid activity losses upon the first reuse. This chapter reports the preparation of an active, reusable supported catalyst-organic framework containing a rhodium complex of **13** for the cycloisomerization of 1,6-enynes.

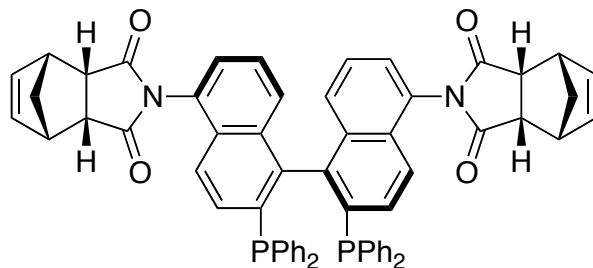


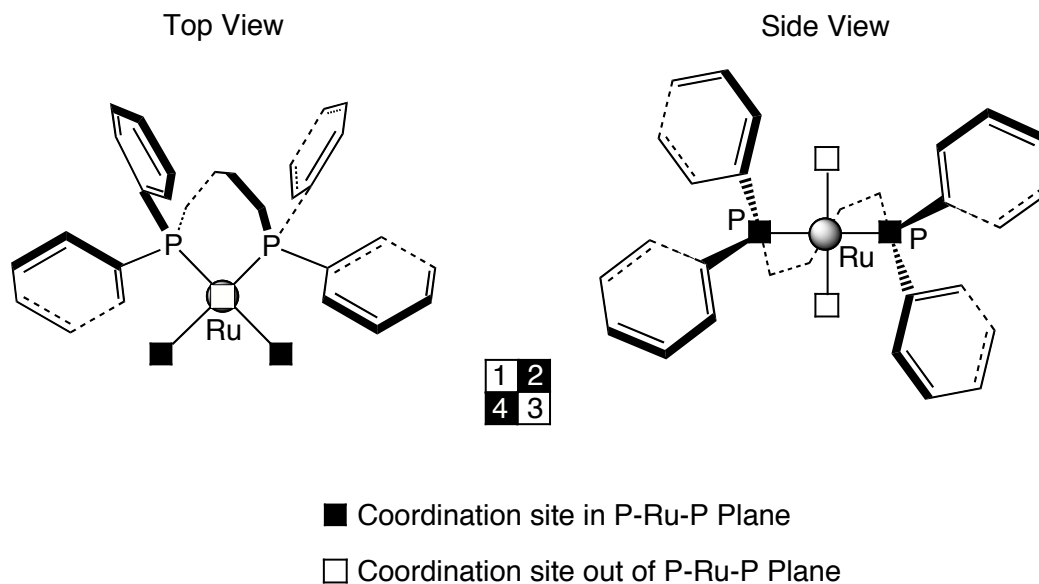
**Figure 2-1:** (*R*)-5,5'-dinorimido BINAP, **13**, a ROMP-active ligand used in the preparation of Catalyst-Organic Frameworks.

## Results and Discussion

### Section A: Synthesis of (*R*)-5,5'-Dinorimido-BINAP (**13**)

BINAP (BINAP = 2,2'-bis(diphenylphosphino)-1,1'-binaphthyl) is one of the most extensively utilized chiral phosphine ligands in enantioselective catalysis<sup>89</sup>. BINAP is extensively utilized because it is not easily oxidized, it is conformationally rigid, and often affords high enantioselectivity. This high enantioselectivity is, in part, a result of  $C_2$ -dissymmetry, at the large projection of the equatorial phenyl rings on phosphorous atoms into the spatial domain of the metal centre. This projection results from the 7-membered ring formed by the coordination of BINAP. Figure 2-2 shows the equatorial phenyl rings of BINAP projecting in a  $C_2$ -dissymmetric array into the spatial domain of the metal centre<sup>90</sup>, forming sterically congested quadrants. These features make BINAP one of the few chiral ligands used in industry<sup>91</sup>. Further discussion on the use and properties of BINAP and related ligands are beyond the scope of this

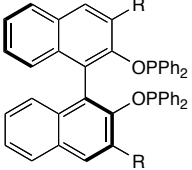
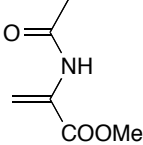
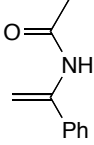
dissertation. The interested reader is directed to several review articles available in the literature.<sup>92, 93</sup>



**Figure 2-2:** Chiral environment of a (*S*)-BINAP-Ru complex as described by Kitamura *et al.*<sup>90</sup>. The binaphthyl skeleton is omitted for clarity

There are several possible avenues to modify BINAP with functional groups that will undergo polymerization. BINAP has been functionalized at the phosphine-aryl groups, and the 3', 4', 5' and 6' positions of the binaphthyl rings<sup>89</sup>. For example, functionalization at the 3,3'-positions results in hindered rotation about the phenyl-phosphorous bond, which can enhance the *ee*. As seen in Table 2-1, Zhang *et al.* showed that substitution at the 3,3'-position of a BINAP phosphinite ligand enhanced the *ee* of several Rh-catalyzed hydrogenations<sup>94</sup>.

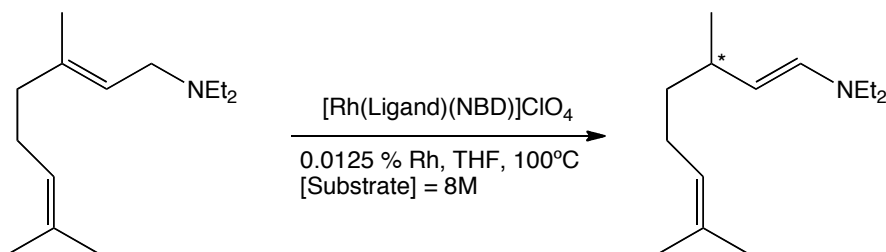
**Table 2-1:** Rh(I)-catalyzed asymmetric hydrogenation of dehydroamino acids using BINAP phosphinite ligands.

R Group	Substrate	Substrate
		
Me	95 % <i>ee</i>	67 % <i>ee</i>
Ph	>99 % <i>ee</i>	94 % <i>ee</i>
H	73 % <i>ee</i>	28 % <i>ee</i>

Reactions were carried out with 1 mol % Rh using the *in situ* generated catalyst from  $[\text{Rh}(\text{COD})_2]\text{PF}_6$  and 1.5 equiv of ligand, at RT under 3 atm  $\text{H}_{2(\text{g})}$ .

More commonly, BINAP is functionalized at the 5,5'-positions, largely because electrophilic aromatic substitution reactions with BINAP dioxide are directed towards the 5,5'-positions. Amine- and other nitrogen containing functional groups at the 5,5'-position generally have a positive effect on selectivity<sup>95</sup>, which is believed to be due to electron donation from the lone-pair electrons on the nitrogen atom to the naphthyl  $\pi$ -system. This was first illustrated by Okano *et al.* using (*R*)-5,5'-diamino BINAP (**16**)<sup>95</sup> in the asymmetric isomerization of N,N-diethyl geranylamine to the corresponding enamine (Table 2-2).

**Table 2-2:** Rh(I)-catalyzed isomerization of N,N-diethyl geranylamine using **5** at 100°C in THF.

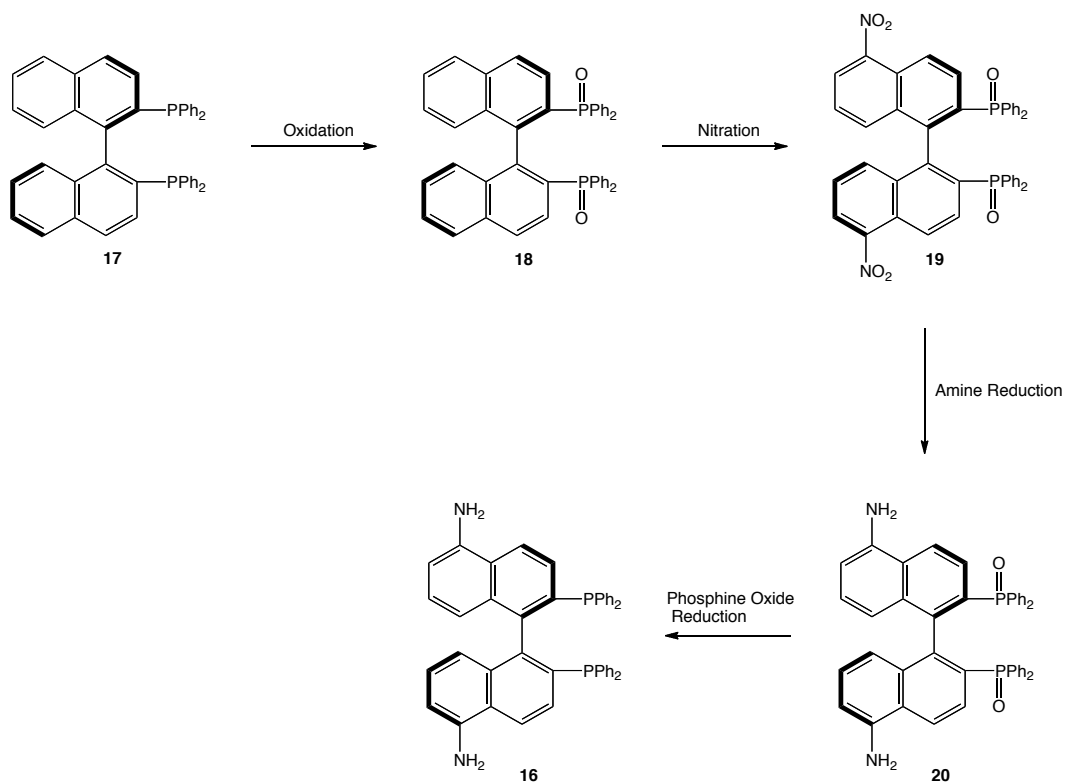


Ligand	% Conversion to Enamine			
	1 Hour	3 Hours	6 Hours	15 Hours
BINAP	3.2	8.6	-	83.0
<b>16</b>	12.3	39.6	66.8	95.9

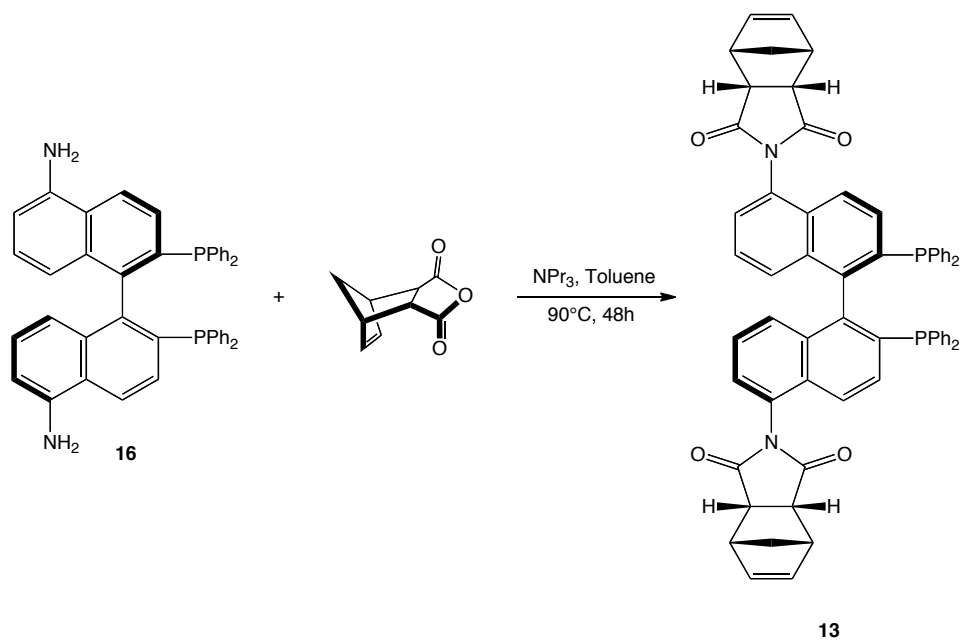
**16** was chosen as a starting point because it is easily prepared, it has demonstrated enhanced selectivity and reactivity in asymmetric catalysis<sup>95, 96</sup> and it has previously been used in the immobilization of BINAP-based catalysts<sup>57</sup>. (*R*)-5,5-diamino BINAP, **16**, was initially synthesized in this group using a procedure similar to Scheme 2-1<sup>95</sup>. Specifically, (*R*)-BINAP (**17**) is treated with hydrogen peroxide to yield (*R*)-BINAP dioxide (**18**). Nitration with acetic anhydride, nitric acid and catalytic sulphuric acid yields (*R*)-5,5'-dinitro BINAP dioxide (**19**). Reduction of the nitro groups produces (*R*)-5,5'-diamino BINAP dioxide (**20**). The original literature procedure for this step called for a stannous chloride reduction in acidic medium. Sullivan found that hydrogenation of **19** over Pd/C is vastly superior to this method, due to its shorter reaction times and

simplified workup<sup>96</sup>. The hydrogenation proceeds under 45 psig (psig = gauge pressure) H<sub>2(g)</sub> at 50°C in 6 h to provide **20** in near quantitative crude yield. Purification by flash chromatography gives pure **20** in 87% yield. The Pd/C used for hydrogenation of the nitro groups is recovered and reused. **20** is then reduced to the free phosphine (**16**) using trichlorosilane/triethylamine in toluene.

Direct attachment of a ROMP-active group to **16** was carried out by condensation between *cis*-5-norbornene-*endo*-2,3-dicarboxylic anhydride and **16**. The *endo*- configuration anhydride was chosen over the *exo*- configuration purely due to the price difference. Condensation of (**16**) with *cis*-5-norbornene-*endo*-2,3-dicarboxylic anhydride gives (*R*)-5,5'-dinorimido-BINAP, henceforth referred to as N-BINAP (**13**), in 75% yield, as shown in Scheme 2-2.



**Scheme 2-1.** Synthesis of (*R*)-5,5'-diamino BINAP (**16**). Synthetic means are described fully in text.



**Scheme 2-2:** Synthesis of ROMP active ligand, (*R*)-5,5'-dinorimido-BINAP (**13**).

The  $^{31}\text{P}$  NMR spectrum of **13**, as seen in Figure 2-4, contains signals from a mixture of distinct diastereomeric rotamers<sup>88</sup>, which are illustrated in Figure 2-3. Specifically it contains two non-classical doublets and two singlets. The diastereomers arise due to hindered rotation around the nitrogen-arene bonds, the rate of which is slow relative to the NMR timescale, resulting in the formation of atropisomers that are differentiated by NMR spectroscopy. Axial chirality as a result atropisomerism has been noted in other aryl imides with sufficiently high barriers to rotation<sup>97</sup>. As seen in Figure 2-3, two atropisomers of **13** are  $C_2$ -dissymmetric ( $R,R,R$  and  $S,R,S$ ), and one is non  $C_2$ -dissymmetric ( $S,R,R$  and the equivalent  $R,R,S$ ). The  $C_2$ -dissymmetric rotamers each have a singlet in the  $^{31}\text{P}$  NMR at  $\delta = -12.9$  and  $\delta = -13.2$  ppm respectively. The non  $C_2$ -dissymmetric atropisomers have one doublet for each phosphorous centre due to the loss of the  $C_2$ -rotation axis, resulting in the inequivalency of the phosphorous centers, leading to phosphorous-phosphorous coupling. This P-P coupling results in the formation of an AB system. Interestingly, one can easily prepare rotamerically pure **13** by heating it in toluene to  $90^\circ\text{C}$ ; resulting in the precipitation of a single  $C_2$ -dissymmetric isomer in near quantitative yields. This allows for the isolation of a single rotamer for use in subsequent experiments. Dissolution of rotamerically purified **13** shows a single signal in the  $^{31}\text{P}$  NMR at  $\delta = -13.2$  ppm, corresponding to one of the  $C_2$ -dissymmetric isomers. Figure 2-5 shows that over time at



room temperature, additional signals for the other rotamers grow into the spectrum indicating that the rotation around the nitrogen-arene bond is slow at room temperature. As expected, the initial signals that grow in (Figure 2-5b) are from the  $(R,R,S)$  and  $(S,R,R)$  non  $C_2$ -dissymmetric atropisomers, followed by the signal from the other  $C_2$ -dissymmetric atropisomer  $(R,R,R)$  or  $(S,R,S)$ , as the non  $C_2$ -dissymmetric isomer is the intermediate between the  $C_2$ -dissymmetric isomers.

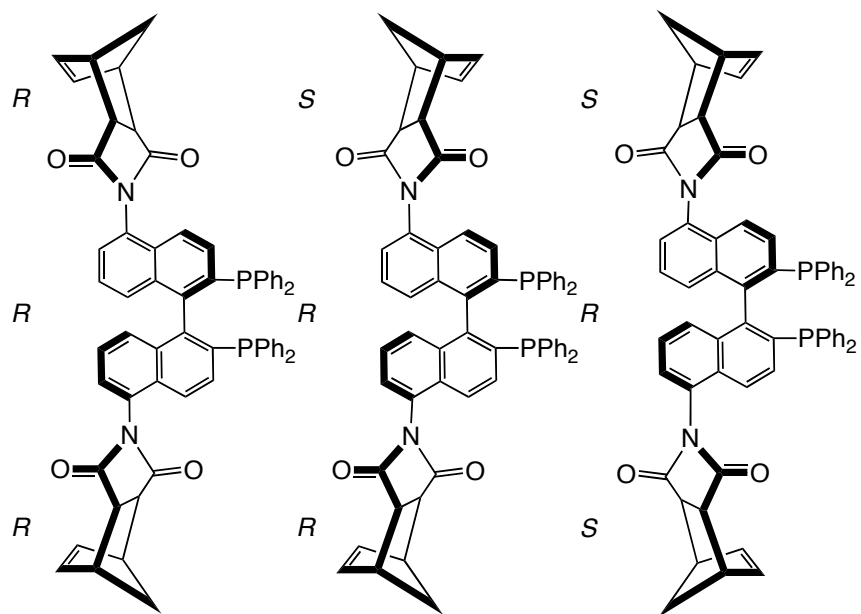


**Figure 2-3:** Diastereomeric rotamers of 13.

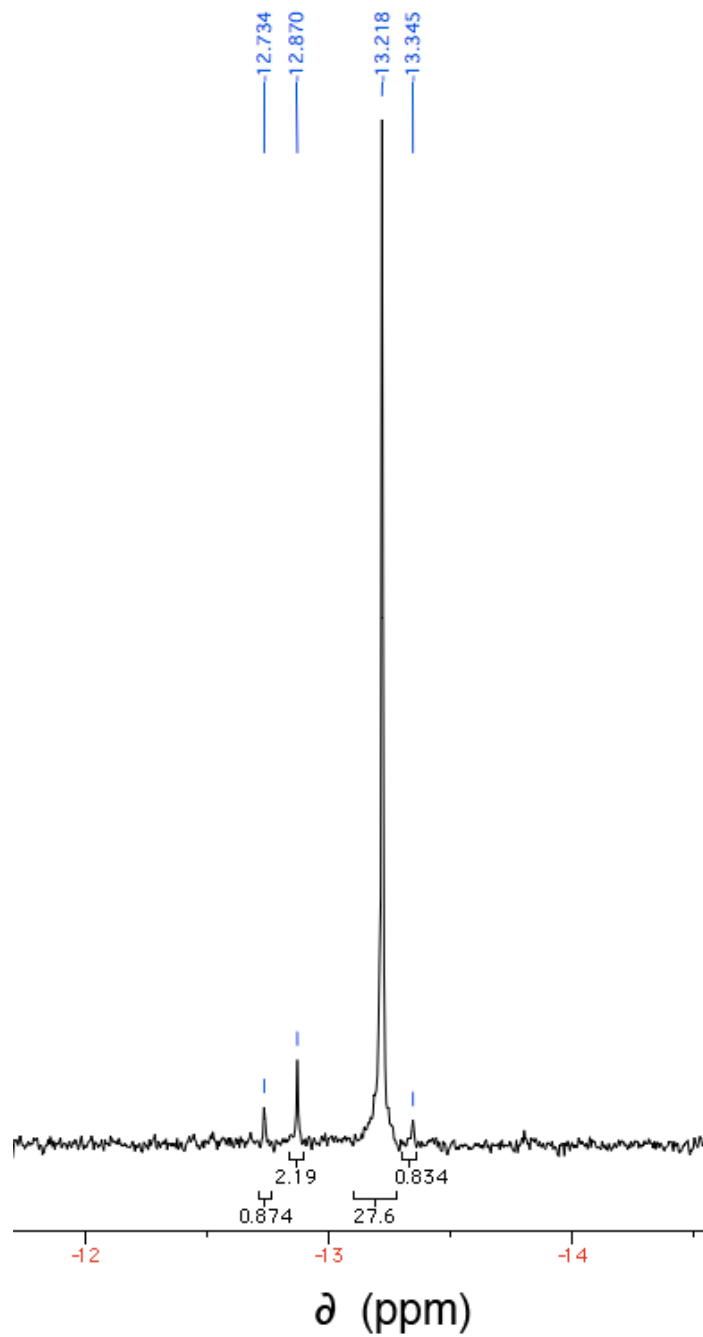


**Figure 2-4:**  $^{31}\text{P}$  NMR of one isomer of **13** after 5 minutes at room temperature (162.1 MHz,  $\text{CD}_2\text{Cl}_2$ .)

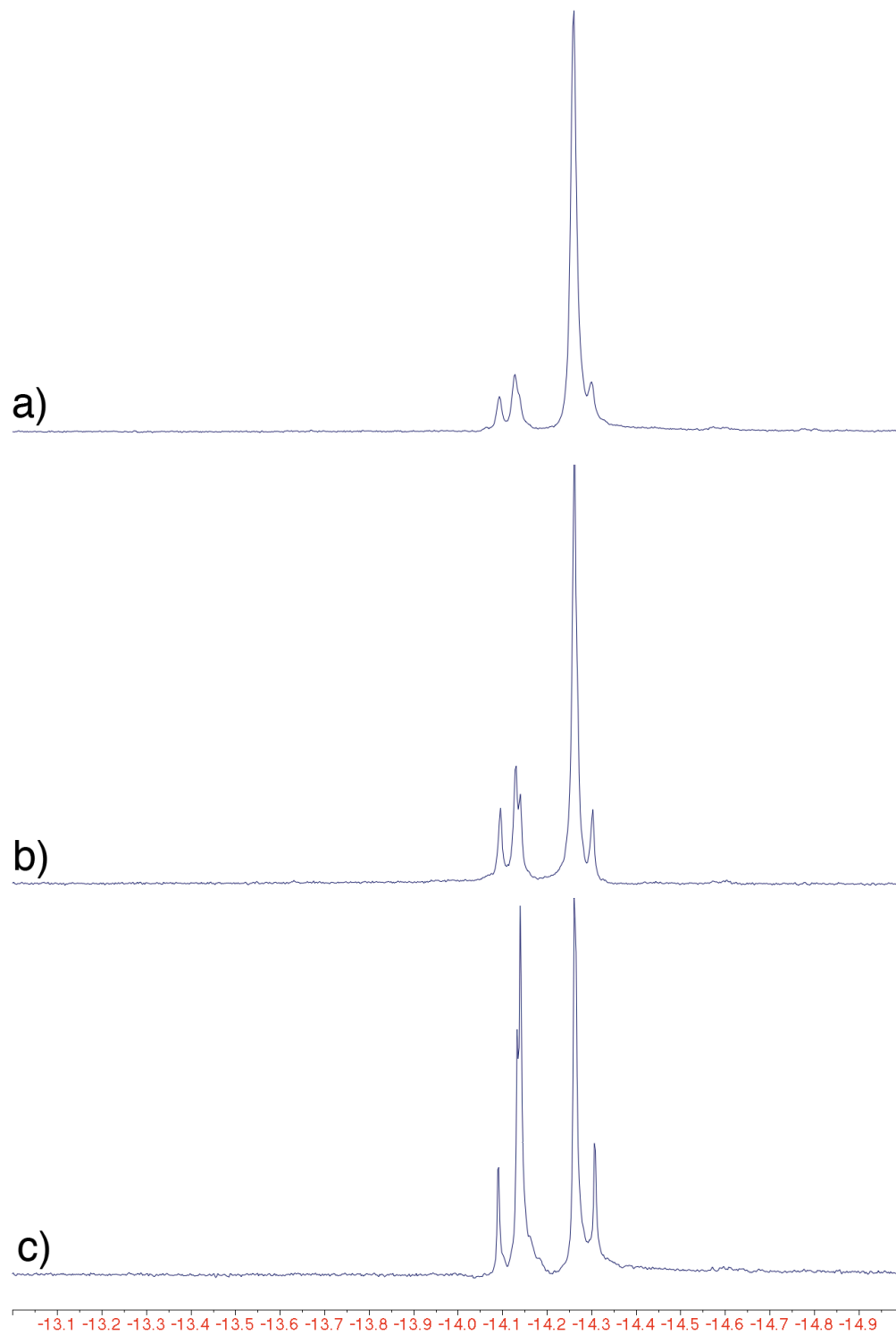


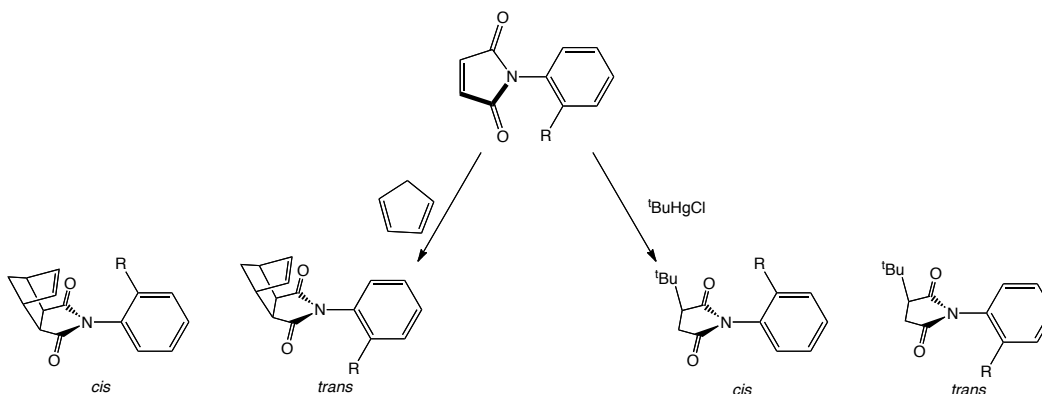
**Figure 2-5:**  $^{31}\text{P}$  NMR spectra of **13** in  $\text{CD}_2\text{Cl}_2$  recorded at a) 30 minutes, b) 60 minutes and c) 18 hours. (202.3 MHz,  $\text{CD}_2\text{Cl}_2$ , 27°C)

The hindered rotation around the aryl-imide bond results from both steric and electronic effects. The imide-nitrogen and the aryl-carbon are both  $sp^2$  hybridized, and the nitrogen's lone pair can donate into the  $\pi^*$  orbitals of the naphthalene ring, resulting in partial N-C double bond character. Additionally, steric interactions between the imide carbonyl groups, and the ortho-substituent on the aryl ring will disfavour a coplanar arrangement of the two moieties. Indeed, x-ray crystallography has shown that N-aryl imides twist  $\sim 90^\circ$  relative to the arene ring when prepared from 2,5-di-*tert*-butylaniline in order to reduce the steric interactions.<sup>98</sup>

Curran *et al.* found with a series of N-aryl maleimides that bulkier substituent groups at the *ortho*-position on the N-arene ring lead to higher barriers to rotation. Consequently, bulkier substituents also resulted in high selectivities in both the radical, and Diels-Alder reactions with alkyl mercury compounds and with cyclopentadiene, respectively<sup>99</sup> (Table 2-3). With the ortho-substituent being a *tert*-butyl group, only the *trans*- isomer from the Diels-Alder reaction was formed. Similar trends were observed with the addition of <sup>t</sup>BuHgCl. It was noted that upon equilibration for relatively short times (10 – 30 min), the kinetic ratio of *trans*- to *cis*-isomers decreased in all cases except for the <sup>t</sup>Bu substituent, which did not form the *cis*-isomer at all, even after equilibration at 140°C for one week. This aforementioned study by Curran *et al.* illustrates the relationship between

rotation and steric crowding. Similar steric and electronic effects are the likely source of atropisomerism in **13**.

**Table 2-3** Atropisomer ratios obtained from the Diels-Alder and radical reactions of N-aryl maleimides.



R-Substituent	Diels-Alder Reactions		Radical Reaction	
	<i>trans:cis</i> ratio	After Equilibration	<i>trans:cis</i> Ratio	After Equilibration
Et	4.6	1.1	1.2	1.1
<sup>i</sup> Pr	6.1	1.4	8.7	1.8
<sup>t</sup> Bu	<i>trans</i> -only	<i>trans</i> -only	12.5	2.5

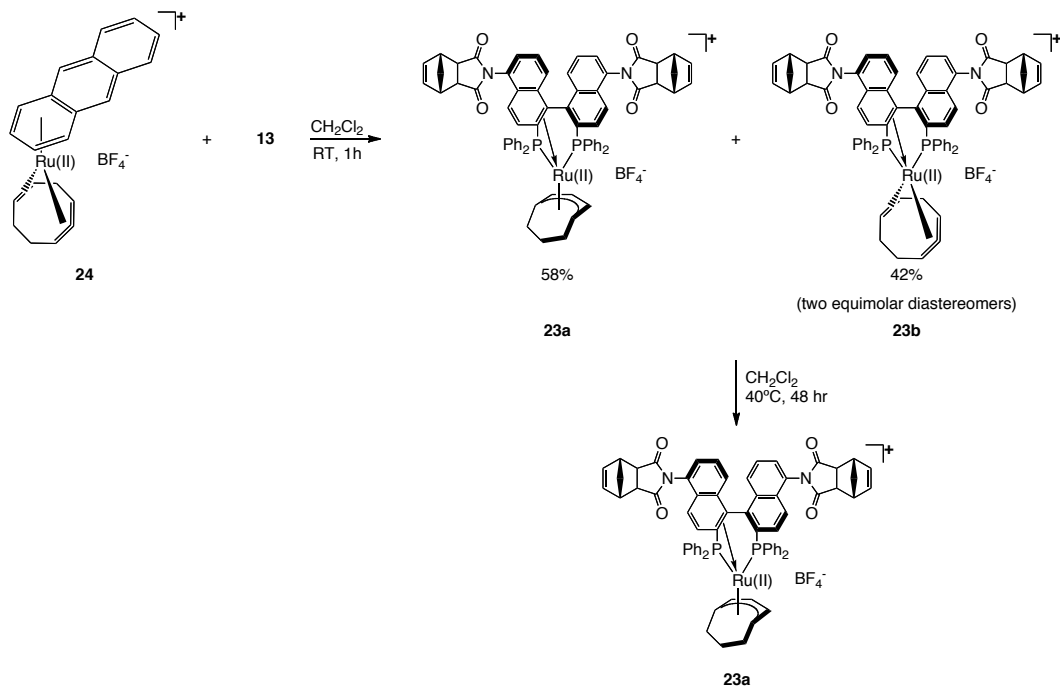
Upon coordination of **13** to a metal centre we observed that the metal was capable of influencing the atropisomerism of the ligand. Interestingly, the  $^{31}\text{P}$  signals coalesce in the case of  $[\text{Rh}(\text{NBD})(\text{N-BINAP})]\text{BF}_4$  (**21**) while distinct signals are observed for  $[\text{RhCl}(\text{N-BINAP})]_2$  (**22**). The coalescence of the  $^{31}\text{P}$  signals indicate that the phosphorus centres have become equivalent as a result of rapid rotation about the C-N

imide bond on the NMR timescale. If the naphthalene rings are relatively electron-rich, there would be less donation from the imide-nitrogen p-orbital to the naphthalene  $\pi^*$  orbital, resulting in less C-N double bond character, and a decrease in the electronic contribution to its hindered rotation. When an aryl phosphine coordinates to a metal centre, it does so through  $\sigma$ -donation from the phosphorous atom to the metal, and  $\pi$ -back donation from a metal d-orbital to an empty p-aryl  $\pi$  or  $\pi^*$  orbital on the phosphine. Increasing the amount of  $\pi$  back donation from the metal to the ligand would increase the electron density of the ligand, and conversely weaken the imide-aryl  $\pi$  interaction.

### **Section B: Preparation of ROMP-Active Catalyst Monomers**

In preliminary work done for this dissertation,  $[\text{Ru}(\text{N-BINAP})((1\text{-}3;5\text{-}6\text{-}\eta)\text{-C}_8\text{H}_{11})]\text{BF}_4$  (**23**) was synthesized as a convenient entry into carbonyl hydrogenation catalysis. The aim was to use **23**, as seen in Scheme 2-3, to prepare a heterogeneous ester hydrogenation catalyst via alternating-ROMP assembly. Previous results from our laboratory showed that product inhibition by primary alcohols limits the turnover numbers for ester hydrogenation under mild conditions (4atm  $\text{H}_{2(\text{g})}$ ,  $0^\circ\text{C}$ ) using  $[\text{Ru}((R)\text{-BINAP})(\text{H})_2((R,R)\text{-dpen})]$  as a catalyst. The studies showed that primary alcohols form ruthenium alkoxides that are unreactive to esters under these conditions. The reasoning for this early project was that if

heterogeneous catalysis were used for these ester hydrogenations, product inhibition could be avoided by choosing high Ru loadings per run to minimize product inhibition, and then reuse the heterogeneous catalyst, or use a flow reactor, to achieve high turnover numbers.



**Scheme 2-3:** Preparation of a ROMP active **23** for the asymmetric hydrogenation of ketones.

**23** was synthesized by reaction of racemic [Ru((1-3;5-6-η)-C<sub>8</sub>H<sub>11</sub>)(η<sup>6</sup>-anthracene)]BF<sub>4</sub> (**24**) and **13** in dichloromethane. Other workers in our laboratory showed that **24** readily reacts with a variety of diphosphines via displacement of the η<sup>6</sup>-anthracene ligand. Indeed, **24** reacted with **13** via displacement of the anthracene ring to form a mixture

of products. We proposed that the mixture consisted of the (1-5- $\eta$ )-C<sub>8</sub>H<sub>11</sub> product **23a** in 58% yield, and a 1 : 1 mixture of the (1-3;5-6- $\eta$ )-C<sub>8</sub>H<sub>11</sub> diastereomers **23b** in 42% yield. The diastereomers of **23b** yields signals at  $\delta = 35.6$  and  $\delta = 32.4$  ppm in the <sup>31</sup>P NMR spectrum. It is known that heat induces the isomerization of (1-3;5-6- $\eta$ )-C<sub>8</sub>H<sub>11</sub> rings to the (1-5- $\eta$ )-coordination mode<sup>100</sup>. Figures 2-6 and 2-7 show the <sup>1</sup>H and <sup>31</sup>P spectra recorded of the mixture of products before and after reflux for 48 hr. In the <sup>1</sup>H NMR spectra a sharp multiplet at  $\delta = 6.76$  ppm is lost upon reflux along with a broad signal at  $\delta = 3.17$  ppm. Signals from the (1-5- $\eta$ )-ring system correlating to a broad apparent triplet at  $\delta = 5.4 - 5.7$  ppm along with a broad signal at  $\delta = 4.6 - 4.8$  ppm grow larger. A broad peak at  $\delta = 2.20$  ppm also grows during reflux; this signal corresponds to one of the terminal methine C-H found on the (1-5- $\eta$ -C<sub>8</sub>H<sub>11</sub>) rings. Characteristic evidence of the (1-5- $\eta$ )-ring system in the <sup>1</sup>H NMR spectrum is the broad, high-field quartet at -0.2 ppm. This characteristic peak is due to the conformation of the ring system, as shown in Figure 2-8<sup>100</sup>, where the three methylene bridges flip out of the plane of the conjugated system that allows the endo-proton to interact with the  $\pi$  system.

Prior to reflux, the <sup>31</sup>P NMR spectrum obtained showed signals for **23b** at  $\delta = 32.3, 35.5,$  and  $46.9$  ppm. These are in accordance with the analogous [Ru(1-3;5-6- $\eta$ )-C<sub>8</sub>H<sub>11</sub>](BINAP)]BF<sub>4</sub> complex prepared by Wiles *et al.*<sup>101</sup>. The <sup>31</sup>P NMR spectrum after reflux agrees with that of



[Ru(BINAP)((1-5- $\eta$ )-C<sub>8</sub>H<sub>11</sub>)]BF<sub>4</sub> as prepared by Wiles *et al.*, with signals at  $\delta = -5.9$  and 65.4 ppm<sup>101</sup>. The spectra observed after reflux together indicate the presence of the (1-5- $\eta$ )-C<sub>8</sub>H<sub>11</sub> ring in **23a**. The inequivalency of the <sup>31</sup>P signals is due to the irregular binding mode of the ligand. Specifically, one of the naphthalene ring units is coordinated edge on in an  $\eta^2$  fashion<sup>102</sup>, to fulfill the requirements for 18 e<sup>-</sup> around Ru. This mode of coordination is referred to as  $\kappa^4\eta^2$  and has been noted before in compounds analogous to **23**, [Ru(diphosphine)((1-5- $\eta$ )-C<sub>8</sub>H<sub>11</sub>)]BF<sub>4</sub><sup>101</sup>. The rotation about the N-arene bond causes the phosphorous signal to appear as a broad multiplet.

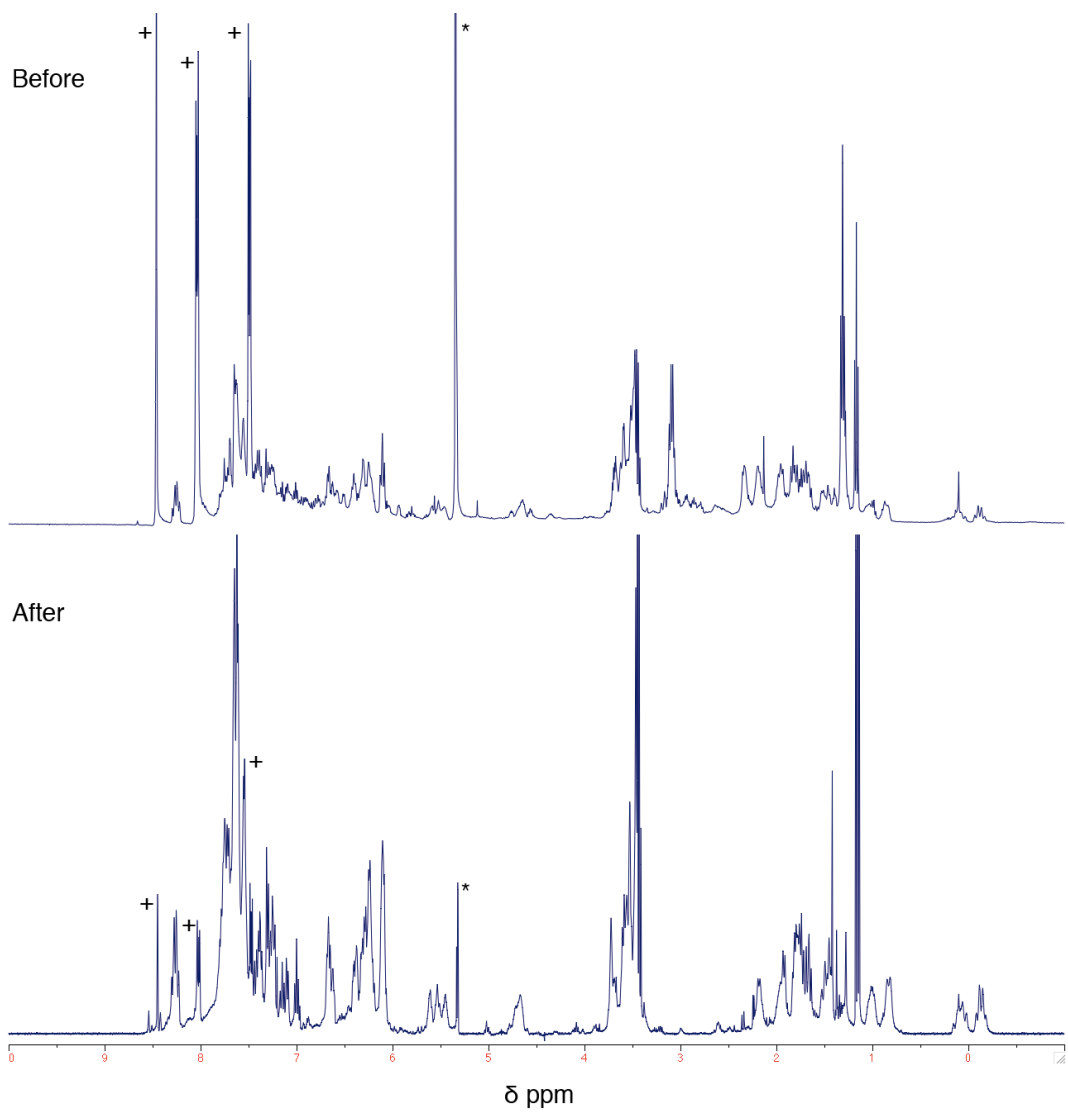


**Figure 2-6:**  $^1\text{H}$  NMR Spectrum of  $[\text{Ru}(\text{C}_8\text{H}_{11})(\text{N-BINAP})]\text{BF}_4$  (**23**) before and after reflux at  $40^\circ\text{C}$  for 48h. (399.8 MHz,  $27^\circ\text{C}$ ,  $\text{CD}_2\text{Cl}_2$ .) \* = residual solvent signal, + = displaced anthracene.



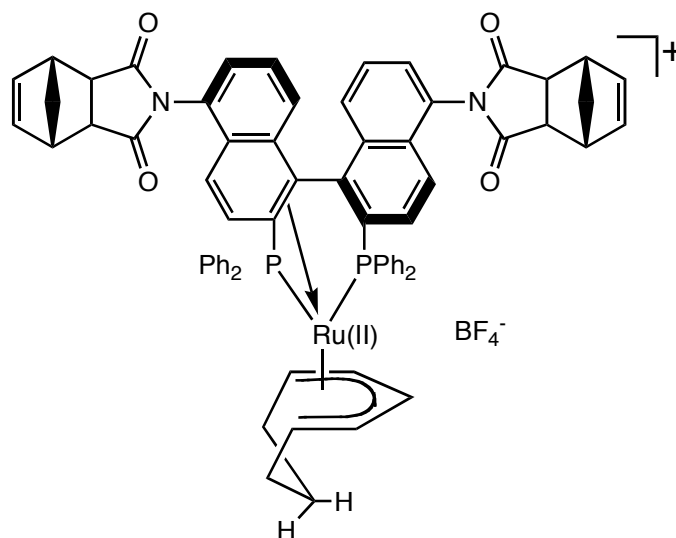
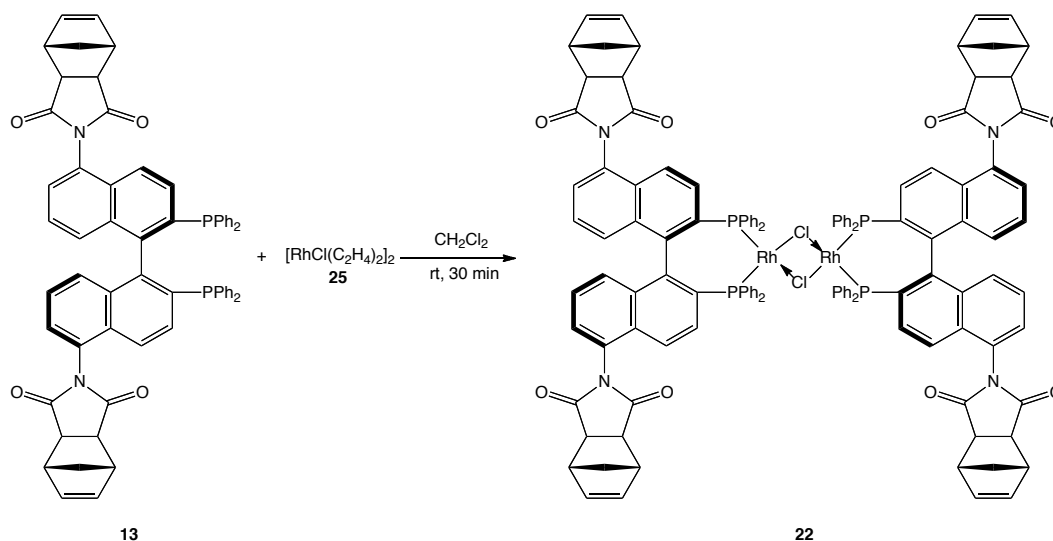


**Figure 2-8:** Conformation of the thermodynamically stable isomer of  $[\text{Ru}(\text{C}_8\text{H}_{11})(\text{N-BINAP})]\text{BF}_4$ , (**23a**).

As discussed in Sections C and D, as part of the preliminary studies for this research, **23a** was then incorporated into a catalyst-organic framework with alternating-ROMP assembly, and the immobilized catalyst was evaluated for the hydrogenation of esters. This system proved to be moderately active and reusable, as discussed in Section D. The activity and the catalyst and its' reusability, however, was difficult to reproduce, and it was decided that the focus of the project would change to the synthesis, characterization, and immobilization of a rhodium-(N-BINAP) based system to catalyze the cycloisomerization of 1,6-enynes. For these studies, the Rh-containing polymerization monomer was synthesized as shown in Scheme 2-4. The dimer  $[\text{RhCl}(\text{N-BINAP})]_2$  (**22**) was prepared *in situ*, by addition of dissolved rotamerically pure **13** to a slurry of

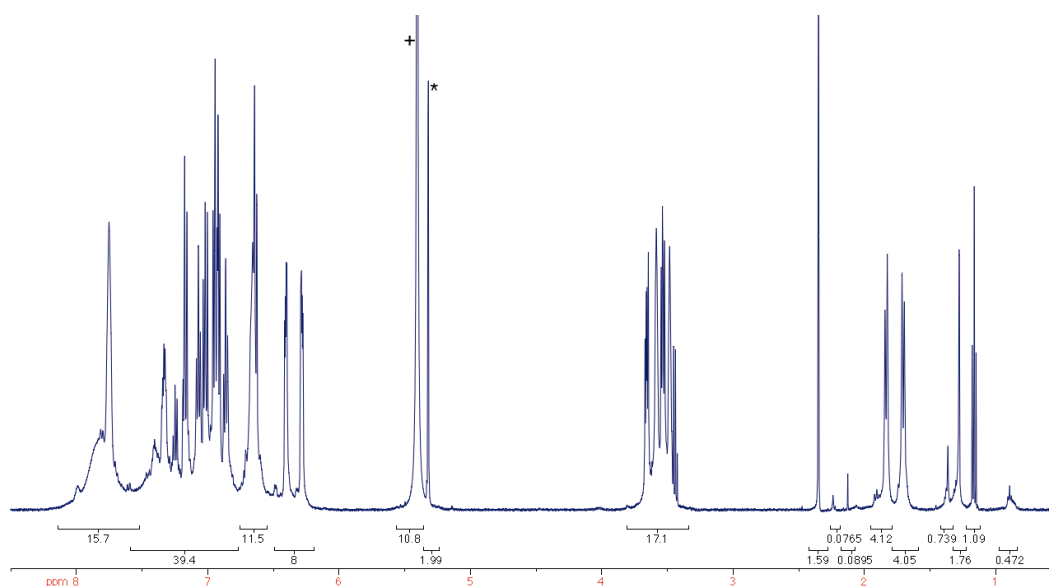
$[\text{RhCl}(\text{C}_2\text{H}_4)_2]_2$  (**25**) in  $\text{CD}_2\text{Cl}_2$ . This nets **22** through loss of the labile ethylene ligands in **25**. Characterization of **22** was carried out *in situ*, by NMR spectroscopy ( $^1\text{H}$ ,  $^{31}\text{P}$ ,  $^{13}\text{C}$ ) as attempts to isolate **22** caused some decomposition through an uninvestigated mechanism. As a result, we used **22** as a ROMP monomer without isolation, as often is the practice in the literature for diphosphine dimers prepared in this manner<sup>80</sup>.



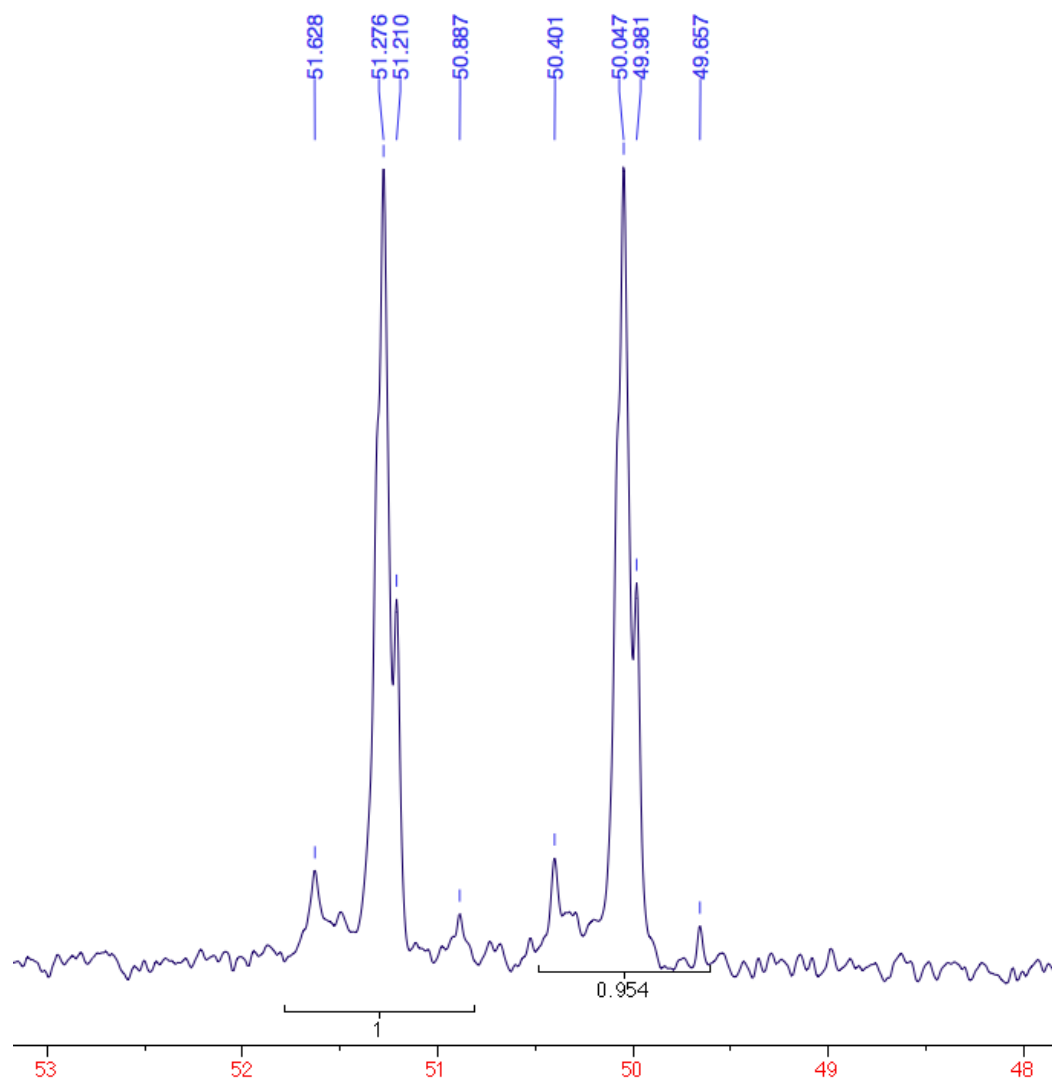
**Scheme 2-4:** Preparation of ROMP active Catalyst Monomer, **22**.

The reaction between **13** and **25** was carried out with 10% excess **25** to avoid possible formation of bis complexes such as  $[\text{Rh}(\text{BINAP})_2]^+$  through disproportionation<sup>103</sup>. Figures 2-9 and 2-10 show the  $^1\text{H}$  and  $^{31}\text{P}$  NMR spectra of one reaction between **25** and **13** after 5 min. The  $^1\text{H}$  NMR spectrum shows signals for residual ethylene ( $\delta = 5.4$  ppm). The undissolved **25** is removed before alternating ROMP polymerization by

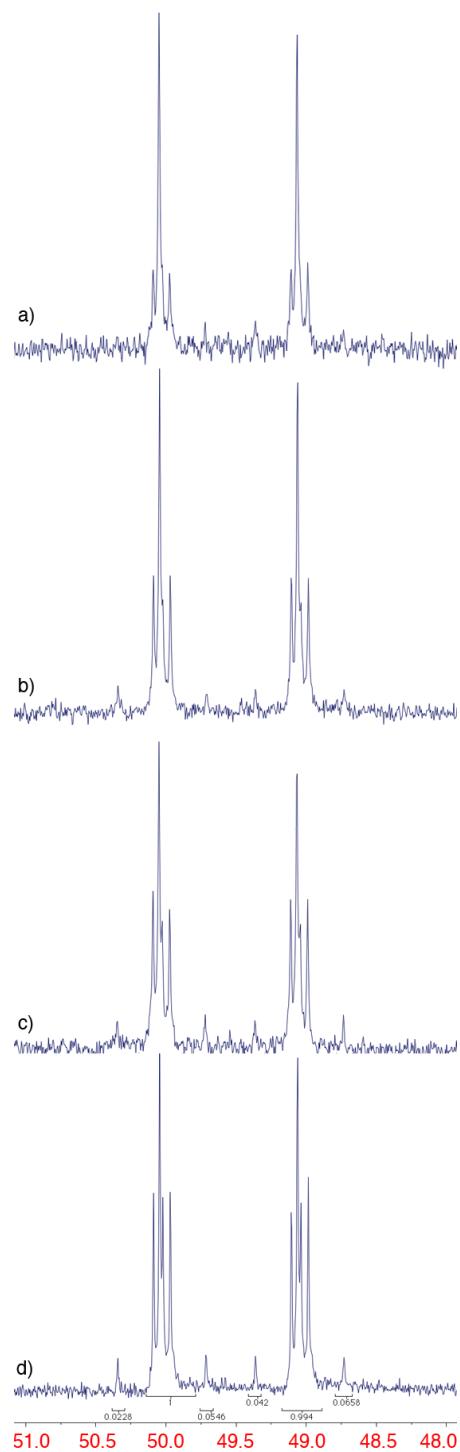
decanting the solution off the remaining solid. The  $^{31}\text{P}$  NMR spectrum of **22** consists of a doublet of multiplets due to coupling between Rh and P, with  $^1J_{\text{Rh-P}} = 199$  Hz, and the presence of the N-C rotamers. The preparation with excess **25**, and the Rh-P coupling constant, is consistent with the literature for the analogous  $[\text{RhCl}(\text{diphosphine})]_2$  species<sup>104</sup>. No  $^{31}\text{P}$  signal of free ligand was observed. Further, the main diastereomeric rotamer formed is that from addition of the  $\text{C}_2$ -disymmetric **13** to **25**.



**Figure 2-9:**  $^1\text{H}$  NMR of **22** taken at  $27^\circ\text{C}$ . \* = residual  $\text{CH}_2\text{Cl}_2$  signals; + = residual  $\text{C}_2\text{H}_4$  signals. (399.8 MHz,  $\text{CD}_2\text{Cl}_2$ ,  $27^\circ\text{C}$ ).



**Figure 2-10:**  $^{31}\text{P}$  NMR of  $[\text{RhCl}(\text{N-BINAP})]_2$  (**22**) recorded 15 minutes after mixing. (162.1 MHz, 27°C,  $\text{CD}_2\text{Cl}_2$ .)



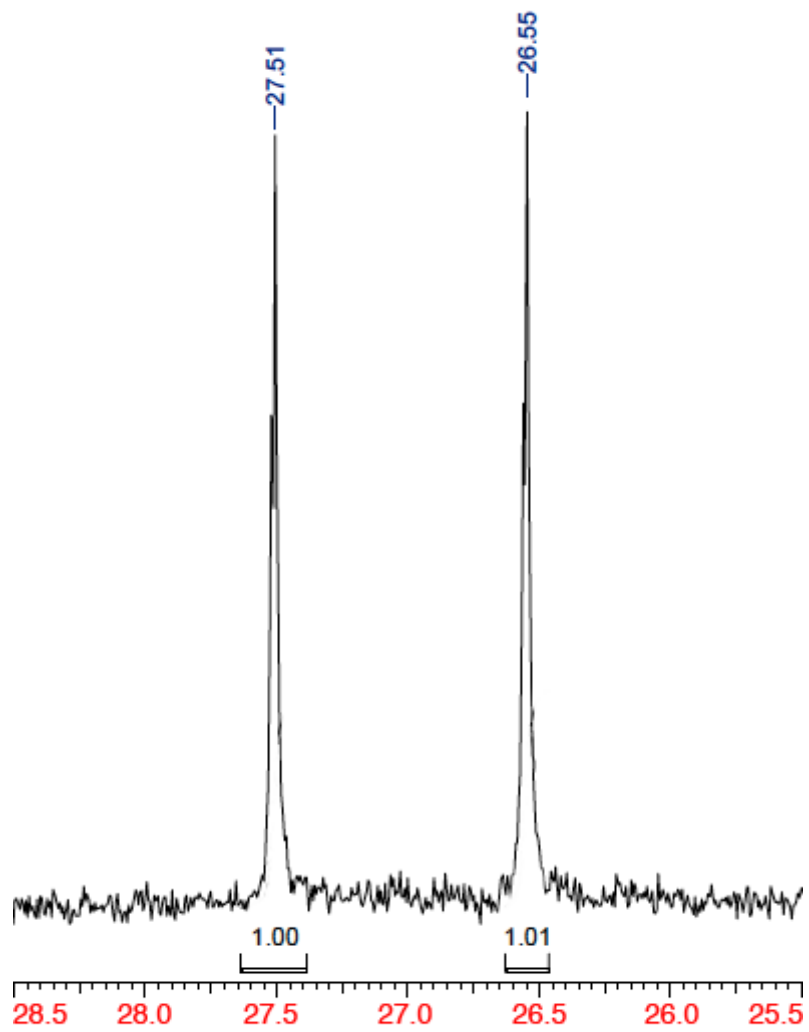
**Figure 2-11:**  $^{31}\text{P}$  NMR of  $[\text{RhCl}(\text{N-BINAP})]_2$  (**22**) recorded a) 15 minutes, b) 30 minutes, c) 60 minutes and d) 90 minutes after mixing. (162.1 MHz,  $27^\circ\text{C}$ ,  $\text{CD}_2\text{Cl}_2$ .)



Figure 2-11 shows the  $^{31}\text{P}$  NMR spectra recorded over time for a sample of **22** at room temperature. At 15 minutes, the signals from the non  $C_2$ -dissymmetric isomers begin to grow in on either side of the signal from the  $C_2$ -dissymmetric rotamer, as the non  $C_2$ -dissymmetric isomers are the intermediate between the two  $C_2$ -dissymmetric isomers. At thirty minutes another signal very similar in chemical shift to the  $C_2$ -dissymmetric rotamer has begun to grow in; this is the other  $C_2$ -dissymmetric rotamer. As well, the peak heights of the non-dissymmetric signals have increased after 30 minutes. From 30 minutes on, the AB system of the non-dissymmetric rotamers is readily apparent.

The disparity between peak intensities is a key feature of an AB system, where the difference in signal position in Hertz is very similar to the coupling constant,  $J$ . After 90 minutes the less intense signals are better observed with  $^2J_{\text{P-P}} = 52$  Hz for the non-dissymmetric rotamers. These experiments show that rotation about the C-N bonds occurs when **13** is coordinated to the Rh(I) centre in the chloro-bridged dimer **22**, and that this rotation is slower than in the free ligand. Specifically, signals from the non-dissymmetric isomers of **13** are more apparent in less time for the free ligand than for **22**, indicating that rotation about the imide-naphthyl C-N bond in **13** is faster. Experiments to determine the precise difference in rate were not carried out. This increased rate of rotation is most likely due to more electron density in the naphthyl  $\pi$ -system of **13** than of **22**.

Conversely, in  $[\text{Rh}(\text{NBD})(\text{N-BINAP})]\text{BF}_4$  (**21**) (NBD = norbornadiene, prepared for another project), the  $^{31}\text{P}$  NMR spectrum (Figure 2-12) contains only a sharp doublet with  $^1J_{\text{RhP}} = 156$  Hz. The NMR equivalence of the phosphorous in **21** is caused by rapid rotation about the C-N bond at room temperature. Cooling to  $-40^\circ\text{C}$  slows this rotation relative to the NMR timescale. Presumably, the increased rate of rotation about the imide-naphthyl bond in **21** is due to greater electron donation from the  $d\pi$ -orbitals of Rh to the aromatic  $\pi$ -system on BINAP in **21** compared to **22**, however, sigma effects cannot be ruled out by this preliminary interpretation.



**Figure 2-12:**  $^{31}\text{P}$  NMR of **21** at room temperature. (162.1MHz,  $\text{CD}_2\text{Cl}_2$ ,  $27^\circ\text{C}$ ).

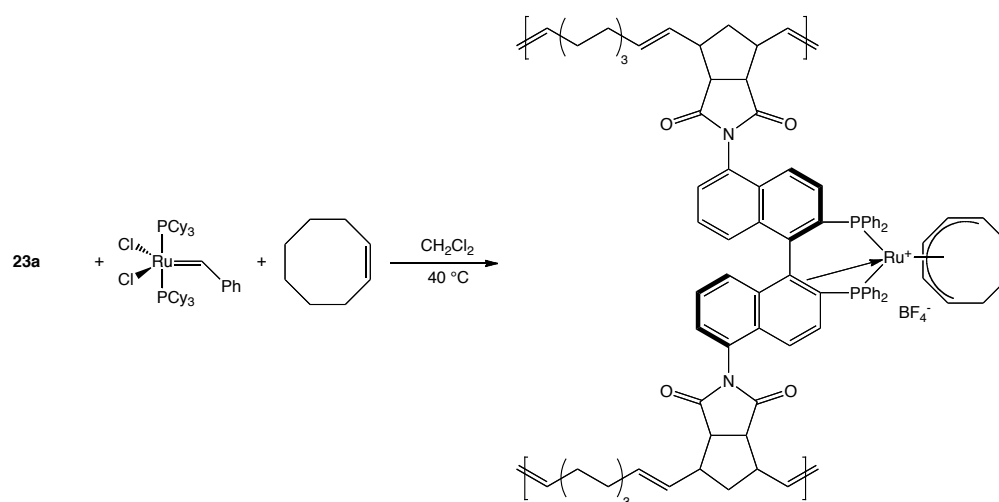
## Section C: Preparation of Catalyst-Organic Frameworks through Alternating-ROMP Assembly.

As shown previously (Chapter 1, Scheme 1-9), direct ROMP of complexes containing **13** does not occur, or is quite sluggish using the 1<sup>st</sup> and 2<sup>nd</sup> generation Grubbs' metathesis catalysts because the steric crowding around the norimido olefin groups is too large<sup>85</sup>. Specifically, although catalytic ROMP does not occur with 1<sup>st</sup> generation Grubbs' catalyst, one event of ring-opening metathesis does. The resulting Ru-alkylidene is too crowded to allow further metathesis reactions with another complex of **13**. To successfully assemble the catalyst-organic framework, a co-monomer was introduced that was intrinsically less reactive, or strained, than the norimido olefin group in **13**, but also less crowded. The cyclic olefin chosen as a spacer monomer was *cis*-cyclooctene (COE). Through judicious choice of a less strained and crowded cyclic olefin, the polymerization was designed so that the norimido group reacts first, but due to steric hindrance is unable to react further. The COE co-monomer reacts to insert a C<sub>8</sub> spacer with the Ru-alkylidene attached to a primary carbon. This alkylidene is much less crowded, and reacts with another norimido group to form a new, crowded Ru-alkylidene. This cycle of insertion of COE followed by a norimido olefin will continue until completion, and hence the process is known as alternating-ROMP. A three-dimensional cross-linked lattice is produced

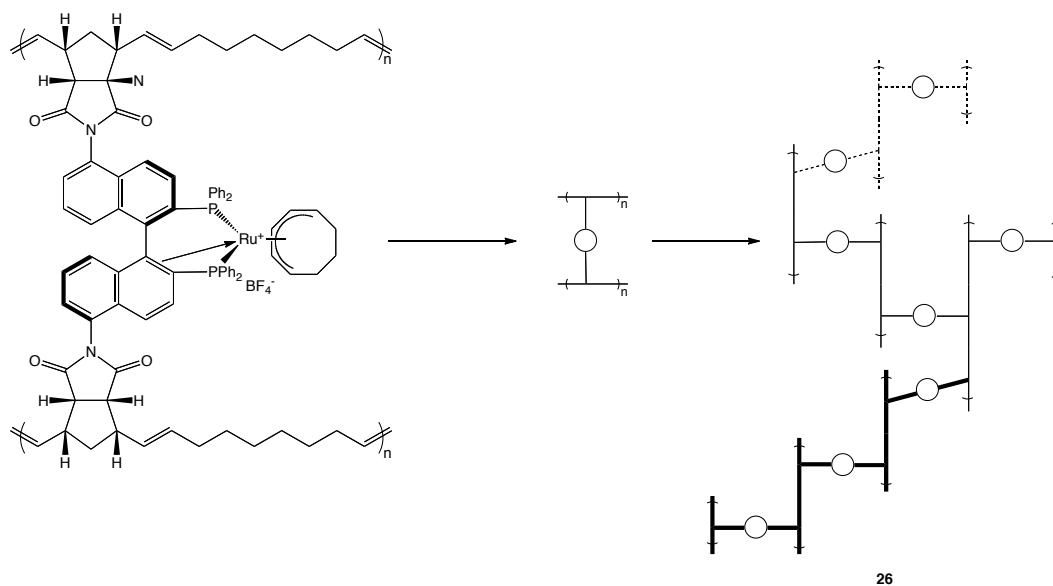
from the alternating ROMP assembly, and we refer to this process as the it the assembly of a catalyst-organic framework rather than polymerization.

For this research, alternating-ROMP assembly of the Ru complex **23a** (Scheme 2-5) was carried out using mixtures of COE, **23a**, and Grubbs' 1<sup>st</sup> generation ROMP catalyst, [RuCl<sub>2</sub>(PCy<sub>3</sub>)<sub>2</sub>(CHPh)], in a ratio of 80 : 20 : 1. The alternating ROMP assembly of **23a** and COE was complete after reflux in CH<sub>2</sub>Cl<sub>2</sub> for 48 hours, Scheme 2-6 shows the predicted three-dimensional structure of the catalyst-organic framework (**26**). This proposed three-dimensional structure is likely similar to that proposed by Ralph *et al.* for the previously prepared Ru containing framework **15** (Scheme 1-9). The differences would be in the nature of the ancillary ligands on Ru, and that the catalyst centres are cationic in **26**. After the alternating-ROMP assembly of **26** was complete as shown by <sup>1</sup>H and <sup>31</sup>P NMR spectroscopy (Figure 2-13), 8 equiv of (1*R*,2*R*)-diphenyl-1,2-ethylenediamine (dpen) (per ruthenium centre) were added to displace several double bonds of the (1-5-η)-C<sub>8</sub>H<sub>11</sub> ring and of the η-κ BINAP coordination to generate the catalyst-organic framework **27** with a Ru centre with coordinated dpen. From unpublished results by another student in our laboratory, we believe that the dpen displaces a coordinated olefin from the (1-5-η)-C<sub>8</sub>H<sub>11</sub> ring system, yielding an allylic system, as well as the coordinated olefin from the κ-coordinated BINAP. Figure 2-14 shows the <sup>1</sup>H and <sup>31</sup>P NMR spectra after addition of dpen. The apparent

$^{31}\text{P}$  NMR inequivalency of the phosphorous centres is not due to the  $\kappa$ -coordination mode of N-BINAP, which has been lost, but instead results from the coordination of dpen. One phosphorous is trans to a nitrogen in dpen, while the other is trans to the allylic species. In the  $^1\text{H}$  NMR spectrum it is apparent that the upfield signals from the interaction of the methylene protons with the (1-5- $\eta$ )- $\text{C}_8\text{H}_{11}$  ring system are lost; this is expected upon coordination of dpen. Given that this was exploratory work into a heterogeneous catalytic system, no further characterization of the supported catalyst was attempted. After addition of dpen, the supersaturated solution of the catalyst-organic framework **27** was then slowly evaporated over the  $\text{BaSO}_{4(s)}$  support.



**Scheme 2-5:** Preparation of catalyst-organic framework using **23a**.



**Scheme 2-6:** Expected three-dimensional structure of catalyst organic framework **26**.

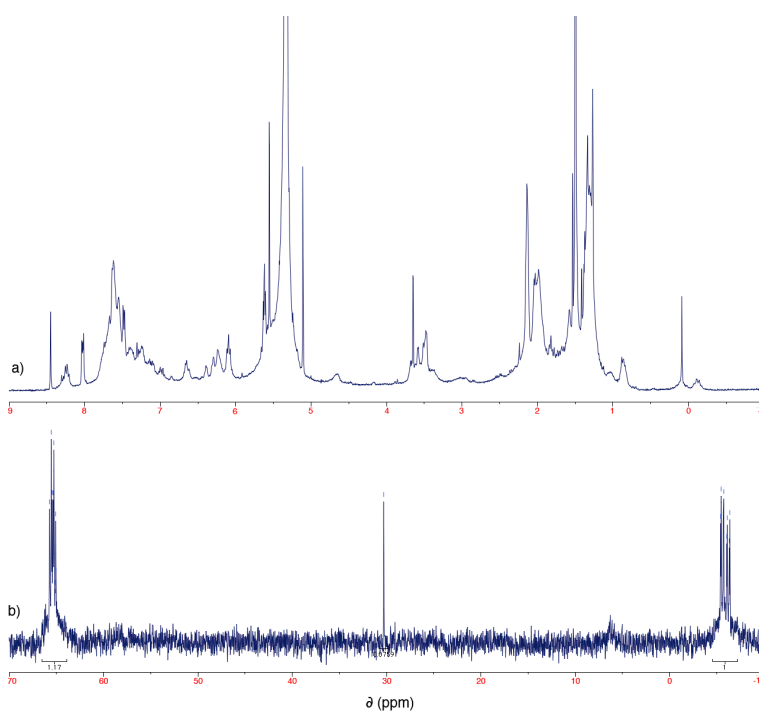


**Figure 2-13:** NMR spectra recorded of the prepared catalyst-organic framework **26** from the alternating-ROMP assembly of **23a** with COE. a)

$^1\text{H}$  NMR spectrum (400 MHz,  $\text{CD}_2\text{Cl}_2$ ,  $27^\circ\text{C}$ ), b)  $^{31}\text{P}$  NMR spectrum (162.1 MHz,  $\text{CD}_2\text{Cl}_2$ ,  $27^\circ\text{C}$ ).

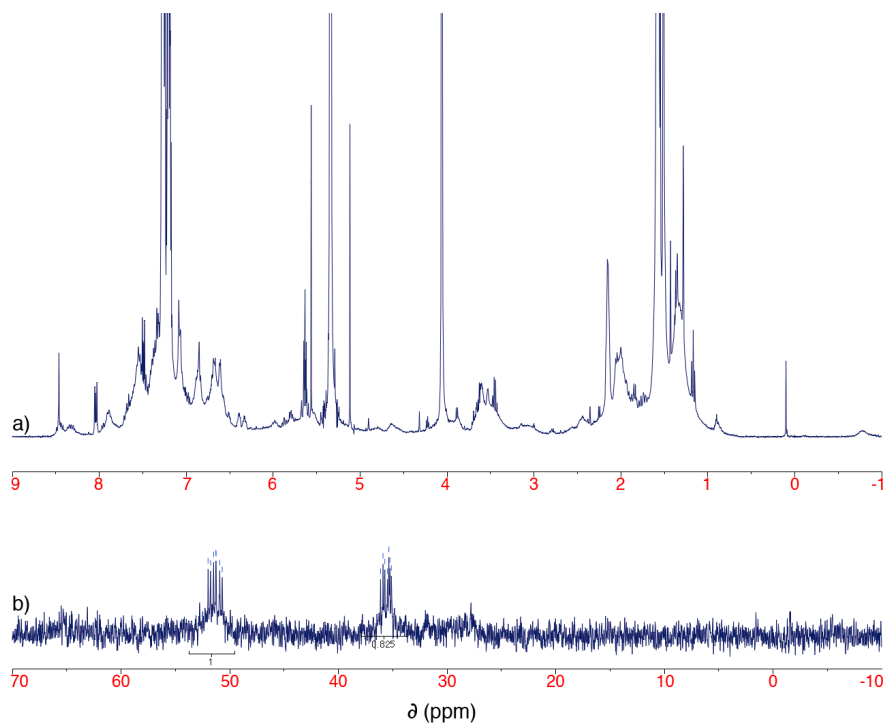


**Figure 2-14:** NMR spectra recorded for the catalyst-organic framework **27** prepared through alternating-ROMP assembly of **23a** with COE after the addition of dpen. a)  $^1\text{H}$  NMR spectrum (400 MHz,  $\text{CD}_2\text{Cl}_2$ ,  $27^\circ\text{C}$ ), b)  $^{31}\text{P}$  NMR spectrum (162.1 MHz,  $\text{CD}_2\text{Cl}_2$ ,  $27^\circ\text{C}$ ).

As is common to complexes of **13**, the Rh dimer does not readily undergo ROMP in the absence of a spacer monomer. The alternating-ROMP assembly of the Rh complex **22** (Scheme 2-7) was carried out using mixtures of COE, **22**, and Grubbs' 1<sup>st</sup> generation ROMP catalyst, **1** (Figure 1-1), in a ratio of 120 : 10 : 1. The resulting catalyst-organic framework, shown in Scheme 2-8, is expected to be quite different from



the Ru frameworks **27** and the framework as prepared by Ralph<sup>88</sup>. The  $\mu$ -Cl ligands in the Rh(I)-dimer **22**, will act as an additional crosslinking agent, that bridges the catalyst centres in the catalyst-organic framework **28**. This additional crosslinking likely alters the rigidity and solubility of the framework. We found that in concentrations greater than  $6.5 \times 10^{-3}$  M in DCM, the resulting polymer is insoluble and precipitates. As anecdotal evidence from these exploratory studies, the assembly as performed by Ralph had concentrations as high as  $1.0 \times 10^{-2}$  M, with the assembled framework remaining in solution, indicating that the solubility of **28** is less than that of **27** or the framework as prepared by Ralph. In keeping with the literature procedure for cycloisomerization of enynes using  $[\text{RhCl}(\text{BINAP})]_2$ , the bridging  $\mu$ -Cl ligands are abstracted with a silver salt, typically  $\text{AgSbF}_6$ , to activate the rhodium centres towards cycloisomerizations. It is possible that the presence of the chloro- bridges during the alternating ROMP assembly of **28** results in the Rh centres existing as pairs within proximity of each other after abstraction of the chloride bridge with silver. Miyashita *et al.* reported the preparation of the dimer  $[(\text{Rh}(\text{BINAP}))_2]^{2+}$  (Figure 2-15)<sup>52</sup>. These researchers demonstrated that the phenyl rings of BINAP bridge the Rh centres in this dimer by coordinating to another rhodium centre in an  $\eta^6$  fashion. It is well known that hydrogenation of  $[\text{Rh}(\text{BINAP})(\text{NBD})]^+$  in coordinating solvents such as MeOH, THF, and acetone gives the solvento species  $[\text{Rh}(\text{BINAP})(\text{sol})_2]^+$

and free norbornane. The solvento species is capable of undergoing oxidative additions, and is generally believed to be an active catalyst in a variety of reactions. In the absence of coordinating solvents, hydrogenation of NBD results in formation of a dimer with  $\eta^6$ -phenyl rings, with 18-electron rhodium centres.

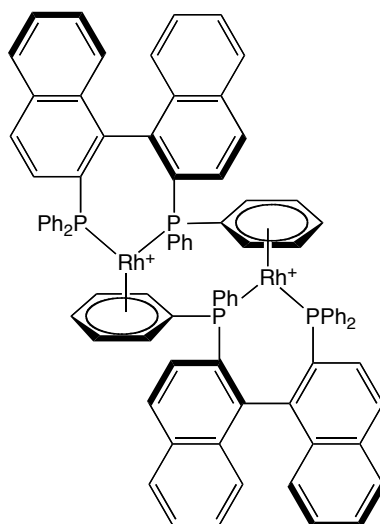


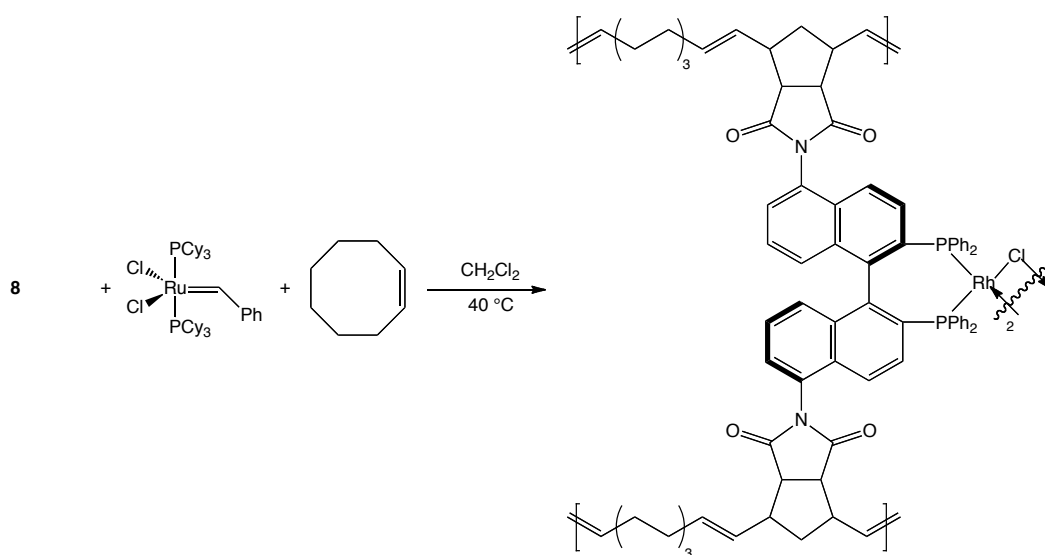
**Figure 2-15:** Dicationic, inactive Rh-dimer formed upon hydrogenation of  $[\text{Rh}(\text{BINAP})(\text{NBD})]^+$ .

ROMP assembly of **22** yields two diphosphine-rhodium centres in very close proximity to one another. After abstraction of the chloro bridge by Ag(I) to facilitate the entrance into catalysis, it is therefore possible for Rh-Rh interaction and cooperativity. In the absence of a coordinating solvent or substrate, the Rh-arene interaction illustrated in Figure 2-13 would be possible within the catalyst-organic framework. Although this bonding interaction yields two 18 electron centres, it has been shown that this is a weak bonding interaction, and in the presence of coordinating

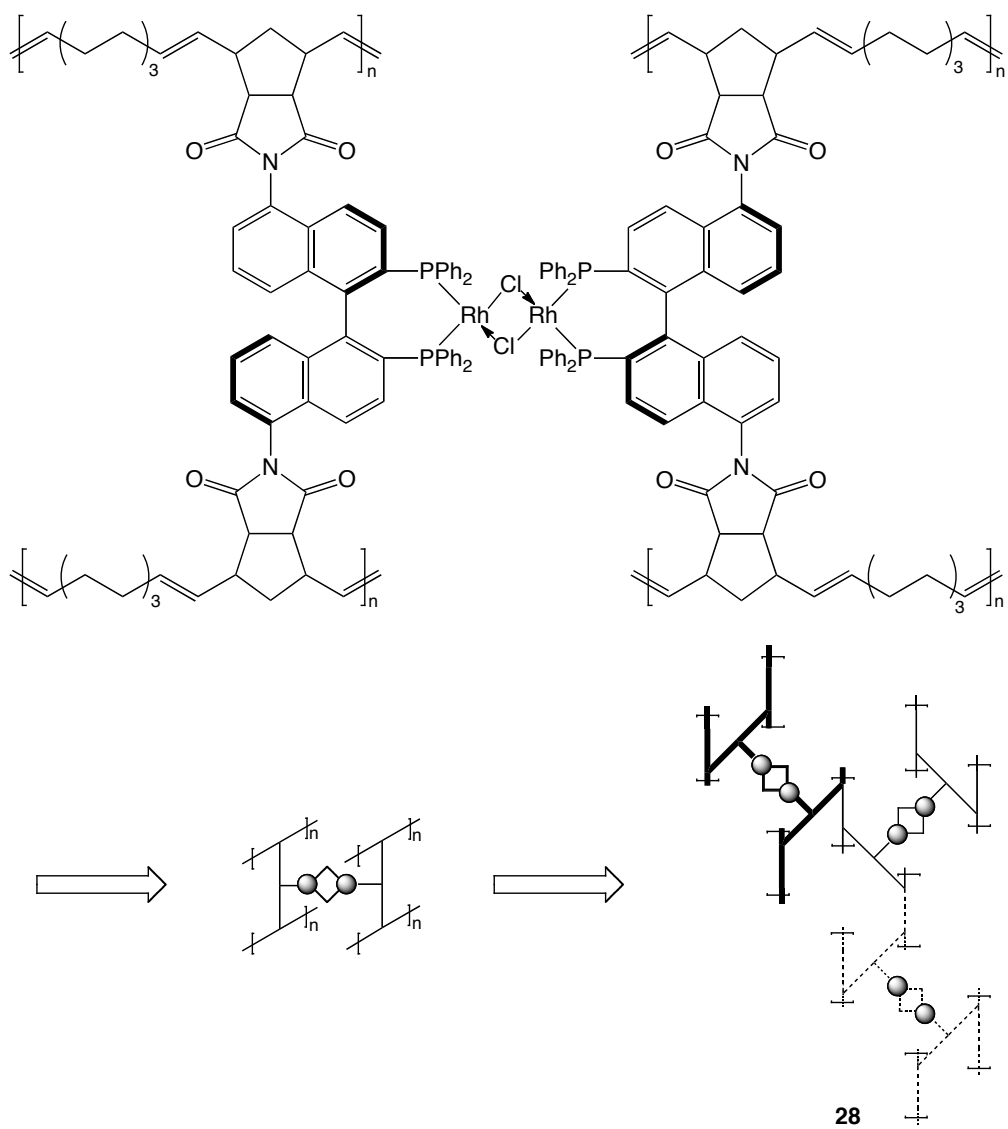
solvents or substrates the bonding interaction is disfavoured<sup>52</sup>. Furthermore, it is possible that this weak-bonding interaction could stabilize the active centres during reuse.

As stated previously in this section, ROMP assembly of **22** alone is not expected to occur unless a spacer monomer like *cis*-cyclooctene (COE) is used<sup>88</sup>. During preliminary studies by Sullivan, both *cis*-cyclooctene and *cis*-cyclododecene were investigated as co-monomers, as well as the use of different metathesis polymerization catalysts. In the course of trial polymerizations both Grubbs' 1<sup>st</sup> (**1**, Figure 1-1) and 2<sup>nd</sup> generation (**2**, Figure 1-1), and Hoveyda-Grubbs' (**3**, Figure 1-1) catalysts were used. The ratio of COE : dimer : metathesis catalyst was maintained at 120 : 10 : 1. From the studies done, **1** was the preferred catalyst. Unpublished results from our lab indicated that activation kinetics of **1** are better than those of **2**. Specifically *in situ* <sup>31</sup>P NMR spectra showed that the amount of free PCy<sub>3</sub> present in solution during the alternating-ROMP assembly was greater for the 1<sup>st</sup> generation catalyst, showing that the rate of initiation is faster than propagation for 1<sup>st</sup> generation Grubbs' which should result in a narrower molecular weight distribution. The rate of propagation, however, is slower than the 2<sup>nd</sup> generation catalyst. A slower rate of propagation may result in a higher degree of regularity in the alternating polymerization. Preliminary studies showed that *cis*-cyclooctene in combination with **1** produced a catalyst-organic framework

that was less soluble, and thereby able to sustain more reuses, than the frameworks made from the other spacer co-monomers, or ROMP catalysts made under the specified conditions. The alternating-ROMP assembly was complete in 16 hours, as indicated by  $^1\text{H}$  and  $^{31}\text{P}$  NMR, affording the generalized structure illustrated by Scheme 2-7 and 2-8. Figure 2-16 shows the  $^{31}\text{P}$  NMR spectrum of the complete ROMP-assembly reaction. The  $^{31}\text{P}$  signals of the polymer are found at  $\delta = 50.4$  ppm ( $^1J_{\text{Rh-P}} = 195\text{Hz}$ ), whereas the monomer is found at  $\delta = 50.6$  ( $^1J_{\text{Rh-P}} = 199\text{Hz}$ ).



**Scheme 2-7.** Preparation of catalyst-organic framework (**28**) through alternating-ROMP assembly.



**Scheme 2-8:** Three-Dimensional structure of **28** after alternating ROMP assembly.

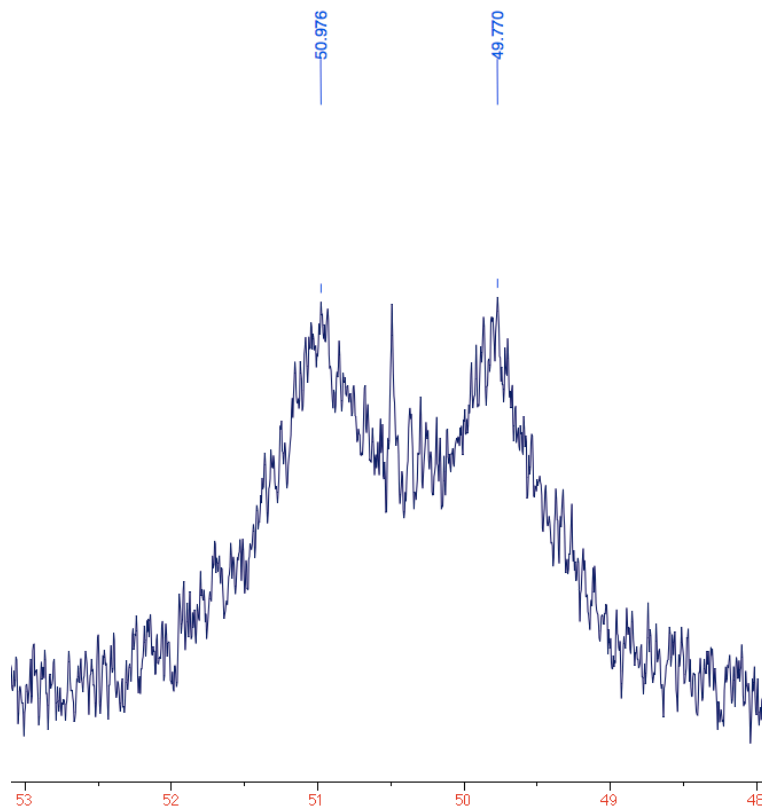


**Figure 2-16:**  $^{31}\text{P}$  NMR of alternating-ROMP assembled catalyst-organic framework **28**. (161.2 MHz, 27°C,  $\text{CD}_2\text{Cl}_2$ .)

Figure 2-17 shows the  $^1\text{H}$  NMR spectra of a ROMP assembly of **28** at room temperature over the course of 24 hours. This figure shows the consumption of COE and the norimido olefin moieties over the course of polymerization and the growth of the bridgehead proton signals at  $\delta = 3.1$  and 3.4 ppm. Figure 2-17 also shows the  $^1\text{H}$  NMR after polymerization is complete, with the indicated bridgehead protons. These were first noted by Ralph *et al*<sup>88</sup>, and are a general indicator for complete polymerization.

Investigations into the nature of the polymerization were attempted, after a sample of **22** was prepared, followed by addition of the spacer monomer COE and **1**. Respective  $^1\text{H}$  and  $^{31}\text{P}$  NMR spectra were recorded over time during polymerization at room temperature. From *in situ* peak-height comparison of alkene signals, a general rate of reaction can be determined. A  $^1\text{H}$  NMR spectrum recorded minutes after mixing the metathesis catalyst and the solution of **22** and COE showed that polymerization had already begun at room temperature. The broad signal at  $\delta = 3.1$  ppm that corresponds to the bridgehead protons, labeled b and c in Figure 2-17, indicates that polymerization is occurring. After three hours reaction time, 52.5 % of the norimido unit had been consumed and only 28.8 % of the *cis*-cyclooctene had. While less COE has been consumed, there was initially three times the amount of COE present in comparison to the norimido moiety. When normalized, the ratio of COE to norimido consumed is  $\sim 1.7$ . This indicates that the polymerization is not truly alternating, as approximately 5 COE are consumed for every 3 norimido units; not 1 : 1 as was evidenced by Ralph<sup>88</sup>. After 7 hours reaction time at room temperature, 80.2 % of the norimido and 55.5 % of the COE monomer units were consumed, again corresponding to a normalized ratio of  $\sim 1.7$ . The entirety of the norimido units had been consumed within 24 hours, whereas only 80% of the spacer monomer

COE was. At the end of polymerization the ratio of COE to norimido consumed was ~2.4.

During polymerization a peak was present at  $\delta = 5.4$  ppm in the  $^1\text{H}$  NMR spectrum that is the same shape and chemical shift as poly(COE) made by ROMP<sup>105</sup>. The intensity of this peak increased as the alternating ROMP assembly proceeded. The consumption of the norimido groups was nearly complete after 7 hours, and at this point, the peak at 5.4 ppm began to grow in more quickly, with a comparable increase in the rate of consumption of COE. We propose that the peak at 5.4 ppm is from the olefin groups connecting COE monomers that have been polymerized by ROMP. These signals may arise from two COE's joined during the alternating ROMP assembly, or by ROMP of COE alone as a side reaction during the alternating-ROMP assembly. We note that small amounts of poly(COE) are present in the MeOH washes after the alternating-ROMP assembly is complete. Thus, ROMP of only COE occurs to some extent during the alternating ROMP assembly. The amount of poly(COE) present in the reaction mixture is relatively small, however, showing that most of the metathesis catalyst is involved in the alternating-ROMP assembly. Once all the norimido groups are incorporated into the framework, the remaining COE begins to polymerize. As stated above, the ratio of COE to norimido groups consumed during the alternating-ROMP assembly, that is before depletion of the norimido groups, is ~1.7 : 1. This ratio shows



that the degree of alternation is not 1 : 1 for this system. As stated above, most of the remaining COE reacted after the alternating assembly is complete, resulting in a ratio of COE consumed to norimido groups reacted of ~2.4. We therefore postulate that the ratio of COE to norimido groups within the framework is ~1.7 : 1, and that some portion of the remaining COE was grafter to the outside of the framework as poly(COE). In parallel, a small amount of the COE is consumed to make pure poly(COE).

There were also signals at  $\delta = 4.9$  ppm (doublet of doublets) and  $\delta = 5.8$  ppm (multiplet) present in all the spectra recorded. This pattern is indicative of a terminal alkene group that likely formed by metathesis reactions between COE and the residual ethylene found in solution after preparation of **22**. The identity of the terminal alkene was confirmed in an experiment wherein COE was polymerized with **1** in a 120 : 1 molar ratio at room temperature. Figure 2-18 shows the  $^1\text{H}$  NMR spectrum recorded 10 minutes after mixing, showing the formation of poly(COE), labeled b. The next spectrum was recorded after excess  $\text{C}_2\text{H}_{4(g)}$  was added to the polymerization reaction. The spectrum recorded after the addition contained the same peaks at  $\delta = 5.8$  and 4.9 ppm, labeled c. One reason that the degree of alternation is ~1 : 1.7, and not 1 : 1 for this system is the steric hindrance between the opposite ends of the dimer (**22**, Scheme 2-4). More specifically, the crystal structure of the Ir analogue,  $\text{IrCl}((S)-$

$\text{BINAP})_2$  is known<sup>106</sup>. This compound is not planar; instead it is “butterfly shaped”, with the angle between the coordination planes of the Ir centres being  $126^\circ$ . It is likely the Rh dimer **22** has a similar structure. This butterfly shape imparts a greater degree of steric hindrance about the norimido groups in **22**, that is not present in the Ru monomer **13** used by Ralph. We propose that the greater degree of hindrance in **22** decreases the net reactivity of the norimido groups to ROMP relative to COE, resulting in more incorporation of COE into the framework.

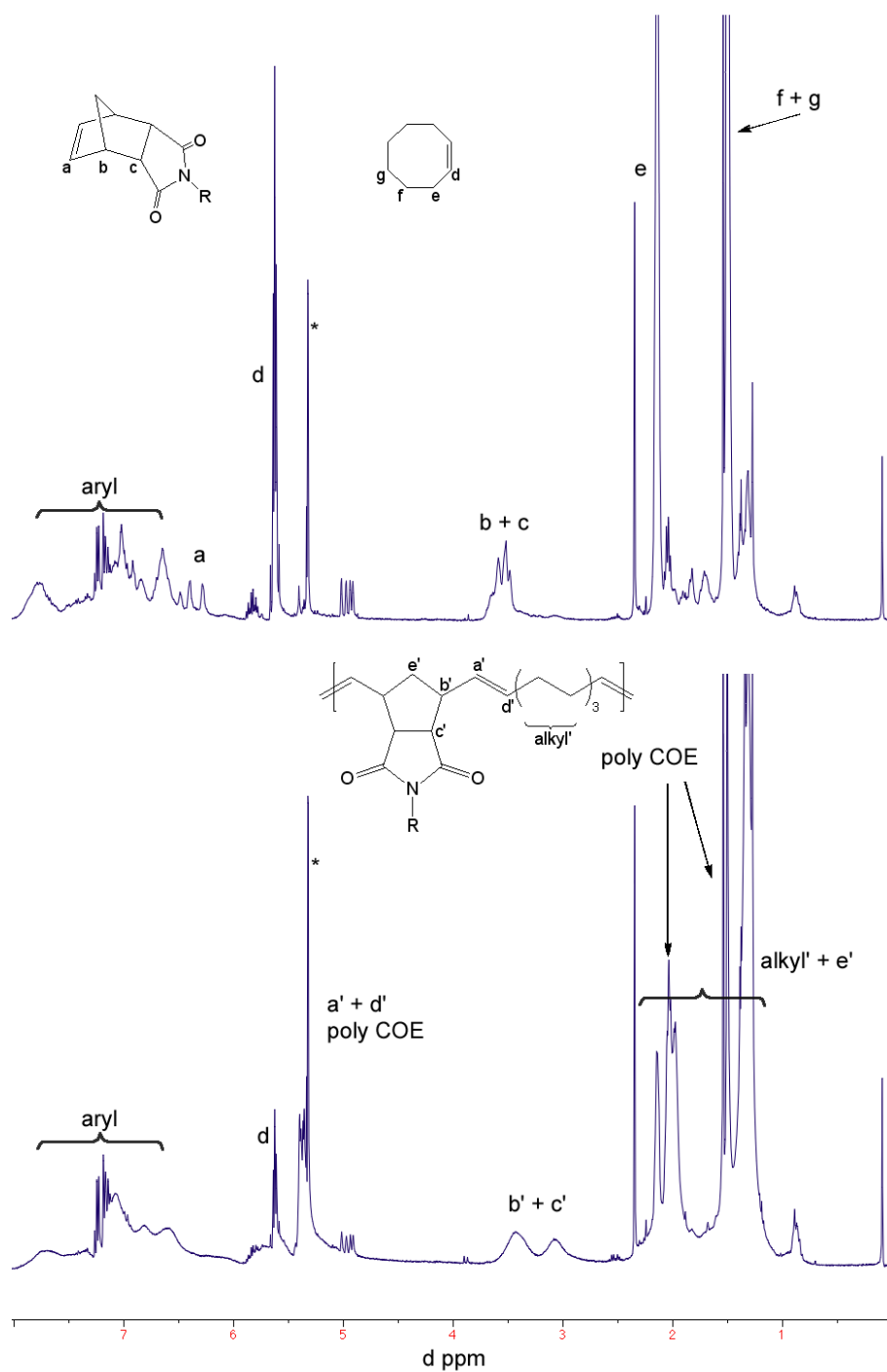
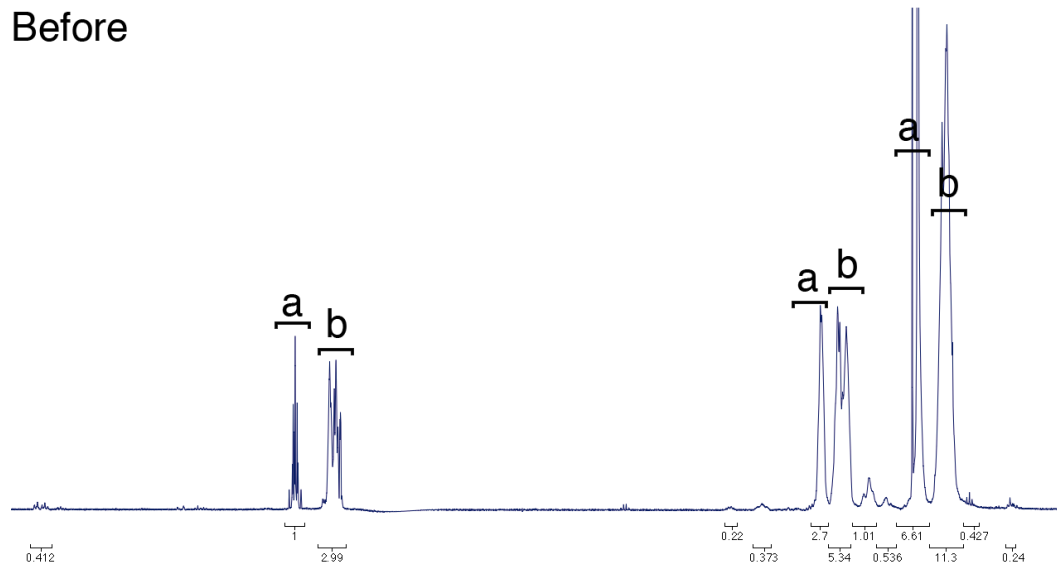


**Figure 2-17:**  $^1\text{H}$  NMR Spectra during alternating-ROMP assembly of **22** and COE with **1** at RT a) 0 hr (before addition of Grubbs' I), b) 24hr. \* = Residual  $\text{CH}_2\text{Cl}_2$ . (399.8 MHz,  $\text{CD}_2\text{Cl}_2$ , 27.0°C)

Before



After

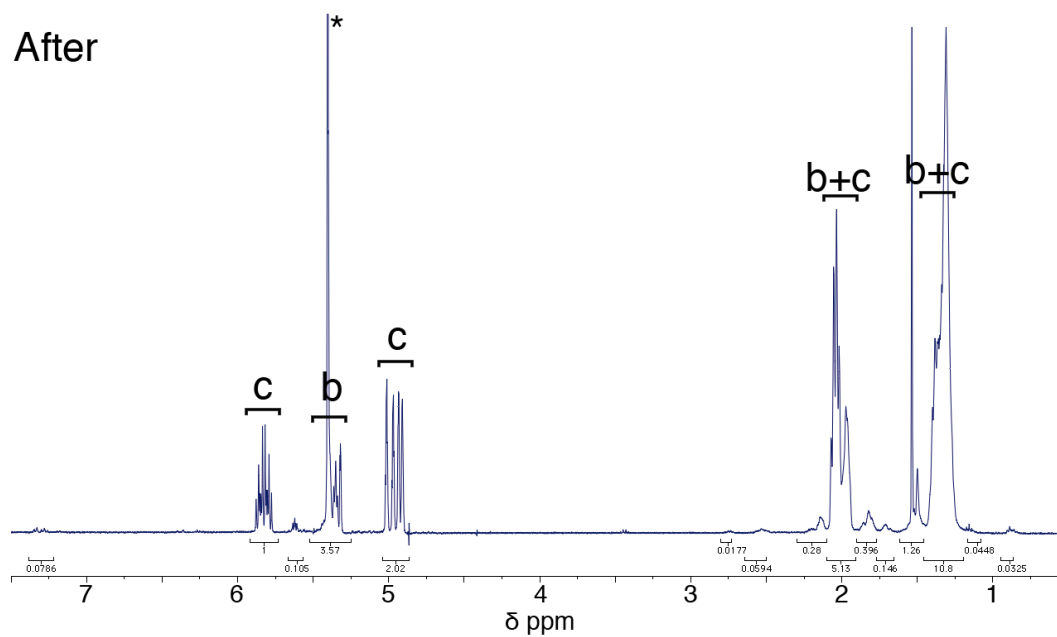


**Figure 2-18:**  $^1\text{H}$  NMR spectra of COE polymerization before and after addition of excess  $\text{C}_2\text{H}_4(\text{g})$ . (399.8 MHz,  $\text{CD}_2\text{Cl}_2$ ,  $27.0^\circ\text{C}$ )

The methods we used to obtain a rough characterization of the dimer and polymer for this preliminary study include elemental analysis,  $^{13}\text{C}$  NMR spectroscopy, and mass spectrometry. Efforts to obtain mass spectra, either the metal-containing monomer **22**, or the catalyst-organic framework **28** were not successful. The methods we attempted included ESI-MS and MALDI-TOF mass spectrometry. It was found that **22** would not ionize through positive mode electrospray ionization (ESI-MS(pos)); the only  $m/z$  detected was that attributed to THF. That is, no ions that could reliably be attributed to **22** were detected through ESI-MS; MALDI-TOF mass spectrometry on **22** was also unsuccessful. Specifically, although ionization events occurred, the highest  $m/z$  species detected corresponded to a dimer with one phosphorous of one of the (*R*)-5,5'-dinorimido-BINAPs in the dimer being oxidized and one  $\mu\text{-Cl}$  being abstracted,  $[\text{Rh}_2\text{Cl}(\text{N-BINAP})(\text{N-BINAPO})]$ . Attempts to carry out mass spectrometry (ESI-MS, MALDI-TOF) on the catalyst organic framework **28** did not result in observation of ions; the only  $m/z$  detected were attributed to THF in the case of ESI-MS. Elemental analysis indicated that the framework **28** was comprised of 70.31 % carbon, 1.92 % nitrogen and 7.23 % hydrogen. Assuming the ratio of COE to monomer incorporated into the framework was 12 : 1 (i.e., all the COE added was incorporated into the framework), the calculated values are 75.05 % carbon, 1.59 % nitrogen, and 7.44 % hydrogen. The preliminary NMR studies described

as above estimate that the amount of COE incorporated into the framework is between 1.7 and 2.4 COE per norimido olefin. Considering the notorious difficulties associated with obtaining elemental analyses of polymers, at best, we can conclude that the results from the NMR analysis and the elemental analysis are consistent, but not conclusive. Although more thorough characterizations may be possible using gel permeation chromatography (GPC), dynamic and static light scattering experiments, as well as TEM on a lacey carbon substrate, such studies are beyond the scope of this dissertation, which was to prepare, carry out preliminary analysis, and then evaluate the activity of the desired catalyst-organic framework.

After alternating-ROMP assembly of **28** was complete, the reaction mixture was diluted with  $\text{CH}_2\text{Cl}_2$  to prevent precipitation, and to help with deposition of the framework on a  $\text{BaSO}_{4(s)}$  support. Mass transport to and from the active sites is a common issue in heterogeneous catalysis because the polymer matrix often impedes diffusion<sup>107</sup>. By supporting the framework as a thin film on  $\text{BaSO}_4$ , our objective was to minimize the diffusion distance through the polymer backbone. Also, the density of active sites in the catalyst-organic framework, defined roughly as the ratio of catalyst to spacer monomers, is high, relative to catalytic polymers made by radical polymerizations. The diluted reaction mixture was added to  $\text{BaSO}_4$ , and the solvent was slowly evaporated under reduced pressure.

Average rhodium loadings of this catalyst are  $1.1 \times 10^{-5}$  mol Rh per gram of support. The supported polymer catalyst was washed with methanol to remove any low molecular weight poly(COE).  $^{31}\text{P}$  and  $^1\text{H}$  NMR show that the washings contained only poly(COE), indicating that **22** was entirely consumed during alternating-ROMP assembly and incorporated into the catalyst-organic framework.

#### **Section D: Investigations into the Hydrogenation of Esters using a Supported Noyori-Type Ketone Hydrogenation Catalyst.**

The primary objective for the preparation of immobilized catalysts is reuse, or the application of the catalyst system to a flow reactor. The reduction of ester substrates to primary alcohols is considered a difficult transformation<sup>108</sup>, and often requires use of stoichiometric main-group hydride reagents. The use of catalyst hydrogenation would eliminate the need for stoichiometric Al-H and B-H reagents, which can react violently with water, and upon use, generate stoichiometric amounts of waste. Milstein *et al.* reported the hydrogenation of esters using a Ru-pincer ligand catalyst to hydrogenate different unactivated esters under low pressures, but also at high temperatures (100 equiv ester, 115°C, 5.3 atm H<sub>2</sub>, 4-24hr, 10.5-100% yield)<sup>109</sup>. More recently, Saudan *et al.* have reported several homogeneous Ru catalyst systems that are capable of high turnover frequencies and numbers under moderately high

temperatures and pressures in the presence of large amounts of base (2000-10000 equiv, 60-100°C, 10-50 atm, 15min–16hr, 20–500 equiv base, 47-100% yield)<sup>110-112</sup>. It has been shown previously in our laboratory that the Noyori catalyst, *trans*-[Ru((*R*)-BINAP)(H)<sub>2</sub>((*R,R*)-dpen)], catalytically hydrogenates esters under very mild conditions (60 equiv ethyl hexanoate, -20°C, 4 atm, 4hr, 4 equiv KN(Si(CH<sub>3</sub>)<sub>3</sub>)<sub>2</sub>, 23% yield) with esters, but suffers from product inhibition by corresponding alcohol products<sup>113</sup>. We note that lactones are less susceptible to product inhibition than acyclic esters. This product inhibition is most likely through the addition of the formed primary alcohols to the Ru-amide formed during catalysis, yielding a Ru-alkoxide. These primary Ru-alkoxides are more stable than the secondary Ru-alkoxides generated from ketone hydrogenation, and ketones are intrinsically more reactive than esters. The combination of these phenomena results in product inhibition. The aim of this project was to avoid product inhibition by isolating and reusing the catalyst as part of a framework.

The heterogeneous hydrogenations of ester substrates were done in the following manner. Batch reactions were set up in a stainless steel autoclave, which was charged with the supported catalyst, followed by the ester (50 equiv), and then base (5 equiv) in THF. The vessel was sealed, pressurized to 36 atm H<sub>2(g)</sub> and heated at 50°C with vigorous stirring. The <sup>1</sup>H NMR spectrum recorded of an aliquot showed complete conversion



after 23 hours. Thus, 50 turnovers were completed in the first run. A procedure was then developed to isolate and reuse the catalyst, where the supported catalyst was allowed to settle, and the reaction mixture was removed through inverse filtration. Then, the catalyst was rinsed with two portions of THF, stirred vigorously, and the solution was removed through inverse filtration. The reactor was then charged with another set of substrate and base, and the reaction was resumed. Remarkably, the catalyst sustained a total of 7 reuses; however, there was a decrease in activity that was apparent upon the first reuse. The results from this experiment are shown in Table 2-4.

The catalyst suffered from approximately 30% loss in activity between runs 1, 2, and 3. This decrease in activity is partially reversed by use of 10 equiv of potassium *t*-butoxide after the third run. The additional base reacts to deprotonate one of the amine groups on dpen, followed by elimination of alkoxide to generate the Ru-amide. We noted that this increased amount of base did not permanently increase the activity of the catalyst; losses of ~30% were noted for each subsequent run after run 5. Although very promising at the time, this novel reactivity was difficult to reproduce in the laboratory, and attempted hydrogenations of other substrates were not successful.

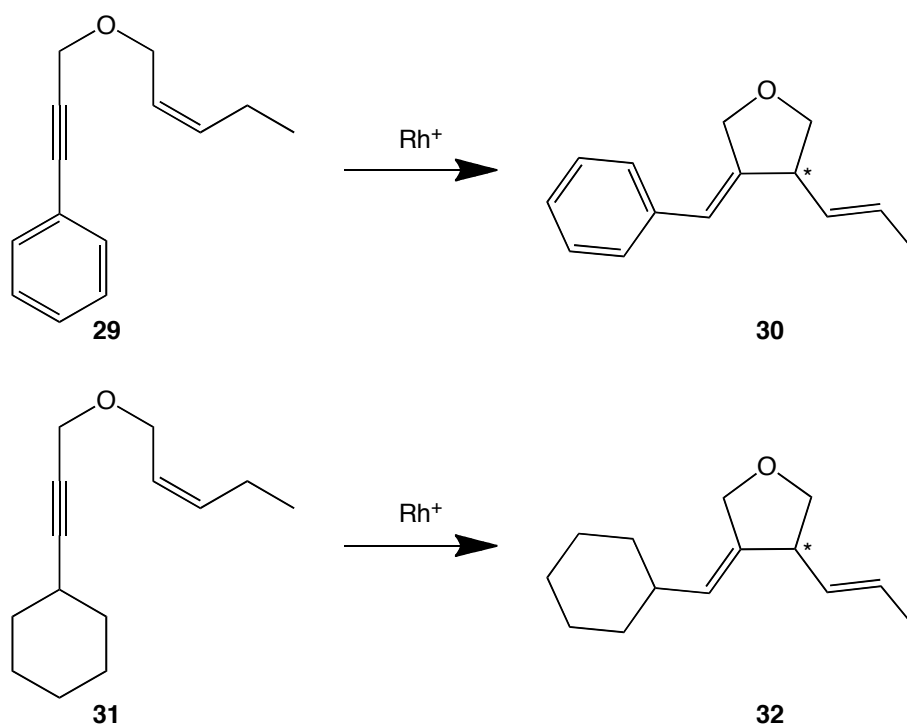
**Table 2-4:** Hydrogenations of Methyl Benzoate in THF, through reuse of Catalyst-Organic Framework.

Run #	Temperature (°C)	Time (h)	% Conversion <sup>a</sup>
1	50	23	>99.0
2	50	23	70.0
3	50	23	48.0
4 <sup>b</sup>	50	23	88.4
5	50	23	94.0
6	50	23	65.2
7	50	23	21.0
8	50	23	14.1

<sup>a</sup>Conversion determined by <sup>1</sup>H NMR spectroscopy. <sup>b</sup>For this run, and all subsequent runs, 10 equiv of <sup>t</sup>BuOK were used to compensate for the initial decrease in activity.

## **Section E: Investigations into the Efficacy and Reusability of the Immobilized Catalyst for the Cycloisomerization of 1,6-Enynes**

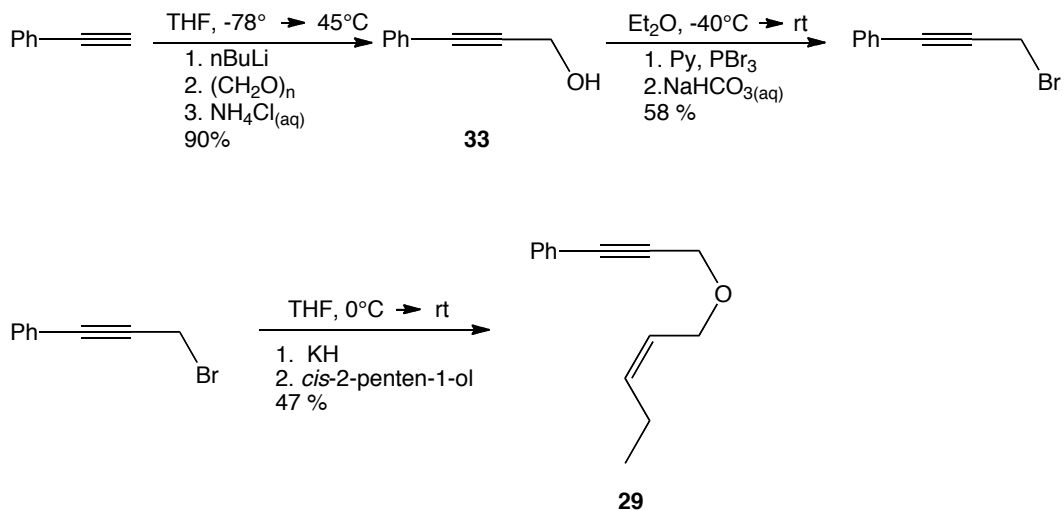
The substrates used in the studies of the efficacy of the catalyst are shown in Scheme 2-9. They were synthesized following a modification of the literature procedure for the preparation of the phenyl substrate **29**<sup>80</sup>. The literature synthesis, although functional, suffered from the difficult purification of nearly all the intermediate and final products. Upon modification of the synthesis, purification became far simpler as one of the reactants used in the modified preparation is volatile. This volatility makes the chromatography used to purify the final substrate molecule easier, as one of the unreacted starting materials can be removed through evaporation under reduced pressure. As an added benefit, the new synthetic method chemically modified the common reagent used in both syntheses, allowing for a larger stock of substrates while minimizing the number of transformations required for the given alkyne.



**Scheme 2-9:** 1,6-Enyne substrates used in the evaluation of the catalyst organic framework.

To date, the preparation of cyclohexyl substrate, ((*Z*)-3-pent-2-enyloxy-prop-1-yl)cyclohexane (**31**), and the subsequent cycloisomerization to the product (*Z*)-3-(cyclohexylmethylene)-4-((*E*)-prop-1-enyl)tetrahydrofuran (**32**), have not been reported in literature. To the best of our knowledge, **31** has only been used for intramolecular cycloisomerizations in our laboratory. The best reported homogeneous catalyst for the cycloisomerization of **29** is generated from 10 mol% each of  $[\text{Rh}(\text{COD})_2]\text{BF}_4$  and (*R*)-BINAP in 1,2-dichloroethane at 50°C, producing **30** in 93 % yield and 99 % *ee*<sup>80</sup>; however, this corresponds to a poor TON

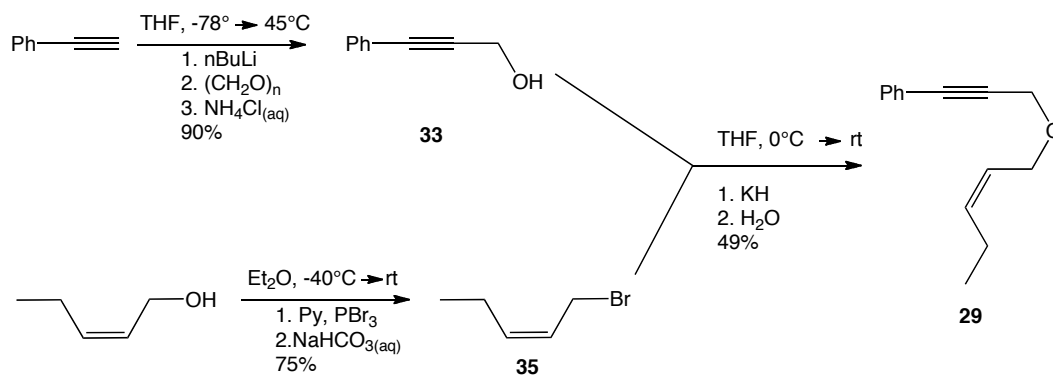
of 9.3. For catalysis to be considered industrially viable, TON of 1000 or higher per batch reaction are on the low end of acceptability<sup>114</sup>.



**Scheme 2-10:** Literature Procedure for the Synthesis of ((*2Z*)-3-Pent-2-enyloxy-prop-1-yl)benzene, **29**.

As seen in Scheme 2-10, the literature procedure for the synthesis of **29** requires that 3-phenyl-2-propyn-1-ol (**33**), prepared from phenylacetylene, be converted into the corresponding bromide, and the bromide is reacted with *cis*-2-penten-1-ol to form **29**. This was initially adapted for the synthesis of **31**, through preparation of 2-cyclohexyl-2-propyn-1-ol (**34**) from cyclohexylacetylene. A more efficient procedure is to convert *cis*-2-penten-1-ol into the corresponding bromide instead. *Cis*-2-penten-1-ol is commercially available, inexpensive, and can be converted to the bromide, *cis*-2-penten-1-bromide (**35**) and stored in gram quantities. **35** can then be reacted with a number of different propargyl

alcohols, to prepare a number of substrates with one less step, rather than individually converting each propargyl alcohol into the bromide. Finally, **35** is volatile, so an excess was used to ensure completion of the ether formation. The excess **35** can simply be removed by vacuum. This modified procedure is illustrated in Scheme 2-11.



**Scheme 2-11:** Modified Preparation of (2*Z*)-3-Pent-2-enyloxy-prop-1-yl)benzene, **29**.

Previous students in this group have prepared immobilized catalyst-organic frameworks based upon **21** for the cycloisomerization of **29** and **31**; however these frameworks were either totally inactive, or suffered from rapid loss of activity. Initial studies involved the use of 1,2-dichloroethane (DCE) or tetrahydrofuran (THF) as solvent. In the case of DCE the catalyst polymer dissolved, causing notable rhodium leaching. THF as solvent resulted in no observed catalytic activity whatsoever. The system was active, however, in 1,4-dioxanes. Although DCE is the favoured solvent for homogeneous cycloisomerization reactions, and 1,4-dioxane

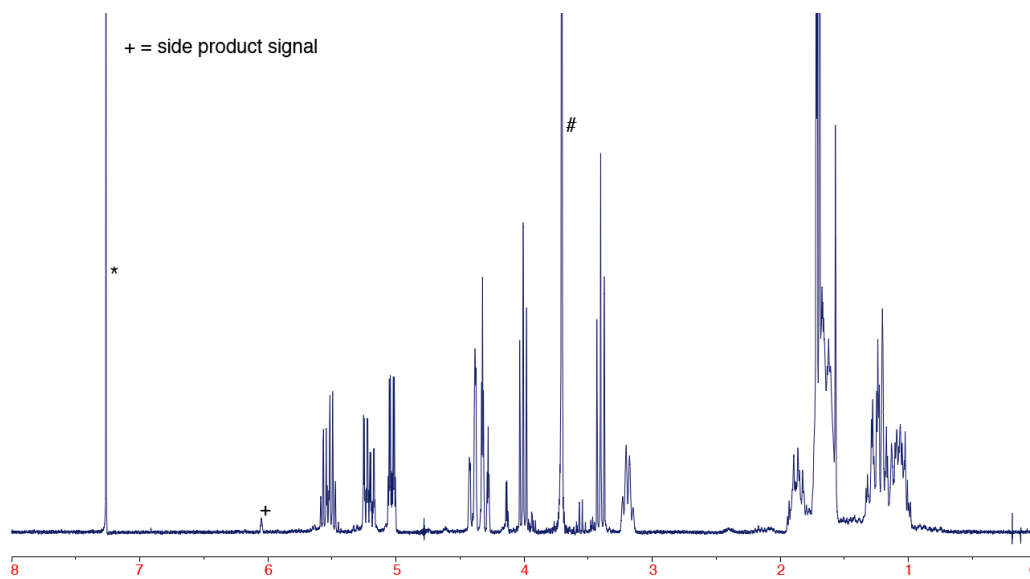
exhibits poor activity as a homogeneous solvent, the activity of the cyclization using the heterogeneous system was greater for 1,4-dioxane than for DCE. 1,4-dioxane displays lower toxicity when compared to 1,2-dichloroethane; maximum concentrations allowed in pharmaceuticals are 380 and 5 ppm respectively<sup>115</sup>.

Initial batch reactions were carried out with a semi-sacrificial run of 20 equiv (per rhodium) of substrate **31**, added to the supported catalyst, followed by 1,4-dioxane. This loading of 20 equiv of substrate per rhodium is already twice the loading of common literature reactions. The loading of substrate was to act as a means of preparation of the catalyst for later, silver-free runs, as well as to swell the polymer if that was required. Two equiv (per rhodium) of silver (I) hexafluoroantimonate ( $\text{AgSbF}_6$ ) were added as a slurry in this solvent.  $\text{AgSbF}_6$  is the preferred additive for this cyclization<sup>80</sup> because the  $\text{SbF}_6^-$  anion is weakly coordinating. The steric hindrance combined with the poor coordinating ability of the ion means that it will not interact notably with the rhodium centres during catalysis. After three hours at 60°C <sup>1</sup>H NMR spectroscopy showed complete conversion to the cyclized product, **32**, with minimal side product formation, as shown in Figure 2-19. To our knowledge, this is the first successful cycloisomerization of **31**.

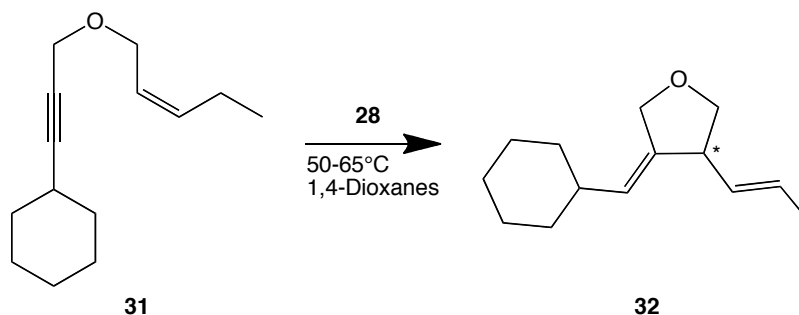
For these reactions a procedure was devised to isolate the immobilized framework **28** without loss in activity. The catalyst was

washed several times with dioxanes, without letting the catalyst/support dry. It has been found that the catalyst, after an initial run of 20 equiv of substrate, was able to handle a loading upwards of 100 equiv per run, for a total of six runs, without additional AgSbF<sub>6</sub>. Although the activity was higher than other previous attempts at making this catalyst; there was still a decrease in activity over time. This drop in activity was countered by increasing the reaction temperature, as shown in Table 2-5. There was no appreciable difference in quality of products over the runs, and the catalyst achieved 620 turnovers over the seven runs done with the substrate, with excellent *ee*. The <sup>1</sup>H NMR spectrum of the reaction product **31** is shown in Figure 2-19. The reaction was only stopped when the substrate stock had been depleted. A final run was attempted, with the methyl-containing substrate (2*Z*)-1-(2-butyn-1-yloxy)-2-pentene), which was only used to indicate that the catalyst was not deactivated. This was the first attempt at optimization of this system, and affords remarkably higher turnovers than the homogeneous system reported to date in the literature.





**Figure 2-19:**  $^1\text{H}$  NMR spectrum of **32** as prepared through reuse of catalyst-organic framework **28**. (399.8 MHz,  $\text{CDCl}_3$ ,  $27.0^\circ\text{C}$ ) \* = residual  $\text{CHCl}_3$ , # = residual 1,4-dioxanes, + = side product signal.

**Table 2-5:** Cycloisomerization of **31** through reuse of Catalyst Framework**28<sup>a</sup>**

Run Number	Temperature (°C)	Time (h)	Conversion (%) <sup>c</sup>
1 <sup>b</sup>	60	3	>99
2	50	18	>99
3	50	22.5	>99
4 <sup>d</sup>	50	22	<99
	65	4	>99
5	65	19.5	>99
6	65	24	>99
7	65	24	>99

<sup>[a]</sup>The reaction was carried out in 0.2M **31** in 1,4-dioxane under the following conditions: Sub./Rh. = 100/1 except for run 1. <sup>[b]</sup>This was carried out in 0.1M **31** in 1,4-dioxane at 60°C under the following conditions: Sub./AgSbF<sub>6</sub>/Rh. = 20/2/1. Temperature was decreased to 50 after the initial run. <sup>[c]</sup>Conversion determined by <sup>1</sup>H NMR. <sup>[d]</sup>Reaction was incomplete after 22h at 50°C, so the reaction was warmed to 65°C for 4 hours.

We found that the *ee* of **32** could not be determined with chiral HPLC or GC, so a procedure utilizing chiral NMR shift reagents was devised. Europium tris[3-(heptafluoropropylhydroxymethylene)-(+)-camphorate] (**36**) was repeatedly added to a sample of racemic **32** in benzene- $d^6$ . Upon addition of **36**, the triplet at  $\delta = 3.41$  ppm shifts downfield, and initially broadens to an apparent singlet. Upon further additions, this singlet shifts to approximately  $\delta = 4.5$  ppm and begins to split into an apparent doublet, due to separation of enantiomers of **32**. Further additions drive this doublet downfield to  $\delta = 6.4$  and  $6.3$  ppm, where the two signals show 1 : 1 integration. This gradual shift of the signal at  $\delta = 3.41$  upon addition of **36** is shown in Figure 2-20. Upon addition of **36** to **32** prepared using catalyst-organic framework **28**, only a broad, apparent singlet is observed, without detectable minor enantiomers, when compared to the racemic sample of **32** prepared (Figure 2-21). The small peak at  $\delta = 6.4$  ppm is attributed to a side product, as upon addition of racemic **32** (Figure 2-21c) the signals attributed to **32** shift upfield, whereas the signal in question does not. From these experiments, we conclude that the *ee* of compound **32** is over >99%, and this value is only limited by the signal: noise ratio of the NMR spectra.

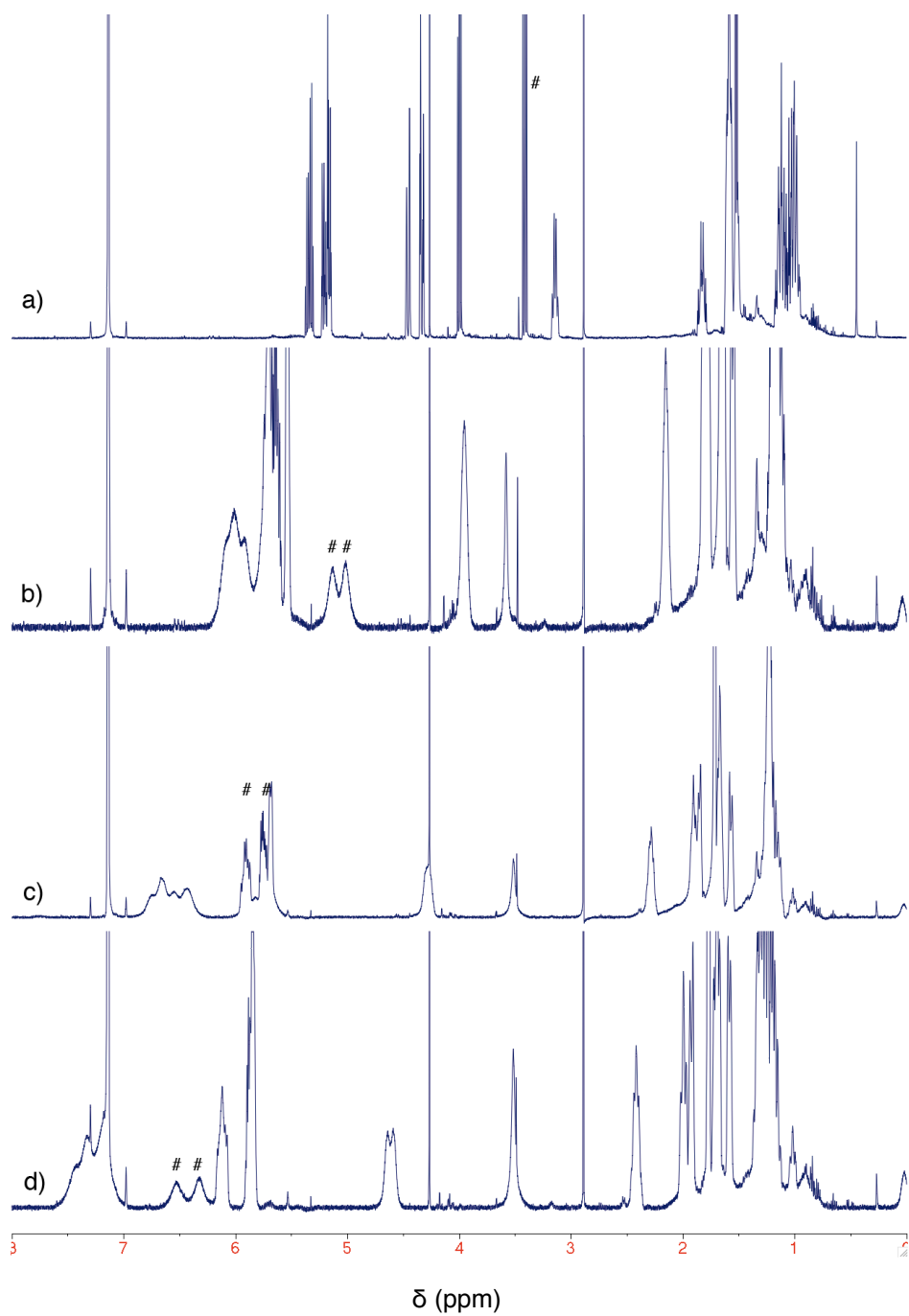


**Figure 2-20:** Effects of addition of **35** in the  $^1\text{H}$  NMR spectra of a sample of  $(\pm)$ -**32**. (500 MHz,  $\text{C}_6\text{D}_6$ ,  $27^\circ\text{C}$ ). a) 0 mol %; b) 4 mol %; c) 6 mol %; d) 8 mol %.

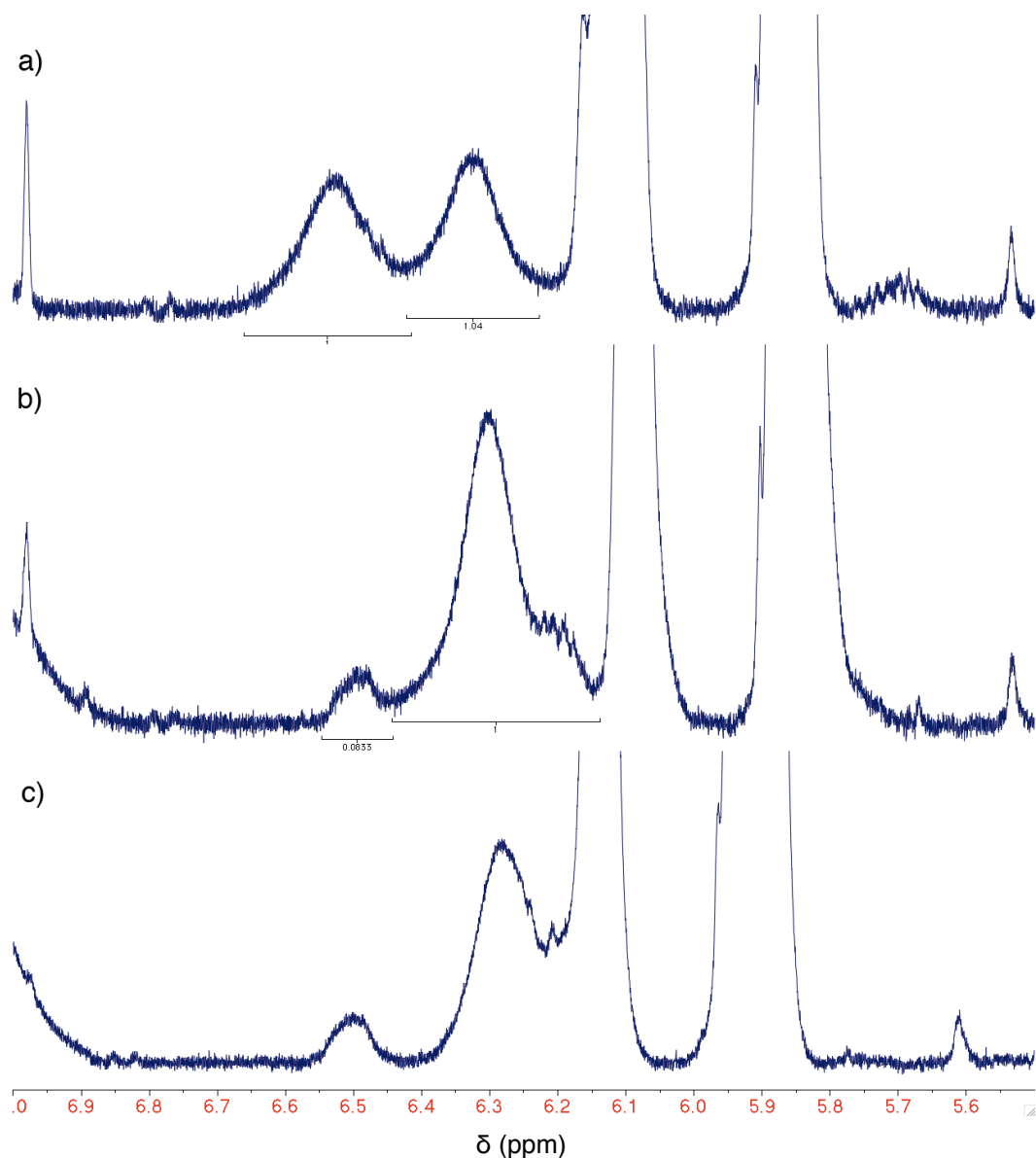


**Figure 2-21:** Determination of the *ee* of **32** using ~8 mol % of **35** through  $^1\text{H}$  NMR spectroscopy. (500 MHz,  $\text{C}_6\text{D}_6$ ,  $27^\circ\text{C}$ ) a) racemic **32** prepared using  $[\text{Rh}(\text{NBD})_2]\text{BF}_4$ ; b) **32** prepared using framework **28** as the catalyst; **32** as prepared in b with racemic **32** added.

Catalyst-organic framework **28** was also active towards the cycloisomerization of **29**. These experiments were carried out with the

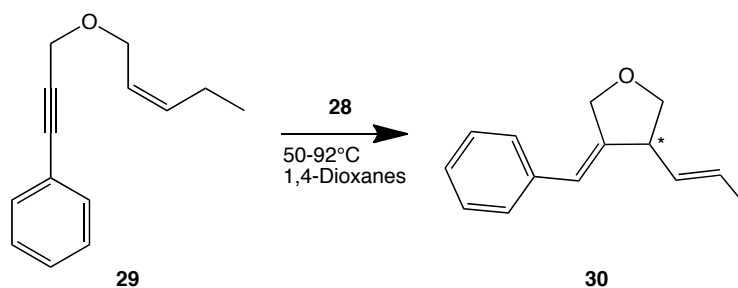
same procedure as for **31** and the results are shown in Table 2-6. As was reported in the literature, the rate of reaction and overall TON were lower for **29** than for **31**. This slower rate of reaction may be due to competitive  $\eta^6$ -binding of the aromatic ring on the substrate or product to Rh. The  $\eta^6$ -coordination mode is not possible with **31**. Accordingly, higher temperatures and reaction times are required for the cyclization of **29** than are needed for **31**. Chiral GC data of racemic samples of **30** were compared to the samples of **30** prepared using **28**. The *ee* for **30** prepared using **28** was greater than 99.9%, with the peak from the minor product not being detectable within the rejection limits of the GC (0.025% of major peak integration). In total, 396 turnovers were achieved for the phenyl substrate, with the *ee* being >99.9% for each run.

Chiral GC-MS was also attempted on **30** and **32**, using the same conditions as previously noted for **30**. These experiments further confirm the identities of the peaks as had been determined through previous spiking experiments, and also provide low-resolution mass spectra of those peaks, which confirmed the parent ion of substrate **31** and cyclization product **32** to be at a *m/z* of 206. The peaks attributed to substrate **29** and cyclization product **30** were found at 200, as was expected due to the lower molecular mass for the phenyl-containing substrate and product. The experimentally obtained *m/z* values are in

accordance with the expected  $m/z$  values. As previously noted, no  $ee$  data for **32** was obtained from these experiments.

**Table 2-6:** Cycloisomerization of **29** through reuse of Catalyst Framework

**28<sup>a</sup>**



Run Number	Temperature (°C)	Time (h)	Conversion (%) <sup>c</sup>	$ee^d$ (%)
1 <sup>b</sup>	60	3	>99	>99.9
2	50	18.5	18	
	70 <sup>e</sup>	42	96	>99.9
3	70	24	47	
	70	45	88	
	70	48	91	>99.9
4	80	22.25	48	
	80	45.5	81	
	80	51	85	
	80	69.5	97	>99.9
5	92	46	53	>99.9

<sup>[a]</sup> The reaction was carried out in 0.1 M solution of **29** in 1,4-dioxane under the following conditions: Sub./Rh. = 20/1; except for run 1.

<sup>[b]</sup> Sub./AgSbF<sub>6</sub>/Rh = 20/2/1; after the first run, temperature was decreased to 50°C. <sup>[c]</sup> Conversion determined by <sup>1</sup>H NMR. <sup>[d]</sup>  $ee$  determined by chiral GC analysis. <sup>[e]</sup> After the decrease to 50°C, the temperature was increased as needed for completion of reaction.

Investigations were then carried out on the utilization of solvents less toxic than 1,4-dioxanes for the cycloisomerization of **31**; cyclopentylmethyl ether (CPME), 2-methyltetrahydrofuran (2MeTHF), 1,2-dimethoxyethane (DME) and methanol. The procedure for these experiments was equivalent to that for the reuse studies, with the exception of the catalyst loading being 1 mol % Rh instead of 5 mol % Rh. In every case the first run was successful; the supported catalyst cycloisomerized the substrate into product with greater TON offered than the homogeneous system. Although successful in terms of TON for the first run, any reuse attempted after the initial run did not result in cycloisomerization. The most successful runs were done with 2-MeTHF as solvent. Results from this set of experiments are shown in Table 2-7. A possible source for the allowed reuse of the catalyst in 1,4-dioxanes, but not in other solvents, is coordination of the solvent itself to the active centres. Coordination of THF to rhodium is known<sup>116</sup>, as well as the coordination of 1,4-dioxanes<sup>117</sup>. As a result, there is the inherent possibility of coordination of 1,4-dioxanes to unsaturated coordination sites in the absence of substrate or product. 1,4-dioxanes would be a better ligand than 2-MeTHF, as the Rh is stabilized more through one bidentate 1,4-dioxane molecule than through two monodentate 2Me-THFs. There is also the possibility of bridging  $\eta^6$ -phenyl rings from the opposing BINAP-type moiety in the polymer chain, as previously discussed<sup>52</sup> (Figure 2-15), that could form in the absence of



coordinating substrate or product. However, given the inability to reuse the framework to the same scale as was observed in 1,4-dioxanes, this  $\eta^6$ -phenyl coordination is unlikely to be the cause of reusability.

**Table 2-7:** Cycloisomerization of **31** In Different Solvents.

Run #	Solvent	Loading Sub:Ag:Rh	Temperature (°C)	Time (h)	Conversion (%) <sup>a</sup>
1	CPME	100 : 2 :1	50°C	19.5	50
2	CPME	100 : 2 :1	50°C	19.5	0
1	2MeTHF	100 : 2 :1	50°C	19.5	100
2	2MeTHF	100 : 2 :1	50°C	3	40
2b <sup>b</sup>	2MeTHF	200 : 2 :1	50°C	23	67
3	2MeTHF	100 : 2 :1	50°C	23	36
1	DME	100 : 2 :1	50°C	18	50
1b <sup>c</sup>	DME	100 : 2 :1	70°C	5.75	100
2	DME	100 : 2 :1	70°C	19	0
1	MeOH	100 : 2 :1	50°C	20.5	64
2	MeOH	100 : 2 :1	50°C	20.5	0

All reactions were carried out in 0.2 M solution of **31** in the shown solvent. Temperature and loadings are shown in the table. <sup>[a]</sup>Conversion determined by <sup>1</sup>H NMR <sup>[b]</sup> This run is denoted as such because another 100 equiv of substrate was added to the previous reaction flask without removal of products. The 67% yield (134 turnovers) includes the 40 turnovers from Run 2. <sup>[c]</sup>The temperature of Run 1 with 1,2-DME was increased to 70°C for another 5.75 hours to yield 100 % conversion.

Once the initial optimizations for reusability and solvent choice were completed, the initial activity of catalyst-organic framework **28** was tested to determine if a sacrificial initial run was required. The first batch reaction requires less than one fifth of the time of all subsequent runs; it is believed that the reuse procedure used was possibly deactivating the catalyst. To test this theory, a cycloisomerization reaction was set up using an initial loading of 100 equiv of **29** (per Rh), in 1,4-dioxanes at 70°C. Differing from the previous experiments was the amount of silver (I) hexafluoroantimonate, at 5 eq (per Rh), the amount used was increased due to the low solubility of the silver salt in the solvents used. An aliquot was taken at 150 minutes; the <sup>1</sup>H NMR spectrum recorded confirmed that the reaction was complete. Instead of washing the catalyst and attempting reuse, the reaction was charged with another 100 equiv of **29**. Another aliquot was taken at 135 minutes, and this was again seen to be nearly complete by <sup>1</sup>H NMR spectroscopy, with ~180 turnovers. Another 100 equiv of **29** were added to the vessel, and the reaction was maintained overnight. Another aliquot was taken and completion of the reaction was noted through <sup>1</sup>H NMR spectroscopy after another 15 hours. The catalyst was not rinsed with 1,4-dioxane, instead the reaction mixture was removed through inverse filtration, and the vessel was charged with 100 equiv **29**, and 1,4-dioxane. An aliquot removed at 5.5 hours indicated 84% conversion by <sup>1</sup>H NMR spectroscopy, so an additional batch of substrate

was added (100 equiv), and the reaction was allowed to run overnight. After 17 hours, an additional 98 turnovers were noted. Total TON for this reaction reached 482; a number comparable to that of previous reuse. These studies show that a sacrificial run to induce catalytic activity through polymer swelling of the catalyst-organic framework is not needed for this system. The results from this experiment are shown in Table 2-8. Also discussed in this table is a high-loading run of **29** in 1,4-dioxanes; results indicate that high-loading reactions of **29** are feasible, but take longer to complete.

**Table 2-8.** Cycloisomerization of **29** at 70°C in 1,4-dioxanes Using Further Additions of Substrate before Attempted Reuse .

Loading (Sub:Rh:AgSbF <sub>6</sub> )	Conversion (%)	TON	ee (%)
300:1:5	100	300	>99.9
200:1 <sup>a</sup>	91	182	>99.9
500:1:5	35	175	N/A

<sup>a</sup> used same catalyst as previous, AgSbF<sub>6</sub> addition was not necessary. Total TON for the catalyst is 482.

Stemming from the discovery that the catalyst did not need to be activated with a sacrificial low loading of substrate, higher loading reactions were then attempted. The initial loadings were of 1000 equiv of **31** per Rh. The procedure was similar to the higher-loading batch reactions of **29**. Briefly, the reaction vessel was charged with 5 equiv of

AgSbF<sub>6</sub> (per Rh) along with **31**. The substrate, as in a 2M solution in 1,4-dioxanes was added to the catalyst-organic framework **28**/Ag mixture moments prior to immersion in a 70°C oil bath. An aliquot taken at 120 minutes reaction time indicated that the reaction was 20% complete (by <sup>1</sup>H NMR), a rate comparable with homogeneous reactions; however, further aliquots indicated that the rate decreased over time. Aliquots taken at 22 hours indicated 50% conversion by <sup>1</sup>H NMR spectroscopy, and after 50 hours, 80% of the starting material had reacted.

This reaction was repeated, as above, with 2MeTHF as solvent. The results from these experiments are summarized in Table 2-9. The reaction proceeded well in 2MeTHF. An aliquot at 120 minutes indicated 50% conversion (500 TO) to the desired product by <sup>1</sup>H NMR spectroscopy, with 63% conversion after 240 minutes, at which point the no further reaction was noted. In accordance, a 500 : 1 : 5 substrate : Rh : AgSbF<sub>6</sub> cycloisomerization of **31** was set up in 2MeTHF. The reaction was complete within 2 hours, a TOF of 250 hr<sup>-1</sup>. Attempts at further reuse of this catalyst were unsuccessful. Furthermore, this rate is directly comparable, if not better than literature, wherein 10 equiv of substrate will typically be cyclized in 10 minutes.

**Table 2-9.** Cycloisomerization of **31** with High Loadings of Substrate at 70°C.

Loading (Sub : Rh : AgSbF <sub>6</sub> )	Solvent	Time (h)	Conversion (%)	TON
1000:1:5	1,4-dioxanes	45	80.0	800
1000:1:5	2MeTHF	4	63.0	630
500:1:5	2MeTHF	2	100	500

These results indicate that the initial rate of reaction for the BaSO<sub>4</sub> supported catalyst is comparable to, and possibly even higher than, the homogeneous reaction, but also that there is an upper limit on the number of turnovers that the catalyst affords. From this result, it was decided that all other high-loading batch reactions be attempted at 500 equiv.

Currently, the supported polymer-based catalyst, **28**, for the intramolecular cyclization of 1,6-enynes is the most successful catalyst in the cycloisomerization of **29**, as well as **31**, affording TONs of 482 and 620, respectively. Accordingly, **28** is also capable of high-loading cycloisomerization reactions of **29** and **31**, through only a small change in reaction conditions. The catalyst-organic framework **28** is also capable of batch reactivity for **31** of up to 500 equiv of substrate; a loading on the order of 50 times greater than anything found in the literature for straightforward 1,6-enyne cycloisomerizations.

## Chapter 3

### Concluding Remarks

Utilizing the methodology developed by the Bergens' group for the immobilization of transition metal-BINAP based metal containing monomers using alternating-ROMP assembly, a Rh-BINAP based immobilized catalyst-organic framework was prepared. The prepared catalyst-organic framework was used for the cyclization of **29** and **31** in 1,4-dioxanes; catalyst loadings during reuse were 1 mol % Rh after an initial batch reaction of 5 mol % Rh. This loading per run is 10 times lower than Rh loadings found in literature for this cyclization, and the product was formed with minimal side reactions, forming the 1,3-diene and the *cis*-1,4-diene. The cyclization of **31** has not been disseminated in literature, and during homogeneous reactions forms a complex mixture of side products; when cyclized using the catalyst organic framework the amount of side reactions are minimal.

Higher-loading single batch reactivity was observed with 2-MeTHF as solvent, with loadings as low as 0.2 mol % Rh reacting to completion in 2 hours. This rate is nearly equal to the homogeneous reaction, where 10 turnovers by the catalyst are accomplished within 2 to 10 minutes at room temperature.

These results indicate that solvent choice is crucial for the type of activity desired. The homogeneous solvent, 1,2-dichloroethane was not a

prudent choice for heterogeneous catalysis; it was found that the solvent would dissolve the catalyst-organic framework. Initially replaced by 1,4-dioxanes, a higher-boiling solvent that affords a greater range of temperatures for catalysis, this solvent also affords catalyst reusability, probably through coordination of the ether-oxygen to rhodium. Later studies, after high-loading reactions were sluggish in 1,4-dioxanes, used 2-MeTHF as solvent for the high-loading single-batch reactions. 2-MeTHF affords a faster rate of reaction at the expense of reusability; any reuse attempted with this solvent was not successful.

The initial rate of reaction for the heterogeneous intramolecular cyclization is nearly equal with the homogeneous reaction, a very promising result. Normally, the rate of reaction for an immobilized catalyst is much slower than for the homogeneous; having a system where the rates are nearly equal, but the immobilized catalyst is able to withstand higher loadings of substrate is very rare. The short reaction times and high-loadings of Rh used in literature are most likely to stave off side-product formation, making this system unlikely to be used on an industrial scale, even though useful pharmaceutical precursors can be synthesized in a more atom-economical manner. The high-loading single-batch reactions indicate the robustness of the catalyst to large amounts of substrate, and a future goal of this project is to adapt this system to be used in a flow-reactor.

Other future works that are possible is the extension of this system to a rhodium precursor that is not bridged by chloride ligands. The requirement of silver additives for the chloro-bridged system is a negating factor, due to increased costs and waste that precludes the development of large-scale reactions using this system. Further works to be done in this lab include the preparation of a catalyst-organic framework based upon **21** (Chapter 2, Figure 2-12); the diolefin can be removed through hydrogenation as an entryway into catalysis. An immobilized catalyst system that is not hindered by additives is where this project should head

Along with the preparation of an immobilized Rh-BINAP system that does not require activation by silver prior to catalysis, the general scope of reactions possible with this system needs to be tested. Rh-BINAP is a system that has seen many uses, including allylic alcohol and amine isomerizations<sup>56</sup>, hydrogenations<sup>118</sup>, and amination reactions<sup>119</sup>. The isomerization of allylic alcohols is of particular interest for the development of a flow reactor system, as often the product aldehyde has a lower boiling point than the starting material, leading to ease of product separation. This ease of separation is important to atom economy, wherein the starting materials would remain in the flow reactor system until they are converted to the product aldehyde, but also because the catalyst will not display any product inhibition upon removal of product aldehydes or other carbonyl containing compounds. These compounds produced are



possibly useful in other areas of synthetic chemistry. Currently research in our laboratory is focusing on the catalytic isomerization of allylic alcohols and related compounds, with exceptional yield. These current advancements are very promising towards the development of a flow reactor; this is not possible with the cycloisomerization of 1,6-enynes due to inherent product inhibition.

The alternating-ROMP assembly methodology of other complexes of **13** should also be investigated, particularly Pd-BINAP based systems for the asymmetric allylation of prochiral nucleophiles<sup>120</sup>. Accordingly, the synthesis of **13** with the *exo*-dicarboxylic anhydride instead of the *endo*-isomer should also be attempted, and the characteristics of that ligand investigated. Furthermore, Ru based ROMP catalysts were used for this investigation mainly because they were proven to be effective first. Future work should explore utilization of the Schrock catalysts.

The catalyst-organic framework was characterized through NMR spectroscopy during, and after, alternating-ROMP assembly, as well as elemental analysis on the assembled framework. The evidence from the NMR experiments regarding the number of spacer monomers incorporated per norimido olefin matches the elemental analysis obtained. Future characterizations to be performed on framework **28** include both DLS (dynamic light scattering) and GPC (gel-permeation chromatography), which would afford the size distribution of the polymer beads as well as

the molecular weight distribution and average molecular weight, respectively. Precipitation of **28** and the expected non-linearity of the framework, however, would be a challenge to these studies. Other methods to characterize framework **28** that should be considered include solid-state NMR spectroscopy, which would allow framework characterization before and after deposition on support.

## Chapter 4

### Experimental Section

$^1\text{H}$ ,  $^{13}\text{C}$ , and  $^{31}\text{P}$ , NMR spectra were recorded using Varian Inova (300, 400 or 500 MHz) or Varian Unity (500 MHz) spectrometers.  $^1\text{H}$ , and  $^{13}\text{C}$  NMR chemical shifts are reported in parts per million ( $\delta$ ) relative to TMS with the solvent as the internal reference.  $^{31}\text{P}$  NMR chemical shifts are reported in parts per million ( $\delta$ ) relative to a external reference of 85 %  $\text{H}_3\text{PO}_{4(\text{aq})}$ . Gas chromatography analysis was carried out using a Hewlett Packard 5890 chromatograph equipped with a flame ionization detector, a 3392A integrator, and a Supelco Beta Dex<sup>TM</sup> 120 fused silica capillary column (30m x 0.25mm x 0.25 $\mu\text{m}$ , injector: 220 °C, detector: 220 °C, carrier gas: He, 20 psi).

Unless stated otherwise, all operations were performed under an inert nitrogen atmosphere using standard Schlenk and glovebox techniques. Dinitrogen gas (Praxair, 99.998%) was passed through a drying train containing 3Å molecular sieves and Indicating Drierite<sup>TM</sup> before use. All solvents were dried and distilled under a dinitrogen atmosphere using standard drying agents, unless otherwise noted. All common reagents and solvents were obtained from Sigma-Aldrich Co. and used without further purification, unless stated otherwise. The ROMP catalyst bis(tricyclohexylphosphine)benzylidene ruthenium (IV) dichloride (**1**) and (*R*)-BINAP (**17**) were obtained from Strem Chemicals, Inc. and

used without purification. (*R*)-BINAP dioxide (**18**), (*R*)-5,5'-dinitro-BINAP dioxide (**19**), (*R*)-5,5'-diamino-BINAP (**16**) and (*R*)-5,5'-dinorimido-BINAP (**13**) were synthesized according to previously reported procedures<sup>88</sup>. RhCl<sub>3</sub>·xH<sub>2</sub>O was obtained from A.D. Mackay Chemicals Inc. and used without further purification. [RhCl(C<sub>2</sub>H<sub>4</sub>)<sub>2</sub>]<sub>2</sub> was synthesized according to literature procedures<sup>121</sup>. [Ru(η<sup>6</sup>-anthracene)((1-3;5-6-η)-C<sub>8</sub>H<sub>11</sub>)]BF<sub>4</sub> was synthesized with a slight modification of literature methods<sup>122</sup>. BaSO<sub>4</sub> (white reflectance) was obtained from Eastman Chemical Co., Inc. and washed thoroughly with CH<sub>2</sub>Cl<sub>2</sub>, then MeOH and dried under vacuum before use.

#### **Synthesis of (*R*)-5,5'-diamino-BINAP dioxide (**20**).**

A glass autoclave equipped with a ½" stir bar was charged with 0.912g of (*R*)-5,5'-dinitro-BINAP dioxide (**19**) (1.22mmol) along with 0.1368g of 5 wt % palladium on carbon (6.43 x 10<sup>-5</sup> mol of Pd). The autoclave was purged with H<sub>2(g)</sub> for 20 min, then charged with 15 mL EtOH (degassed with H<sub>2(g)</sub> for 20 min). The vessel was sealed, pressurized to 45 psig, and lowered into a 50°C oil bath with moderate stirring for 3 hours. Aliquots taken at 3 hr indicated that the reaction was complete by <sup>1</sup>H and <sup>31</sup>P NMR. The reaction mixture was filtered to remove the Pd/C; which was then washed with EtOH (3 x 10 mL) and CH<sub>2</sub>Cl<sub>2</sub> (2 x 10 mL) in succession until the washings ran colourless. Filtrate was concentrated

under reduced pressure, and was purified with flash chromatography (neutral alumina, 93 : 7 CH<sub>2</sub>Cl<sub>2</sub> : EtOH, R<sub>f</sub> = 0.75). Fractions collected were monitored by TLC. From the pure fractions, the volatile solvents were removed under reduced pressure, giving 87% yield. The spectroscopic data was in accordance with literature.<sup>88</sup> <sup>1</sup>H NMR (400 MHz, CDCl<sub>3</sub>): δ ppm 4.12 (br s, 4H), 6.28 - 6.30 (m, 2 H), 6.59 - 6.64 (m, 4 H), 7.21 - 7.27 (m, 9 H), 7.34 - 7.46 (m, 9 H), 7.67 – 7.72 (m, 4 H), 7.81 (d, *J* = 8.20, 2 H); <sup>31</sup>P NMR (162 MHz, CDCl<sub>3</sub>): δ ppm 29.95 (s, 1P).

#### **Synthesis of [Ru(η<sup>6</sup>-anthracene)((1-3;5-6-η)-C<sub>8</sub>H<sub>11</sub>)]BF<sub>4</sub> (24).**

To a round bottom flask equipped with a 1" stir bar, 0.1633 g (5.60 x 10<sup>-5</sup> mol) of [Ru(COD)(η<sup>3</sup>-C<sub>3</sub>H<sub>5</sub>)<sub>2</sub>] and 0.0998 g (5.59 x 10<sup>-4</sup> mol) anthracene were then charged into the round bottom flask. After evacuation and backfilling thrice, 8.13 mL CH<sub>2</sub>Cl<sub>2</sub> was added to the flask while moderately stirring. Both colourless solids netted a clear, colourless solution. While stirring, 77.2 μL of 30% HBF<sub>4</sub> (2.63 x 10<sup>-4</sup> mol) in Et<sub>2</sub>O was added dropwise. Upon addition of the first drop, a brick red solution was observed; addition of the remainder nets a black solution. After stirring for 90 minutes, the colour is once again brick red and clear. Crude product was concentrated under reduced pressure, and then recrystallized from CHCl<sub>3</sub>/Et<sub>2</sub>O, 62% yield.

### Synthesis of $[\text{Ru}(\eta^5\text{-C}_8\text{H}_{11})(\text{N-BINAP})]\text{BF}_4$ (**23**).

Under a Nitrogen atmosphere, 0.0392 g ( $9.0 \times 10^{-5}$  mol) of  $[\text{Ru}(\eta^5\text{-C}_8\text{H}_{11})(\eta^6\text{-Anthracene})]\text{BF}_4$  (**24**) is weighed into a vial, along with 0.0799 g ( $8.5 \times 10^{-5}$  mol) of (*R*)-5,5'-dinorimido-BINAP (**13**) into another. Both solids are dissolved in 0.5 mL  $\text{CH}_2\text{Cl}_2$ , and cannulated into a pre-weighed Schlenk flask, with rinses to effect quantitative transfer. Upon addition of **24** and **13**, the reaction mixture is cloudy-orange. After stirring at room temperature for one hour, the reaction mixture is refluxed at  $40^\circ\text{C}$  for 48 hours to convert all compounds into one isomer, as discussed in Chapter 2. The reaction mixture was cannulated into a pre-weighed round bottom flask, and recrystallized from  $\text{CH}_2\text{Cl}_2/\text{Et}_2\text{O}$ . Yield obtained was 70%.

### Synthesis of $[\text{RhCl}(\text{N-BINAP})]_2$ (**25**).

Under a Nitrogen atmosphere, a solution of 32.2 mg ( $3.40 \times 10^{-5}$  mol) of N-BINAP (**13**) in 0.5 mL  $\text{CD}_2\text{Cl}_2$  was added to a slurry of 7.0 mg ( $1.82 \times 10^{-5}$  mol)  $[\text{RhCl}(\text{C}_2\text{H}_4)_2]_2$  in 0.1 mL  $\text{CD}_2\text{Cl}_2$  in an NMR tube. The NMR tube was shaken, and purged occasionally with  $\text{N}_{2(\text{g})}$  for 30 minutes, before  $^1\text{H}$  and  $^{31}\text{P}$  NMR spectra were obtained. Upon addition of the ligand solution to the rhodium slurry, there was an instantaneous colour change from yellow-orange to brick red, with accompanying evolution of gas. After identification of the target molecule, the prepared compound was used in

further reactions without isolation or purification. Spectrographic data was in accordance with literature precedence, specifically that of  $[\text{RhCl}(\text{BINAP})]_2$ <sup>123</sup>. <sup>1</sup>H NMR (400MHz, CD<sub>2</sub>Cl<sub>2</sub>) δ ppm 1.67 (d, *J* = 8.38 Hz, 2 H), 1.81 (d, *J* = 8.38 Hz, 2 H), 3.48 – 3.53 (m, 4 H), 3.56 – 3.60 (m, 4 H), 6.28 (dd, *J* = 1.99 Hz, 2 H), 6.38 (dd, *J* = 1.99 Hz, 2 H), 6.47 (d, *J* = 4.79 Hz, 2 H), 6.57 (d, *J* = 4.79 Hz, 2H), 6.60 – 6,76 (m, 4H), 6.81 – 6.90 (m, 2H), 6.92 (d, *J* = 7.18 Hz, 2H), 7.05 (m, 2H), 7.22 (t, *J* = 8.64 Hz, 2H), 7.41(m, 6H), 7.73 (br s, 4H), 7.98 (br s, 4 H); <sup>31</sup>P NMR (161 MHz, CD<sub>2</sub>Cl<sub>2</sub>) δ ppm 50.77 (d, *J* = 194.1 Hz 2P).

## **Procedure for the ROMP-Assembly of Catalyst Organic Framework (28)**

### **a) Preparation of Catalyst-Organic Framework**

In an experiment 36.9 mg ( $1.70 \times 10^{-5}$  mol) of  $[\text{RhCl}(\text{N-BINAP})]_2$  (**25**) dissolved in 0.6mL CD<sub>2</sub>Cl<sub>2</sub>, as generated immediately before, is used. To this solution, 26.6 μL ( $2.40 \times 10^{-4}$  mol) of COE is added to **25** under a Nitrogen atmosphere, and the tube is shaken. The colour of solution remained brick-red. This is then cannulated under inert atmosphere into a Schlenk tube equipped with a stir bar, and rinsed in with 1.0 mL CH<sub>2</sub>Cl<sub>2</sub>. 1.5 mg ( $1.82 \times 10^{-6}$  mol) of trans-RuCl<sub>2</sub>(PCy<sub>3</sub>)<sub>2</sub>(=CHPh) (Grubbs 1<sup>st</sup> Generation, **1**) dissolved in 1.1 mL CH<sub>2</sub>Cl<sub>2</sub>, yielding a purple solution, is then added, the vessel sealed, and placed with moderate stirring into an

oil bath at 40°C. This was left, sealed, until ROMP assembly was determined to be complete by  $^1\text{H}$  NMR, typically within 24 hours, as discussed in Chapter 2.

**b) Deposition of Catalyst-Organic Framework onto  $\text{BaSO}_4$ .**

10 g of  $\text{BaSO}_4$  was weighed out in air, and then transferred to a 250 mL Erlenmeyer flask. To this, 50 ml  $\text{CH}_2\text{Cl}_2$  is added, and the flask shook mildly. The slurry is then filtered onto a fritted Buchner Funnel (D Grade). This is rinsed with successive 3 x 50 mL  $\text{CH}_2\text{Cl}_2$ , then 3 x 50 mL MeOH.

3.014 g of washed  $\text{BaSO}_4$  is weighed into a 250 mL round bottom flask equipped with a stir bar and a side arm. This was placed under vacuum to dry overnight while the polymerization was occurring. After drying on hi-vacuum, the flask is backfilled with nitrogen. To this flask, 20 mL of  $\text{CH}_2\text{Cl}_2$  is added, and low stirring applied to affect a slurry. The reaction mixture, a brown solution, which is slightly cloudy due to polymer insolubilities, has 10mL  $\text{CH}_2\text{Cl}_2$  added as dilutant. This diluted reaction mixture is cannulated onto the  $\text{BaSO}_4/ \text{CH}_2\text{Cl}_2$  slurry, affecting a tan-coloured mixture. The reaction vessel is rinsed with 3 x 5 mL  $\text{CH}_2\text{Cl}_2$ , and the slurry is allowed to homogenize with stirring for 20 minutes.

After effective homogenization, the solvent is removed slowly under reduced pressure, with rapid stirring to make certain that the deposition was as uniform as possible. Care was taken to only do the solvent removal at room temperature, and not to heat the flask during removal.



After removal of solvent to dryness, the flask was dried further on the hi-vacuum lines for 1 hour.

After the initial drying, the supported catalyst was rinsed with 3 x 50 mL MeOH. Care was taken to make exposure to MeOH as short-lived as possible, in an effort to not compromise the catalyst. Previously, MeOH portions used for rinsing had been removed by inverse filtration by a cannula equipped with filter paper on one end, but this was not timely. Now, the MeOH portions are collected into another pre-weighed round bottom flask by pure cannula transfer; the filter paper has a tendency to clog, causing rinsing to be the most time-costly part of the deposition. The catalyst, after the final rinse, was dried one hour on hi-vacuum, then immediately placed into the glovebox, and stored free from ambient light.

### **c) Determination of the Loading of the Supported Catalyst-Organic Framework**

The rhodium loading of the supported catalyst-organic framework is determined from the amount of the initial  $[\text{RhCl}(\text{N-BINAP})]_2$  generated for use in polymerization, and the amount of  $\text{BaSO}_4$  weighed out. All steps, the generation, polymerization, and deposition, are assumed to be quantitative in yield. Loadings of  $5.6 \times 10^{-6}$  mol of dimer per gram of support are typical.

## Synthesis of Substrates for the rhodium-Catalyzed Reductive Cyclization of 1,6-Enynes.

Substrates were synthesized according to a modified literature procedure<sup>80</sup>, as shown in Scheme 2-8, in which both preparations utilize *cis*-2-penten-1-bromide. These were synthesized in conjunction with Andrew Sullivan, as well as Elizabeth Corkum.

### Preparation of *cis*-2-Penten-1-Bromide (35).

In 60mL absolute diethyl ether, 5.2 mL *cis*-2-penten-1-ol (4.643 g, 53.4 mmol) and 0.5 mL ( $6.2 \times 10^{-3}$  mol) pyridine are cooled to  $-40^{\circ}\text{C}$ . To this, 2.03 mL phosphorous tribromine ( $\text{PBr}_3$ ) (5.784 g, 21.3 mmol) is added dropwise. Upon addition, a white precipitate is immediately formed. This was allowed to stir and warm to room temperature slowly over 2 hours, then maintained at room temperature for another hour. The reaction was then quenched by addition of 100 mL of concentrated  $\text{NaHCO}_3$  in distilled water. The aqueous layer was extracted 3 x 50 mL  $\text{Et}_2\text{O}$ ; the organic layer was then dried on  $\text{MgSO}_4$  and filtered. Purification was by silica gel flash chromatography using 50 : 1 petroleum ether :  $\text{Et}_2\text{O}$  as eluent,  $R_f = 0.4$ . Yield was 5.973 g (39.8 mmol, 75%).  $^1\text{H}$  NMR (300 MHz,  $\text{CDCl}_3$ )  $\delta$  ppm 1.00 – 1.05 (t, 3H) 2.12 - 2.22 (dq, 2H) 4.01 (d, 2H) 5.56 – 5.72 (m, 2H).

### **Preparation of 3-Cyclohexyl-2-propyn-1-ol (33).**

3-Cyclohexyl-2-propyn-1-ol (**33**) was prepared following the general procedure as described by Hashmi *et al.*<sup>80</sup> Under an inert atmosphere, 5.0 mL (4.20 g, 38.8 mmol) of cyclohexylacetylene in 30 mL absolute THF is cooled to -78°C. 24.3 mL of 1.6 M n-butyllithium in hexanes (38.8 mmol) was then added dropwise. The solution formed was warmed to 0°C, netting a pale-yellow solution. 1.8578 g of paraformaldehyde (61.9 mmol) is then added as a solid, and the solution warmed to room temperature, after which it is heated to 45°C for 90 minutes. This is then cooled to room temperature, upon which it is quenched by addition of 125 mL of 10% NH<sub>4</sub>Cl in distilled water. After separation of the phases, the aqueous layer is extracted with 3 x 50 mL Et<sub>2</sub>O. The organic layer is dried on MgSO<sub>4</sub>, filtered, and the solvent removed via vacuum. Silica gel flash chromatography using 60 : 40 CH<sub>2</sub>Cl<sub>2</sub> : hexanes gave the product **33** as a yellow oil in a yield of 4.962 g (35.9 mmol, 93%). R<sub>f</sub> (CH<sub>2</sub>Cl<sub>2</sub> : hexanes, 60: 40) = 0.3; <sup>1</sup>H NMR (300 MHz, CDCl<sub>3</sub>) δ ppm 1.26 - 1.66 (m, 7 H) 1.69 - 1.81 (m, 2 H) 1.81 - 1.93 (m, 2 H) 2.38 - 2.52 (m, 1 H) 4.33 (d, J = 1.83 Hz, 2 H).

### **((2Z)-3-Pent-2-enyloxy-prop-1-yl)cyclohexene (31).**

In a typical experiment, a 200 mL round bottom flask equipped with a stir bar is charged with 1.301 g of a 30 wt % dispersion of potassium

hydride (KH) in mineral oil (.390 g, 9.7 mmol). The flask is then evacuated and backfilled three times with nitrogen. The KH is then rinsed with 4 x 5 mL dry THF to quantitatively remove all mineral oil. To the KH, another 20 mL THF is added, and the mixture is cooled to 0°C. To the KH, 1.002 g (6.7 mmol) of *cis*-2-penten-1-bromide is added by cannulation under an inert atmosphere, followed by 2 x 5 mL THF as rinse. This is followed by addition of 0.848 g (6.1 mmol) of 3-cyclohexyl-2-propyn-1-ol by cannulation under inert atmosphere, followed by rinsing with 2 x 5 mL THF. Upon addition of the alcohol, gas evolves, and the reaction mixture goes to a bright orange colour. This reaction is allowed to warm to room temperature, and then stirred for three hours, quenched by addition of 50 mL H<sub>2</sub>O, and the aqueous phase extracted with 4 x 50 mL Et<sub>2</sub>O. Organic phase is dried over MgSO<sub>4</sub>, and the solvent removed by reduced pressure. Purification is through flash column chromatography (petroleum ether : ether, 50 : 1). R<sub>f</sub> = 0.3. Yield = 0.667 g, 53%. <sup>1</sup>H NMR (400 MHz, CDCl<sub>3</sub>) δ ppm = 0.91 (t, J = 7.6 Hz, 3 H), 1.15 - 1.29 (m, 3 H), 1.29 - 1.48 (m, 3 H), 1.57 - 1.66 (m, 2 H), 1.67 - 1.76 (m, 2 H), 2.03 (pd, J = 7.39, 1.2 Hz, 2 H), 2.28 - 2.37 (m, 1 H), 4.00 - 4.03 (m, 2 H), 4.03 (d, J = 2.2 Hz, 2 H), 5.35 - 5.57 (m, 2 H); <sup>13</sup>C NMR (101 MHz, CDCl<sub>3</sub>) δ ppm = 14.05, 20.76, 24.70, 25.80, 28.99, 32.52, 57.19, 64.28, 75.82, 90.60, 124.80, 135.74; anal. calcd. for C<sub>14</sub>H<sub>22</sub>O (206.32): C 81.50, H 10.75; found C 81.51, H 10.68.

### Preparation of 3-Phenyl-2-propyn-1-ol (**34**).

This was prepared following the general procedure as described by Hashmi *et al.*<sup>80</sup> Under an inert atmosphere, 5.0 mL (4.65 g, 45.4 mmol) of phenylacetylene in 30 mL absolute THF is cooled to -78°C. 31.3 mL of 1.6 M n-butyllithium in hexanes (50.0 mmol) was then added dropwise. The solution formed was warmed to 0°C, netting a orange-brown solution. 2.052 g of paraformaldehyde (68.2 mmol) is then added as a solid, and the solution warmed to room temperature, after which it is heated to 45°C for 90 minutes. This is then cooled to room temperature, upon which is it quenched by addition of 125mL of 10% NH<sub>4</sub>Cl in distilled water. After separation of the phases, the aqueous layer is extracted with 3 x 50 mL Et<sub>2</sub>O. The organic layer is dried on MgSO<sub>4</sub>, filtered, and the solvent removed via vacuum. Silica gel flash chromatography using 60 : 40 CH<sub>2</sub>Cl<sub>2</sub> : hexanes gave the product **34** as a yellow oil in a yield of 5.431 g (41.1 mmol, 90%). Spectroscopic data was in accordance with what Hashmi *et al.* report<sup>80</sup>. R<sub>f</sub> (CH<sub>2</sub>Cl<sub>2</sub> : hexanes, 60: 40) = 0.35; <sup>1</sup>H NMR (300 MHz, CDCl<sub>3</sub>) δ ppm = 4.53 (s, 2H) 7.27-7.36 (m, 3H) 7.43-7.40 (m, 2H).

### ((**2Z**)-3-Pent-2-enyloxy-prop-1-yl)benzene (**29**).

In a typical experiment, a 200 mL round bottom flask equipped with a stir bar is charged with 1.323 g of a 30 wt % dispersion of KH in mineral oil

(0.370 g, 9.9 mmol). The flask is then evacuated and backfilled three times with nitrogen. The KH is then rinsed with 4 x 5 mL absolute THF to quantitatively remove all mineral oil. To the KH, another 20 mL THF is added, and the mixture is cooled to 0°C. To the KH, 1.021 g (6.8 mmol) of *cis*-2-penten-1-bromide is added by cannulation under an inert atmosphere, followed by 2 x 5 mL THF as rinse. This is followed by addition of 0.818 g (6.2 mmol) of 3-phenyl-2-propyn-1-ol by cannulation under inert atmosphere, followed by rinsing with 2 x 5 mL THF. Upon addition of the alcohol, gas evolves, and the reaction mixture goes to an orange-brown colour. This reaction is warmed to room temperature, and then stirred for three hours, quenched by addition of 50 mL H<sub>2</sub>O, and the aqueous phase extracted with 4 x 50 mL Et<sub>2</sub>O. Organic phase is dried over MgSO<sub>4</sub>, and the solvent removed by reduced pressure. Spectroscopic data was in accordance with what Hashmi *et al.* report<sup>80</sup>. Purification by silica flash column chromatography using 50 : 1 petroleum ether : Et<sub>2</sub>O as eluent, R<sub>f</sub> = 0.2. Yield was 0.610 g (3.0 mmol, 49%) <sup>1</sup>H NMR (400 MHz, CDCl<sub>3</sub>) δ ppm = 1.07 (t, J = 7.5 Hz, 3 H), 2.14 - 2.28 (m, 2 H), 4.25 (d, J=6.6 Hz, 2 H), 4.43 (s, 2 H), 5.56 - 5.64 (m, 1 H), 5.68 - 5.76 (m, 1 H), 7.30 - 7.42 (m, 3 H), 7.47 - 7.56 (m, 2 H); anal. Calcd. For C<sub>14</sub>H<sub>16</sub>O (200.28): C 83.96, H 7.99; found: C 83.60, H 8.36.

## General Procedure for Low-Loading Cyclizations of 1,6-Enyne Substrates Using Supported Catalyst-Organic Framework with Attempted Reuse

In a typical experiment under Argon atmosphere, a thick-walled Schlenk flask (KIMAX) equipped with a Teflon™ valve is typically charged with 0.4736 g of supported catalyst (5.66 mg of “[RhCl(N-BINAP)]<sub>2</sub>”, 2.61 x 10<sup>-3</sup> mmol) under an inert atmosphere. A NMR tube is charged with 0.0036 g AgSbF<sub>6</sub> (1.05 x 10<sup>-2</sup> mmol), and sealed using a rubber septum. The Schlenk flask and NMR tube are then removed from the glovebox, and covered with tin foil to protect the reagents from ambient light. Cyclohexyl substrate **31** and 1,4-dioxanes are bubbled with Ar<sub>(g)</sub> for 30 minutes prior to use. 22 μL of **31** is then added into the flask containing the catalyst, rinsed in with 0.5 mL of 1,4-dioxanes, and stirred for 1 minute. 0.1 mL of 1,4-dioxanes is added to the AgSbF<sub>6</sub>, which is then cannulated onto the substrate/catalyst mixture, along with 5 x 0.1 mL rinse of 1,4-dioxanes. The flask is then sealed with the Teflon™ valve, and the apparatus is placed into an oil bath set at 60°C, stirring is set at 400 rpm. After 2.25 hours, an aliquot is taken by inverse filtration of the reaction mixture under inert atmosphere, and <sup>1</sup>H NMR was utilized to determine amount of conversion. Upon confirmation that the initial batch reaction was successful, the flask was charged with 5 mL 1,4-dioxanes, and stirred

for five minutes. The solvent was removed by inverse filtration, and the catalyst again treated with another 5 mL 1,4-dioxanes.

For catalyst reuse, the solid catalyst was used directly without any downtime or resting period between runs. As soon as the 5 mL rinsings were collected, the flask was charged with 110  $\mu$ L of **31**, and enough solvent to net a 0.2 M solution of substrate (2.61 mL total). The flask was sealed, and the reaction repeated. All further reuses were maintained in this manner.

### **General Procedure for Higher-Loading Cyclizations of 1,6-Enyne Substrates Using Supported Catalyst-Organic Framework**

In a typical experiment under Argon or Nitrogen atmosphere, a thick-walled Schlenk flask (KIMAX) equipped with a Teflon™ valve is typically charged with 0.1011 g of supported catalyst **28** (1.24 mg of “[RhCl(N-BINAP)]<sub>2</sub>”,  $5.74 \times 10^{-4}$  mmol), along with 0.0021 g AgSbF<sub>6</sub> ( $6.11 \times 10^{-3}$  mmol), under an inert atmosphere. The Schlenk flask is then removed from the glovebox, and covered with tin foil to protect the reagents from ambient light. 0.1187 g of **31** (0.575 mmol) is weighed out in air, and bubbled with Ar<sub>(g)</sub> to degas for 30 minutes prior to use. After 30 minutes, 0.6 mL 2MeTHF is added to the substrate. This is then cannulated onto the Rh/Ag mixture, the flask sealed with the Teflon™ valve, and the apparatus is placed into an oil bath set at 70°C, stirring is set at 400. After



two hours, an aliquot is taken by inverse filtration of the reaction mixture under inert atmosphere, and  $^1\text{H}$  NMR was utilized to determine amount of conversion.

### **Determination of Enantiomeric Excess (ee) of (Z)-3-(cyclohexylmethylene)-4-((E)-prop-1-enyl)tetrahydrofuran. (32)**

The ee of **32** was determined through the usage of  $^1\text{H}$  NMR spectroscopy in conjunction with chiral NMR shift reagents. This was required as use of chiral HPLC or GC was unsuccessful at separating the enantiomers. The product of cyclization was concentrated under reduced pressure, and 12.6 mg of **32** ( $6.11 \times 10^{-2}$  mmol) was dissolved in 0.6 mL benzene- $\text{d}^6$ . A solution of 22.1 mg ( $1.9 \times 10^{-5}$  mol) of europium-tris[3(heptafluoropropylhydroxymethylene)-(+)-camphorate] (**36**) in benzene- $\text{d}^6$  was also prepared. All NMR spectra obtained were run on a Varian Inova 500. Experiments were run thusly; after the initial  $^1\text{H}$  NMR spectrum was obtained, 10  $\mu\text{L}$  of the Europium solution was added to the previous NMR sample, and the spectrum was obtained. Additions continued until the signal that originated at 4.02 ppm had shifted to 6.0 ppm. The amount of **36** used corresponded to 20 mol % **32**. From this experiment, it was determined that the ee was >99% and only hindered by the signal to noise ratio of the NMR instrument.

**Determination of Enantiomeric Excess (*ee*) of (*Z*)-3-benzylidene-4-((*E*)-prop-1-enyl)tetrahydrofuran (30).**

Determination of *ee* was done through chiral GC in comparison to the racemic product. Cyclization products were concentrated under reduced pressure, then flushed through a Fluorisil™ plug using CH<sub>2</sub>Cl<sub>2</sub> as eluent to remove any metal residues. The eluted compound was again concentrated under reduced pressure, and a solution was prepared in dichloromethane of 2 mg per mL concentration. The solution was injected into the GC under the following conditions: He carrier gas (20 psig); Temperature program; initial temperature of 100°C, rate of 0.4°C per minute up to 220°C. Retention time for the racemic, Enantiomer 1: 122.6 min, Enantiomer 2: 123.4 min. Starting material eluted at 113.4 min. Absolute configuration was not determined.

## References

1. Saudan, L. A., *Acc. Chem. Res.* **2007**, *40* (12), 1309-1319.
2. Tombo, G. M. R.; Belluš, D., *Angew. Chem. Int. Ed.* **1991**, *30* (10), 1193-1215.
3. Klingler, F. D., *Acc. Chem. Res.* **2007**, *40* (12), 1367-1376.
4. Thayer, A. M., *Chem. Eng. News* **2007**, *85*, 11-19.
5. Smith, S. W., *Toxicol. Sci.* **2009**, *110* (1), 4-30.
6. Finlay, I., *Pain Rev.* **1999**, *6* (4), 303-313.
7. Noyori., R., *Asymmetric Catalysis in Organic Synthesis*. Wiley & Sons, Inc.: New York, 1994; p 378.
8. Trost, B. M., *Angew. Chem. Int. Ed.* **1995**, *34* (3), 259-281.
9. Trost, B. M.; Chung, C. K.; Pinkerton, A. B., *Angew. Chem. Int. Ed.* **2004**, *43* (33), 4327-4329.
10. Drautz, H.; Zähler, H.; Kupfer, E.; Keller-Schierlein, W., *Helv. Chim. Acta* **1981**, *64* (6), 1752-1765.
11. Grabley, S.; Kluge, H.; Hoppe, H.-U., *Angew. Chem. Int. Ed.* **1987**, *26* (7), 664-665.
12. Otomaru, Y.; Senda, T.; Hayashi, T., *Org. Lett.* **2004**, *6* (19), 3357-3359.

13. Garrett, C. E.; Prasad, K., *Adv. Synth. Catal.* **2004**, *346* (8), 889-900.
14. Lu, J.; Toy, P. H., *Chem. Rev.* **2009**, *109* (2), 815-838.
15. Fraile, J. M.; Garcia, J. I.; Mayoral, J. A., *Chem. Rev.* **2009**, *109* (2), 360-417.
16. Simons, C.; Hanefeld, U.; Arends, I. W. C. E.; Maschmeyer, T.; Sheldon, R. A., *J. Catal.* **2006**, *239* (1), 212-219.
17. Maruoka, K., *Org. Process Res. Dev.* **2008**, *12* (4), 679-697.
18. Li, C., *Catal. Rev. Sci. Eng.* **2004**, *46* (3/4), 419-492.
19. Dhakshinamoorthy, A.; Alvaro, M.; Garcia, H., *Adv. Synth. Catal.* **2010**, *352* (4), 711-717.
20. Barbaro, P., *Chem. Eur. J.* **2006**, *12* (22), 5666-5675.
21. Chapuis, C.; Barthe, M.; de Saint Laumer, J.-Y., *Helv. Chim. Acta* **2001**, *84* (1), 230-242.
22. Taylor, R. A.; Santora, B. P.; Gagn<sup>v</sup>©, M. R., *Org. Lett.* **2000**, *2* (12), 1781-1783.
23. Song, C. E.; Lee, S.-g., *Chem. Rev.* **2002**, *102* (10), 3495-3524.
24. Cornejo, A.; Fraile, J. M.; García, J. I.; Gil, M. J.; Luis, S. V.; Martínez-Merino, V.; Mayoral, J. A., *J. Org. Chem.* **2005**, *70* (14), 5536-5544.
25. Saluzzo, C.; Lamouille, T.; Hèrault, D.; Lemaire, M., *Bioorg. Med. Chem. Lett.* **2002**, *12* (14), 1841-1844.

26. Song, C. E.; Yang, J. W.; Roh, E. J.; Lee, S.-G.; Ahn, J. H.; Han, H., *Angew. Chem. Int. Ed.* **2002**, *41* (20), 3852-3854.
27. Abd-El-Aziz, A. S.; May, L. J.; Hurd, J. A.; Okasha, R. M., *J. Polym. Sci., Part A: Polym. Chem.* **2001**, *39* (16), 2716-2722.
28. Kroll, R.; Eschbaumer, C.; Schubert, U. S.; Buchmeiser, M. R.; Wurst, K., *Macromol. Chem. Phys.* **2001**, *202* (5), 645-653.
29. Buchmeiser, M. R.; Kroll, R.; Wurst, K.; Schareina, T.; Kempe, R.; Eschbaumer, C.; Schubert, U. S., *Macromol. Symp.* **2001**, *164* (Reactive Polymers), 187-196.
30. Pugin, B.; Blaser, H.-U., *Top. Catal.* **2010**, *53* (13-14), 953-962.
31. Grubbs, R. H.; Kroll, L. C., *J. Amer. Chem. Soc.* **1971**, *93* (12), 3062-3.
32. Pepper, K. W.; Paisley, H. M.; Young, M. A., *J. Chem. Soc.* **1953**, 4097-4105.
33. Takeda, K.; Oohara, T.; Anada, M.; Nambu, H.; Hashimoto, S., *Angew. Chem. Int. Ed.* *49* (39), 6979-6983.
34. Esteruelas, M. A.; González, F.; Herrero, J.; Lucio, P.; Oliván, M.; Ruiz-Labrador, B., *Polymer Bulletin* **2007**, *58* (5), 923-931.
35. Ivin, K. J., Mol, J. C., *Olefin Metathesis and Metathesis Polymerization*. Academic Press: San Diego, 1997.
36. Grubbs, R. H.; Miller, S. J.; Fu, G. C., *Acc. Chem. Res.* **1995**, *28* (11), 446-52.

37. Savoie, J.; Stenne, B.; Collins, S. K., *Advanced Synthesis & Catalysis* **2009**, *351* (11-12), 1826-1832.
38. Bielawski, C. W.; Grubbs, R. H., *Prog. Polym. Sci.* **2007**, *32* (1), 1-29.
39. Mori, M., *Adv. Synth. Catal.* **2007**, *349*, 121-135.
40. Sabitha, G.; Reddy, S. S. S.; Bhaskar, V.; Yadav, J. S., *Synthesis* **2010**, (7), 1217-1222.
41. Schwab, P.; France, M. B.; Ziller, J. W.; Grubbs, R. H., *Angew. Chem. Int. Ed.* **1995**, *34* (18), 2039-41.
42. Scholl, M.; Ding, S.; Lee, C. W.; Grubbs, R. H., *Org. Lett.* **1999**, *1* (6), 953-956.
43. Hoveyda, A. H.; Kingsbury, J.; Garber, S.; Gray, B. L.; Fourkas, J. T. Recyclable metathesis catalysts. WO0214376 (A2) 2002.
44. Hoveyda, A. H.; Zhugralin, A. R., *Nature (London, U. K.)* **2007**, *450* (7167), 243-251.
45. Cortez, G. A.; Schrock, R. R.; Hoveyda, A. H., *Angew. Chem. Int. Ed.* **2007**, *46* (24), 4534-4538.
46. Slinn, C. A.; Redgrave, A. J.; Hind, S. L.; Edlin, C.; Nolan, S. P.; Gouverneur, V., *Org. Biomol. Chem.* **2003**, *1* (21), 3820-3825.
47. Schrock, R. R.; Hoveyda, A. H., *Angew. Chem. Int. Ed.* **2003**, *42* (38), 4592-4633.
48. Schrock, R. R., *Acc. Chem. Res.* **1990**, *23* (5), 158-65.

49. Tanaka, K.; Böhm, V. P. W.; Chadwick, D.; Roeper, M.; Braddock, D. C., *Organometallics* **2006**, *25* (24), 5696-5698.
50. Hong, S. H.; Grubbs, R. H., *Journal of the American Chemical Society* **2006**, *128* (11), 3508-3509.
51. Kirkland, T. A.; Lynn, D. M.; Grubbs, R. H., *J. Org. Chem.* **1998**, *63* (26), 9904-9909.
52. Miyashita, A.; Yasuda, A.; Takaya, H.; Toriumi, K.; Ito, T.; Souchi, T.; Noyori, R., *J. Am. Chem. Soc.* **1980**, *102* (27), 7932-4.
53. Hayashi, T.; Matsumoto, Y.; Ito, Y., *Tetrahedron: Asymmetry* **1991**, *2* (7), 601-612.
54. Hoegaerts, D.; Jacobs, P. A., *Tetrahedron: Asymmetry* **1999**, *10* (15), 3039-3043.
55. Ping, C.; Zhang, X., *Angew. Chem. Int. Ed.* **2000**, *39*, 4104-4106.
56. Bergens, S. H.; Bosnich, B., *Journal of the American Chemical Society* **1991**, *113* (3), 958-967.
57. McDonald, A. R.; Mueller, C.; Vogt, D.; van, K. G. P. M.; van, K. G., *Green Chem.* **2008**, *10* (4), 424-432.
58. Cai, D.; Larsen, R. D.; Reider, P. J., *Tetrahedron Letters* **2002**, *43* (22), 4055-4057.
59. Hayashi, T.; Takahashi, M.; Takaya, Y.; Ogasawara, M., *Journal of the American Chemical Society* **2002**, *124* (18), 5052-5058.

60. Sorgel, S.; Tokunaga, N.; Sasaki, K.; Okamoto, K.; Hayashi, T., *Org. Lett.* **2008**, *10* (4), 589-592.
61. Alder, K., Diene Synthesis and Related Reaction Types. (Nobel Lecture, 1950). In *Nobel Lectures, Chemistry 1942 - 1962*, Elsevier: Amsterdam, 1964; pp 267-303.
62. Huntsman, W. D.; Hall, R. P., *J. Org. Chem.* **1962**, *27*, 1988-89.
63. Hoffman, H. M. R., *Angew. Chem. Int. Ed.* **1969**, *8*, 556-577.
64. Snieckus, W. O. V., *Angew. Chem. Int. Ed.* **1978**, *17*, 476-486.
65. Mikami, K.; Shimizu, M., *Chem. Rev.* **1992**, *92* (5), 1021-1050.
66. Trost, B. M.; Lautens, M.; Hung, M. H.; Carmichael, C. S., *Journal of the American Chemical Society* **1984**, *106* (24), 7641-7643.
67. Zhang, L.; Sun, J.; Kozmin, S. A., *Adv. Synth. Catal.* **2006**, *348*, 2271.
68. Ikeda, S.-I.; Daimon, N.; Sanuki, R.; Odashima, K., *Chem. Eur. J.* **2006**, *12*.
69. Fürstner, A.; Davies, P. W., *Angew. Chem.* **2007**, *119*.
70. Harrison, T. J.; Dake, G. R., *Org. Lett.* **2004**, *6* (26), 5023-5026.
71. Trost, B. M.; Frederiksen, M. U.; Rudd, M. T., *Angew. Chem. Int. Ed.* **2005**, *44*, 6630.
72. Chatani, N.; Inoue, H.; Morimoto, T.; Muto, T.; Murai, S., *J. Org. Chem.* **2001**, *66* (12), 4433-4436.



73. Cao, P.; Zhang, X., *Angew. Chem. Int. Ed.* **2000**, *39* (22), 4104-4106.
74. Lei, A.; He, M.; Zhang, X., *J. Am. Chem. Soc.* **2003**, *125* (38), 11472-11473.
75. Lei, A.; He, M.; Wu, S.; Zhang, X., *Angew. Chem. Int. Ed.* **2002**, *41* (18), 4.
76. Liu, F.; Liu, Q.; He, M.; Zhang, X.; Lei, A., *Org. Biomol. Chem.* **2007**, *5* (21), 3531-3534.
77. He, M.; Lei, A.; Zhang, X., *Tetrahedron Lett.* **2005**, *46* (11), 1823-1826.
78. Lei, A.; He, M.; Zhang, X., *Journal of the American Chemical Society* **2002**, *124* (28), 8198-8199.
79. Nicolaou, K. C.; Edmonds, D. J.; Li, A.; Tria, G. S., *Angew. Chem. Int. Ed.* **2007**, *46*, 3942-3945.
80. Hashmi, A. S. K.; Haufe, P.; Nass, A. R., *Adv. Synth. Catal.* **2003**, *345* (11), 1237-1241.
81. Lei, A.; Waldkirch, J. P.; He, M.; Zhang, X., *Angew. Chem. Int. Ed.* **2002**, *41* (23), 4526-4529.
82. Horne, D. A.; Fugmann, B.; Yakushijin, K.; Buchi, G., *J. Org. Chem.* **1993**, *58* (1), 62-64.
83. Nicolaou, K. C.; Li, A.; Edmonds, D. J., *Angew. Chem. Int. Ed.* **2006**, *45* (42), 7086-7090.

84. Sayah, R.; Framery, E.; Dufaud, V., *Green Chem.* **2009**, *11* (10), 1694-1702.
85. Ralph, C. K.; Akotsi, O. M.; Bergens, S. H., *Organometallics* **2004**, *23* (7), 1484-1486.
86. Walker, R.; Conrad, R. M.; Grubbs, R. H., *Macromolecules (Washington, DC, U. S.)* **2009**, *42* (3), 599-605.
87. Howell, J.; Goddard, J. D.; Tam, W., *Tetrahedron* **2009**, *65* (23), 4562-4568.
88. Ralph, C. K., Bergens, S. H., *Organometallics* **2007**, *26*, 4.
89. Berthod, M.; Mignani, G.; Woodward, G.; Lemaire, M., *Chem. Rev.* **2005**, *105* (5), 1801-36.
90. Kitamura, M.; Tsukamoto, M.; Bessho, Y.; Yoshimura, M.; Kobs, U.; Widhalm, M.; Noyori, R., *Journal of the American Chemical Society* **2002**, *124* (23), 6649-6667.
91. Takaya, H.; Mashima, K.; Koyano, K.; Yagi, M.; Kumobayashi, H.; Taketomi, T.; Akutagawa, S.; Noyori, R., *J. Org. Chem.* **1986**, *51* (5), 629-35.
92. Noyori, R.; Takaya, H., *Acc. Chem. Res.* **1990**, *23* (10), 345-50.
93. Akutagawa, S., *Appl. Catal., A* **1995**, *128* (2), 171-207.
94. Zhang, X. Ortho substituted chiral phosphines and phosphinites and their use in asymmetric catalytic reactions. 2002.

95. Okano, T. K., H.; Akutagawa, S.; Kiji, J.; Konishi, H.; Fukuyama, K.; Shimano, Y. 5,5'-Diamino or 5,5'-Diacetamido-2,2'-Bis(Diphenylphosphino)-1,1'-Binaphthyls. 1987.
96. Huang, Y.-Y., Deng, G.-J., Wang, X.-Y., He, Y.-M., Fan, Q.-H., *Chinese Journal of Chemistry* **2004**, *22*, 3.
97. Shimizu, K. D.; Freyer, H. O.; Adams, R. D., *Tetrahedron Lett.* **2000**, *41* (29), 5431-5434.
98. Curran, D. P.; Qi, H.; Geib, S. J.; DeMello, N. C., *J. Am. Chem. Soc.* **1994**, *116* (7), 3131-2.
99. Curran, D. P.; Geib, S.; DeMello, N., *Tetrahedron* **1999**, *55* (18), 5681-5704.
100. Itoh, K.; Nagashima, H.; Ohshima, T.; Oshima, N.; Nishiyama, H., *Journal of Organometallic Chemistry* **1984**, *272* (2), 179-188.
101. Wiles, J. A. D., C. J. A.; Hamilton, R. J.; Leong, C. G.; Bergens, S. H., *Organometallics* **2004**, *23*, 4564-4568.
102. Pathak, D. D.; Adams, H.; Bailey, N. A.; King, P. J.; White, C., *J. Organomet. Chem.* **1994**, *479* (1-2), 237-45.
103. Tani, K.; Yamagata, T.; Tatsuno, Y.; Yamagata, Y.; Tomita, K. i.; Akutagawa, S.; Kumobayashi, H.; Otsuka, S., *Angew. Chem. Int. Ed.* **1985**, *24* (3), 217-219.

104. Morimoto, T.; Yamasaki, K.; Hirano, A.; Tsutsumi, K.; Kagawa, N.; Kakiuchi, K.; Harada, Y.; Fukumoto, Y.; Chatani, N.; Nishioka, T., *Org. Lett.* **2009**, *11* (8), 1777-1780.
105. Simon, Y. C.; Coughlin, E. B., *Journal of Polymer Science Part A: Polymer Chemistry* **2010**, *48* (12), 2557-2563.
106. Dorta, R.; Egli, P.; Zuercher, F.; Togni, A., *J. Am. Chem. Soc.* **1997**, *119* (44), 10857-10858.
107. Corain, B.; Zecca, M.; Jerbek, K., *Journal of Molecular Catalysis A: Chemical* **2001**, *177* (1), 3-20.
108. de Vries, J. G. E., C. J., *Handbook of Homogeneous Hydrogenation*. Wiley-VCH: Weinheim, Germany, 2007; Vol. Vol. 1.
109. Zhang, J.; Leitus, G.; Ben-David, Y.; Milstein, D., *Angew. Chem. Int. Ed.* **2006**, *45* (7), 1113-1115.
110. Saudan, L.; Dupau, P.; Riedhauser, J.-J.; Wyss, P. Ruthenium complexes with amine/imine phosphine tetradentate ligands for hydrogenation of esters and lactones to give corresponding alcohols or diols. WO 2006106484 A1, 2006.
111. Saudan, L.; Dupau, P.; Riedhauser, J.-J.; Wyss, P. Ruthenium complexes with amine/imine phosphine bidentate ligands for hydrogenation of esters and lactones to give corresponding alcohols or diols. WO 2006106483 A1, 2006.

112. Saudan, L.; Saudan, C. Hydrogenation of esters with ru/bidentate ligands complexes. WO 2008065588, 2008.
113. Takebayashi, S. B., S. H., *Organometallics* **2009**, *28* (8), 3.
114. Blaser, H.-U., *Rendiconti Lincei* **2007**, *18* (4), 281-304.
115. Dwivedi, A. M., *Int. J. Pharm. Excipients* **2003**, (Apr.-June), 33-37.
116. Weller, A. S.; Mahon, M. F.; Steed, J. W., *J. Organomet. Chem.* **2000**, *614-615*, 113-119.
117. Langer, J.; Kriech, S.; Fischer, R.; Goerls, H.; Walther, D.; Westerhausen, M., *Organometallics* **2009**, *28* (19), 5814-5820.
118. Preetz, A.; Drexler, H.-J.; Schulz, S.; Heller, D., *Tetrahedron: Asymmetry* **2010**, *21* (9-10), 1226-1231.
119. Jin, P.; Huang, Z.; Chen, Z.; Chen, W.; Zhang, J.; Zhang, C. Method for synthesis of L-menthol. 2009.
120. Lozanova, A. V.; Ugurchieva, T. M.; Veselovsky, V. V., *Russ. Chem. Bull.* **2008**, *57* (8), 1787-1789.
121. Cramer, R., *Inorg. Synth.* **1990**, *28* (Reagents Transition Met. Complex Organomet. Synth.), 86-8.
122. Shibasaki, T.; Komine, N.; Hirano, M.; Komiya, S., *J. Organomet. Chem.* **2007**, *692* (12), 2385-2394.
123. Tokunaga, N.; Yoshida, K.; Hayashi, T., *PNAS* **2004**, *101* (15), 5445-5449.